BIOCHEMICAL AND FUNCTIONAL CHARACTERIZATION OF CIRCULAR RNAS DIFFERENTIALLY EXPRESSED IN CISPLATIN-TREATED HELA CELLS

A Thesis Submitted to
the Graduate School of Engineering and Sciences of
İzmir Institute of Technology
in Partial Fulfillment of the Requirements for the Degree of

DOCTOR OF PHILOSOPHY

in Molecular Biology and Genetics

by
Bilge YAYLAK

May 2023
İZMİR

ACKNOWLEDGEMENTS

Firstly, I would like to express my deep appreciation and gratitude to my supervisor Prof. Dr. Bünyamin AKGÜL, for his invaluable guidance, patience, enthusiasm, and support throughout my graduate life. His constructive criticism and sensible feedback have been instrumental in shaping the direction of this thesis.

I would like to express my sincere gratitude to the members of my thesis committee, Prof. Dr. Volkan SEYRANTEPE, Prof. Dr. Hatice Güneş ÖZHAN, Prof. Dr. Ayşe Semra KOÇTÜRK, and Doç. Dr. Ayşe CANER, for their invaluable guidance, contributions, and insightful comments. I would like to thank Dr. İpek ERDOĞAN, who generously gave her time and shared her experiences with me. I thank my fellow labmates, my flatmates, Bengisu GELMEZ and Dilek Cansu GÜRER, for their unwavering support, encouragement, and stimulating discussions. Their love, friendship, and knowledge have been a constant source of strength and inspiration. I would like to thank Şirin Elife CEREN, Cem ÇİFTÇİ, and all non-coding RNA lab members. Their contributions and support helped me to stay focused and motivated. I would also like to acknowledge the research associates and staff at the Integrated Research Center at Izmir Institute of Technology for sharing their expertise.

I would also like to acknowledge the Scientific and Technological Research Council of Turkey (TÜBİTAK) for the financial support under the ARDEB-121038 scientific research project during this study and for the doctoral scholarship under BIDEB-2211-A during my Ph.D. study. Special thanks to the Higher Education Council of Turkey (YÖK) for the scholarship under the YÖK-100/2000 project. I also want to thank Abdi İbrahim Pharmaceutical Industry and Trade Inc. for a doctoral scholarship.

Finally, I would like to extend my heartfelt appreciation to my beloved husband, Çağlar GEDİKSİZ, to my family Ercan YAYLAK, Selma YAYLAK, and Barış YAYLAK and my best friend Bahar LAFÇİ, for their love, patience, and support. Without them, this journey would not have been possible

ABSTRACT

BIOCHEMICAL AND FUNCTIONAL CHARACTERIZATION OF CIRCULAR RNAS DIFFERENTIALLY EXPRESSED IN CISPLATIN-TREATED HELA CELLS

Circular RNAs (CircRNAs) are a novel class of single-stranded, covalently-closed RNA molecules. Functional investigations of the circRNAs provide insight into the mechanisms underlying gene regulation and cellular responses, which could ultimately lead to the development of new therapies for a wide range of diseases. In this thesis, four cisplatin (cis-diamminedichloroplatinum II, CP)-responsive circRNAs, circGALNT2, circBNC2, circBIRC6, and circCLASP1, were validated. The reverse genetics approaches, such as knockdown and overexpression strategies, showed that circCLASP1 is required for the proliferation of HeLa cells. The knockdown of circCLASP1 disrupts proliferation in HeLa, and its overexpression restores impaired proliferation. Further analyses revealed that circCLASP1 knockdown sensitizes HeLa cells against 20 μM and 40 μM cisplatin treatments. Interestingly, an IC_{50} dose of cisplatin causes Annexin V-/7AAD + cell death rather than apoptosis when combined with circCLASP1 knockdown. In light of these findings, five circRNA/miRNA/mRNA regulatory networks were constructed using computational approaches. Additionally, a transcriptomics analysis after circCLASP1 knockdown has supported all of these findings in that muscle cell proliferation genes were significantly altered upon circCLASP1 knockdown in HeLa cells. In conclusion, the findings suggest that the knockdown of circCLASP1 represses proliferation and sensitizes HeLa cells against cisplatin. CircCLASP1-knockdown mediated differential gene expression indicates proliferation, ROS response, iron metabolism, lipid peroxidation, and cell death. Further studies are needed to elucidate the precise mechanism of circCLASP1-mediated cell death and proliferation in muscle cells or liver cells and ROS-related diseases.

Keywords: Circular RNA, Proliferation, Apoptosis, Cisplatin, Transcriptomics

ÖZET

SİSPLATİN İLE MUAMELE EDİLMİŞ HELA HÜCRELERİNDE FARKLI İFADE EDİLEN HALKASAL RNA'LARIN BİYOKİMYASAL VE FONKSİYONEL KARAKTERİZASYONU

Halkasal RNA'lar (HlkRNA'lar) tek sarmallı, kovalent olarak kapalı RNA moleküllerinin yeni bir sınıfıdır. HlkRNA'ların fonksiyonel araştırmaları, geniş bir hastalık yelpazesi için yeni tedavilerin geliştirilmesine yol açabilecek olan, gen regülasyonu ve hücresel tepkilerin altında yatan mekanizmalar hakkında bilgi sağlar. Bu tezde, sisplatine yanıt veren dört hlkRNA, hlkGALNT2, hlkBNC2, hlkBIRC6 ve hlkCLASP1 doğrulanmıştır. Susturma ve aşırı ifade stratejileri gibi ters genetik yaklaşımları hlkCLASP1'in HeLa hücrelerinin çoğalması için gerekli olduğunu gösterdi. hlkCLASP1'in susturulması, HeLa'daki proliferasyonu baskılar ve aşırı ifadesi, baskılama etkisini ortadan kaldırır. Diğer analizler, hlkCLASP1 susturulmasının, HeLa hücrelerini 20 uM ve 40 uM sisplatin uygulamasına karşı duyarlı hale getirdiğini ortaya çıkardı. İlginç bir şekilde, bir IC_{50} dozunda sisplatin uygulaması, circCLASP1 susturulması ile birleştirildiğinde apoptoz yerine Annexin V-/7AAD + hücre ölümüne neden olur. Bu bulguların ışığında, hesaplamalı yaklaşımlar kullanılarak beş circRNA/miRNA/mRNA düzenleyici ağ inşa edildi. Ek olarak, hlkCLASP1 susturulmasını takiben yapılan transkriptomik analiz, kas hücresi proliferasyonu, apoptoz, lipid metabolizması, oksidatif stres tepkisi ve bağışıklık tepkisi genlerinin HeLa hücrelerinde hlkCLASP1 susturması sebebiyle önemli ölçüde değiştiğine dair tüm bu bulguları desteklemiştir. Sonuç olarak, bulgular hlkCLASP1'in susturulmasının proliferasyonu baskıladığını ve HeLa hücrelerini sisplatine karşı duyarlı hale getirdiğini göstermektedir. CircCLASP1 susturulması aracılı farklı gen ifadesi, proliferasyonu, ROS tepkisini, demir metabolizmasını, lipid peroksidasyonunu ve hücre ölümünü göstermiştir. Kas hücrelerinde veya karaciğer hücrelerinde ve ROS ile ilişkili hastalıklarda hlkCLASP1 aracılı hücre ölümü ve proliferasyonunun kesin mekanizmasını aydınlatmak için daha ileri çalışmalar gerekir.

Keywords: Halkasal RNA, Proliferasyon, Apoptoz, Sisplatin, Transkriptomiks

"There and back again."

TABLE OF CONTENTS

LIST OF FIGURES

Figure **Page**

Figure **Page**

Figure **Page**

LIST OF TABLES

Table **Page**

CHAPTER 1

INTRODUCTION

1.1. Apoptosis, Proliferation, and Cell Cycle: A Matter of Cell Fate

1.1.1. Apoptosis and Switch from Pro-survival Signaling to Cell Death Signaling

Apoptosis is an orchestrated cascade of events that are responsible for cell death not only in development but also in adult organisms. Apoptosis was first reported by Carl Vogt in the year 1842 (Vogt 1842). Then Kerr group coined the term 'apoptosis' to describe the morphological changes associated with apoptotic cells in 1972 (Kerr et al. 1972). In the early times of research on apoptosis, efforts were primarily devoted to tissue cell death. Subsequently, scientists described biochemical and morphological changes in apoptosis (Hongmei 2012). Currently, apoptosis is characterized by membrane blebbing, positional organelle loss, chromatin condensation, DNA fragmentation, shrinkage of the cell, fragmentation into membrane-bound apoptotic bodies, and simultaneous engulfment by adjacent phagocytic cells physiologically.

As a biochemical hallmark, inter-nucleosomal cleavage creates a ladder pattern in an electrophoretic gel. Further, a switch of membrane lipid phosphatidylserine from the inner to the plasma membrane's outer side occurs, which serves as a phagocytic signal for neighboring cells. Apoptosis is a silent, non-inflammatory cell death that occurs under physiological conditions and is distinguished from accidental cell death, termed necrosis. Hence, it became a focus of attention during the 1980s. Cytosolic calcium concentration is critical for cell fate, so ion channels such as calcium channels are involved in apoptotic pathways (Hongmei 2012). Additionally, specific receptors, such as the TNF-alpha receptor, TLR, FasL receptor, and the death receptor, participate in caspase-dependent apoptosis triggered by external stimuli such as viral toxins or irradiation (Nagata 2018). Because of its highly regulated nature, apoptosis became an attractive target for

therapeutic interventions. In the past decades, apoptosis research focused mainly on a protein family of caspases. However, ensuing studies have shown that apoptosis still occurred despite its inhibition, suggesting caspase-independent apoptosis (Hongmei 2012). The classical programmed cell death pathway is caspase-dependent apoptosis.

1.1.2. Caspase Dependent Pathways

Caspases 3,7,8 and 9 participate in this type of apoptotic pathway (A. Fraser and Evan 1996; Nicholson and Thornberry 1997; Boldin et al. 1996). These particular cysteine proteases are synthesized as zymogens (Verma, Dixit, and Pandey 2016). The pro-domain of caspases is removed with specific cleavage at two points and generates an active enzyme to promote downstream apoptotic pathways (Verma, Dixit, and Pandey 2016). Finally, macrophages engulf apoptotic cells in efferocytosis (Nagata 2018; Martin, Peters, and Behar 2014). Two main caspase-dependent apoptotic pathways have been identified: intrinsic and extrinsic (De Vries, Gietema, and De Jong 2006). The intrinsic pathway (mitochondrial pathway) is controlled during developmental stages and triggered by genotoxic agents. Bcl-2 (B-cell lymphoma 2) family proteins regulate the intrinsic apoptotic pathway (Nagata 2018). Pro-apoptotic BH-3 only activator proteins, Bim, Bid, Puma, Bax, and Bak, are the critical effectors of apoptosis. Bax and Bak are activated and undergo allosteric changes, allowing them to oligomerize and produce macro-pores to allow cytochrome-c and apoptogenic proteins (e.g., SMAC) release from mitochondrial intermembrane space to the cytosol by causing MOMP (mitochondrial membrane permeabilization (MOMP). The cyt-c release is a direct way to caspase activation. It binds scaffold protein APAF-1 (Apoptotic protease activating protein 1) to create an apoptosome complex (Fig. 1) (Fulda et al. 2010; Singh, Letai, and Sarosiek 2020).

Indirectly, caspase inhibitory protein XIAP is neutralized by SMAC and OMI, and apoptosis sensitivity can be regulated by regulating additional signaling cascades such as NF-κB, JNK, TNFR, and the ubiquitin-proteasome pathway (Fulda et al. 2010; Singh, Letai, and Sarosiek 2020). Those events caused the caspase-9 activation, and executioner caspases

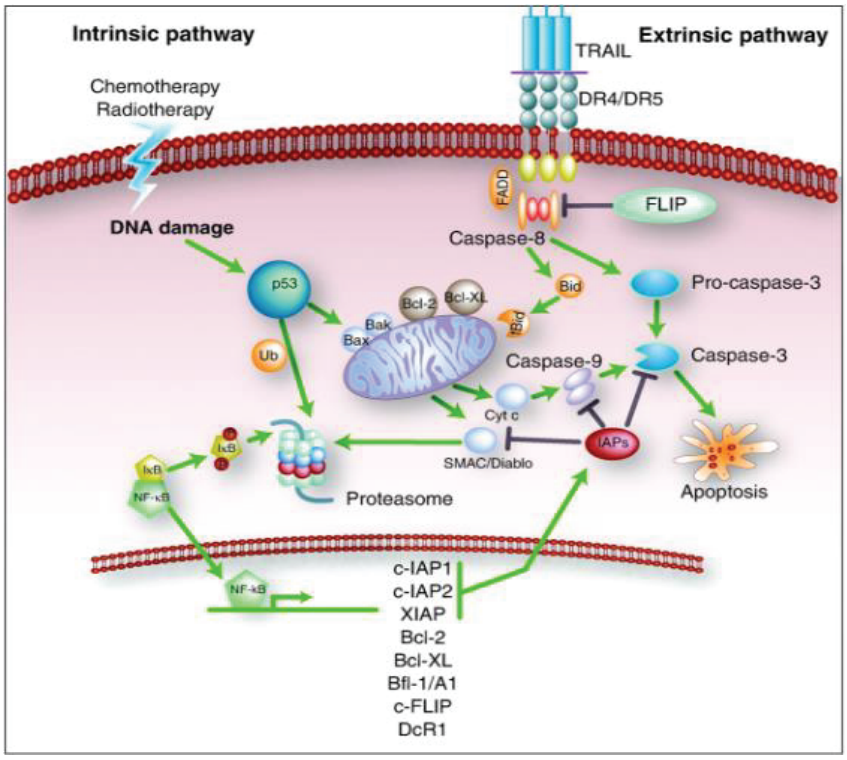

Figure 1.1. Schematic representation of the intrinsic and extrinsic pathways of apoptosis (De Vries, Gietema, and De Jong 2006).

(caspase3,7) were eventually activated (McIlwain, Berger, and Mak 2013). It should be noted that MOMP is the critical and irreversible step of apoptosis and indicates a cellular 'point of no return' (Bhola and Letai 2016). It is essential that incomplete MOMP, which means a small subset of the mitochondrial membrane is exposed to Bax and Bak oligomerization, can be potentially tumorigenic because of the DNA damage caused by post-MOMP-activated DNases (Ichim et al. 2015). Countering this pro-apoptotic chain of events are anti-apoptotic Bcl-2 family proteins: Bcl-2, Bcl-xl, Bcl-w, Bfl-1, and Mcl. These proteins have BH domains, which bind Bax and Bak and sequester their oligomerization to inhibit apoptosis (Hockenbery et al. 1991; Oltvai, Milliman, and Korsmeyer 1993; Westphal, Kluck, and Dewson 2014). Pro-survival Bcl-2 family proteins should be overwhelmed, and Bax and Bak proteins are activated to trigger apoptosis (Singh, Letai, and Sarosiek 2020). In the extrinsic pathway, apoptosis is

triggered by TNF family proteins, TNF-alpha, TRAIL, and FasL(Danial and Korsmeyer 2004; Ashkenazi and Dixit 1998).

These proteins, also known as death factors synthesized as membrane proteins, contain a homotrimeric structure converted to a soluble form after cleavage. The specific receptors for TNF-alpha are DR4/5 (McGrath 2011). The cytoplasmic region of DR4/5 and that of the Fas receptor include a nearly 80-aa part defined as the death domain needed for death signaling. In FasL-triggered apoptosis, FADD is recruited by the Fas death domain, pro-caspase-8, and c-FLIP to form the DISC complex (Schleich et al. 2012). Execution of the extrinsic pathway is proposed to branch into two ways downstream of DISC. In the first pathway, caspase 8 is strongly activated at DISC and activates pro-caspase 3 directly (Dickens et al. 2012).

The bid is cleaved by caspase 8 to form a truncated Bid (t-Bid) and promotes cytochrome c release from mitochondria in the second pathway (H. Li et al. 1998). As mentioned above, the downstream actions of cytochrome c are the same as the intrinsic pathway. The main difference between cells that undergoes Type I and Type II extrinsic pathway is the presence of XIAP (Jost and Vucic 2020). It should be noted that the Fas receptor-ligand-mediated system activated extrinsic apoptosis and played a role in proliferation or cytokine production (Nagata 2018).

1.1.3. Interconnection between Apoptosis, Cell cycle, and Proliferation

Many physiological processes, such as homeostasis, require a perfect balance between proliferation and apoptosis. The proliferation of somatic cells occurs via mitotic division regulated by the cell cycle progression. Apoptotic stimuli affect apoptosis, and apoptosis appears as if they are two contradicting processes. The existing evidence suggests that they are linked to each other. For example, apoptosis is induced by various dominant oncogenes (e.g., c-myc, a mitogen-triggered oncogene), which indicates that apoptosis and cell proliferation are closely linked pathways (Evan et al. 1992). However, while the apoptosis rate changes, the proliferation rate may remain constant. Therefore, there is a link but not a strict relationship between them. Several studies show both positive and negative correlations between apoptosis and proliferation. 7As an example of a positive relationship, Reid et al. have reported that macrophage colony-stimulating

factors appear to induce Fas expression on myeloid progenitor cells (Alenzi 2004; Reid et al. 1998). Thus, it can be said that uncontrolled proliferation can be related to a high level of apoptosis. Various studies have indicated cell cycle regulatory proteins are closely linked with apoptosis through a standard set of factors (Wiman and Zhivotovsky 2017). This linkage has been identified with tumor suppressor genes such as RB and p53 (Engeland 2022). Oncogene c-myc and several cyclin-dependent kinases (CDKs) and their regulators also link the cell cycle and apoptosis(Bhattacharya, Ray, and Johnson 2014; Thompson 1998). Apoptosis and cell proliferation are linked by cell-cycle regulators and apoptotic stimuli that affect both processes (Alenzi 2004; Furuya et al. 1994). The cell cycle is a series of events responsible for cell duplication. The cell cycle consists of 4 stages G1, S, G2, and M. Go or quiescent stage may occur between G1 and S phases during cell differentiation (Z. Wang 2021).

Proper transmission of genetic content into the daughter cell is a key event to producing genetically stable generations. This transmission requires a correct genome duplication during the S-phase and errorless segregation of the duplicated genome in the M-phase, which does not occur until the S-phase is completed (Ovejero, Bueno, and Sacristán 2020). A series of control systems monitor the timing of cell cycle events called checkpoints, which are G1/S, S, G2/M, and M. These checkpoints are activated by DNA damage to hold the cell on a defined stage and allow to repair DNA damage before the cell cycle is complete (Samuel, Weber, and Funk 2002). If the DNA damage is restored, the cell cycle continues. Otherwise, the cell is eliminated by apoptosis (Alenzi 2004). As mentioned above, c-myc is one of the critical key regulators of apoptosis and proliferation (Desbarats et al. 1996; C. Wang et al. 2021). In the normal cellular state, ectopic expression of myc is promoted to enter cells into the cell cycle. However, inhibition of myc leads to cell cycle arrest (Askew et al. 1991; Bretones, Delgado, and León 2015). On the other hand, overexpression of myc induces apoptosis during serum deprivation and hypoxia. In summary, myc acts as a dual switch, activating signals on both apoptosis and proliferation pathways. However, mitogens promote the proliferative pathway through bcl-2, which shuts down the myc-mediated apoptotic pathway (Vermeulen, Berneman, and Van Bockstaele 2003).

1.1.4. p53: Gatekeeper of Life and Death

p53, which has lost its function in nearly half of all cancer types, is involved in different aspects of apoptosis, DNA repair, cell cycle arrest, and genome integrity control (Figure 1.2) (Vousden 2006). p53 activates many genes by transactivation engaged in these processes (e.g., cyclin D1 and G, Bcl-xL, Bax, Fas1, DR5) and inactivation of genes as topoisomerase IIa (Pucci, Kasten, and Giordano 2000). Proliferation is affected by p53 predominately in the G1 phase. DNA damage activates p53 and results in G1 arrest by activating cyclin D/CDKs inhibitor p21 and consequent inhibition of phosphorylation of pRb. Therefore, cells do not progress through G1 to the S phase (J. Chen 2016).

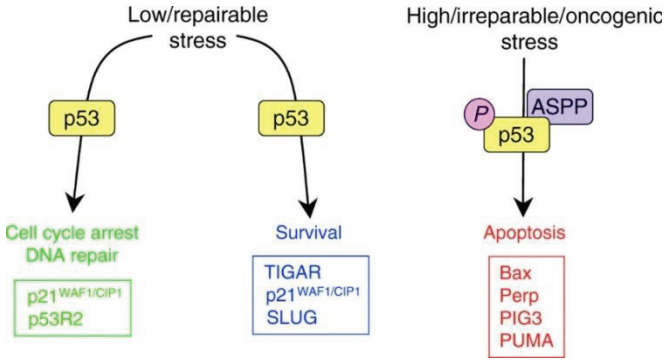

Figure 1.2. Different outcomes of p53 activation (Vousden 2006).

p53 regulates the DNA repair and promotes apoptosis when the damage is overwhelming repair (E. Schneider, Montenarh, and Wagner 1998). It has also been demonstrated that the p53 protein can spread across the mitochondria (Marchenko and Moll 2014). It activates the expression of pro-apoptotic Bax, Apaf-1, Puma, and Noxa and inhibits the expression of the Bcl-2 family. Besides, p53 increases MOMP to facilitate cytochrome c release and consequent induction of apoptosis. (Vermeulen, Berneman, and Van Bockstaele 2003; Wawryk-Gawda et al. 2014). p53 can regulate the CAK complex independently from CDKs to promote growth arrest. It has been shown that p53 upregulation causes G2-M transition arrest in a cell-specific manner (E. Schneider, Montenarh, and Wagner 1998). It also involves a spindle checkpoint and

controls centrosome duplication to prevent mitotic failure (Vermeulen, Berneman, and Van Bockstaele, 2003). However, p53 is always a tumor suppressor, while oncogenic cancer-related mutant p53 may be oncogenic (Oren 2019). It is known that mutation is widespread in cancer cells, but this is not the only reason for the oncogenic features. Currently, p53 is known to be a state-switching protein. Under different physiological conditions, wild-type p53 converts into a 'pseudo-mutant' state to block its canonical tumor-suppressive feature when accelerated cell proliferation is essential or advantageous (Trinidad et al. 2013). In some cancer cells, p53 shows oncogenic GOF mutations in its coding region, and it may stack p53 chronically in its pro-proliferative state (Oren 2019). p53 status is cell-type specific in cancer. For example, the caco-2 (colon adenocarcinoma) cell line does not have a functional p53, while the HeLa cell line (cervical carcinoma) has a WT copy (Smardová et al. 2005; Gartel et al. 2001).

1.1.5. Cervical Cancer and Dysregulation of Apoptosis and Cell-Cycle in HeLa Cells

Cervical cancer (CC) is one of the most commonly diagnosed cancer types in females behind lung, colorectal, and breast worldwide (Pimple and Mishra 2022). In 2008, nearly two-thirds of the new cervical cancer cases were fatal, according to the world health organization. However, the frequency of cervical cancer has decreased due to the high rate of HPV (human papillomavirus) vaccination and increased screening in women in developed countries. It is still the leading cause of women's cancer-related death in underdeveloped countries, with unmeasurable pain and suffering. Although HPV infection seems to be the most crucial cause of CC, smoking, immune suppression, high parity, and oral contraceptive usage are also widely associated with CC (Roura et al. 2016; Dugué et al. 2013). Half of the CC patients were lost in the five years after diagnosis. Thus, it is no exaggeration to state that investigating the molecular mechanism of CC is vital to creating better treatment strategies for CC patients (Lin et al. 2019). E6 and E7 are two fundamental HPV-infected cervical cancer-related oncoproteins (Pal and Kundu 2019). In HPV-infected cells such as HeLa, p53 function is abolished by E6-mediated degradation and transactivation inhibition (H. Zimmermann et al. 1999). Although p53 is expressed ectopically, it cannot perform tumor suppressor functions

(Ajay, Meena, and Bhat 2012; H. Zimmermann et al. 1999). In addition to dysregulation of p53, HPV-related oncogenes inactivate the tumor suppressor gene Rb and suppress the regular cell-cycle checkpoints, leading to abrogating cell division in cervical cancer cells such as HeLa (Goodwin and DiMaio 2000).

Moreover, estradiol activates the essential anti-apoptotic protein Bcl-2 (Q. Wang et al. 2004). Thus, Bcl-2 mediated inhibition of apoptosis cooperates with dysregulated p53 and Rb-mediated uncontrolled cell cycle leading to cancerous phenotype in cervical tissue (D. Chen, Carter, and Auborn 2004). Chemotherapeutic drugs can be used to treat abrogated cell-cycle regulation (Alimbetov et al. 2018). One of the most powerful and commonly used drugs is CP in cervical cancer treatment (Basu and Krishnamurthy 2010)

1.1.6. CP-Induced DNA Damage and the P53-Mediated Downstream Signaling

DNA double-strand breaks (DSB) or single-strand breaks (SSB) caused by chemotherapeutic agents are considered to switch lesions that initiate cell DNA damage response (Woods and Turchi 2013; Jekimovs et al. 2014). It is known that the anti-cancer activity of CP originated from its interaction with chromosomal DNA. However, chemotherapeutic agents like CP induce DNA damage and block cells' DNA damage response mechanism (Florea and Büsselberg 2011; Kiss, Xia, and Acklin 2021). If the cell cannot repair DNA damage and process it through the cell cycle, it is committed to dying eventually. Thus, the signaling pathways regulating apoptosis significantly affect deciding cellular responsiveness to CP. Multiple transporters carry out CP influx, including Na+, K+-ATPase, and SLC transporters (Basu and Krishnamurthy 2010). The primary target of CP is DNA. It is proposed that the intra-strand crosslink between two guanine residues is the critical lesion for CP toxicity. That DNA:: CP complexes block DNA replication and transcription because of the disturbed structure of DNA. The CP-induced DNA damage triggers several essential pathways in the cell (Sedletska, Giraud-Panis, and Malinge 2005).

Cell cycle checkpoints are activated to stop the cell cycle to prevent to inherit damaged DNA into daughter cells and to provide time to restore damaged DNA by DNA damage repair mechanisms or to eliminate genetically unstable cells that have severe

DNA damage by initiating cell death (Basu and Krishnamurthy 2010). The guardian of the genome ‘p53’ has a vital role in CP-induced DNA damage response. In healthy cells, p53 has a short half-life. It regulates the transcription of Mdm2 (E3 ubiquitin ligase), the regulator protein of p53 expression, via a negative feedback loop (Haimei Huang et al. 2004). When DNA damage occurs, ATM/ATR proteins are activated, increasing the stable p53 level in the cell by phosphorylating them. Eventually, the genes involved in DNA repair (e.g., GADD45), cell cycle progression (p21), and apoptosis are trans-activated by p53 (Efeyan and Serrano 2007). Therefore, depending on the DNA damage's severity, the cell decides to live or die. It is shown that overexpressed WT p53 in ovarian cancer cells results in CP sensitivity (Blagosklonny and El-Deiry 1998). Additionally, p21, ATR, and checkpoint kinase 2 (CHK2) have been related to p53-mediated apoptosis (Pabla et al. 2008). Cancer cells have no functional p53 and are more resistant to CP-mediated apoptosis (Basu and Krishnamurthy 2010).

Moreover, p53-mediated CP-triggered cell death is proposed to branch into several pathways. Downregulation of XIAP is the crucial event for p53-mediated apoptosis in response to CP (M. Fraser et al. 2003). On the other hand, PTEN is involved in p53-mediated CP-induced cell death independent from PI3K/AKT pathway (Basu and Krishnamurthy 2010). In particular, p53 exhibits the wild-type phenotype in HPV-infected cervical cancer cell line HeLa. It was reported that CP induces a dramatic increase in the nucleolar level of p53 in HeLa cells due to the escape from E6-mediated degradation. The highest level of p53 was observed 15h after CP treatment, and caspase-3 was activated in almost all of these cells (Wsierska-Gdek et al. 2002). Nonetheless, it has been suggested that several survival signals, including MAPK and AKT signaling, are activated caused by CP treatment and may thus be responsible for the high rate of CP resistance of HeLa cells (L. Zhang et al. 2015). Therefore, it can be suggested that CP treatment may induce the transcription of both apoptotic and survival regulatory pathway genes in HeLa cells.

1.2. Circular RNAs: Beyond Borders of Gene Regulation

Crick's central dogma of biology proposed that RNAs are intermediate messenger molecules that transmit genetic information from DNA to protein (Crick 1958).

Surprisingly, completing the human genome project has revealed that only %2 of the human genome encodes proteins (Comfort 2015). Therefore, the remaining part of the genome was considered 'junk' accumulating across the evolutionary process (Ferreira and Esteller 2018). In the past two decades, a strong correlation was highlighted between the size of these non-coding regions and the biological complexity of the organisms (Taft and Mattick 2003). Intriguingly, it was shown that genes containing large introns have lower transcriptional activity in cancer cells but higher transcriptional activity in neural cells (Ferreira and Esteller 2018; Taft, Pheasant, and Mattick 2007). This information demonstrated the regulatory potential of the non-coding genome coupled with tissue-specific gene expression patterns. The major part of the human genome is in transcriptionally active regions (Djebali et al. 2012). Thus, the particular DNA sequence can be converted into a protein-coded RNA transcript or a non-coding regulatory transcript with different molecular functions (Dhanasekaran, Kumari, and Kanduri 2013; Alexander et al. 2010).

Recent studies have demonstrated that along with DNA methylation and histone modification, non-coding RNAs (ncRNAs) are a type of epigenetic mechanism (Wei et al. 2017). Micro RNA (miRNA), small interfering RNA (siRNA), PIWI-interacting RNA (piRNA), long non-coding RNA (lncRNA), and circular RNA (circRNA) are branches of ncRNAs (Cavalcante et al. 2020). miRNAs, which are single-stranded ncRNA transcripts, originated from hairpin structures. They are involved in post-transcriptional gene silencing by targeting 3'UTR of mRNAs (Ying, Chang, and Lin 2008). Accordingly, siRNAs show the same mode of action and biogenesis pathway as miRNA, but the final siRNA is excised from stem-loop structures (Tomari and Zamore 2005). However, piRNAs are guardians of genome integrity to protect DNA by preventing transposon-induced insertional mutagenesis (Moyano and Stefani 2015). lncRNAs are ncRNA transcripts of 200 nucleotides in length that control transcription, mRNA stability, and translation (Statello et al. 2021). Firstly, piRNAs, siRNAs, miRNAs, lncRNAs, and circRNAs were thought to function independently. It is recently demonstrated that some of these regulatory pathways have interacted, and living organisms perfectly adapted to these multiple regulatory mechanisms (Ferreira and Esteller 2018). The complex regulatory networks built up by ncRNAs are still far from complete. Scientists keep learning as we move forward (Wei et al. 2017).

miRNAs have been a hot topic for the past 20 years. Approximately, about five thousand miRNAs have been identified so far in vertebrates, invertebrates, and plants (M. Li et al. 2009). Thousands of circRNA transcripts have recently been discovered across species from archaea to humans (Qu et al. 2015; Y. Zhang et al. 2013). The first circRNA was reported in the 1980s with an electronic microscope (Wu and Zhou 2019; Hsu et al. 1979). Then, scientists discovered that the DDC gene produces an RNA transcript by spicing exons in a non-canonical order. The abundance of this scrambled transcript is less than one-thousandth of canonical DCC. This phenomenon, called 'exon scrambling (Nigro et al. 1991), suggested the reporting of circRNAs as early as the 1990s. Subsequently, the mouse circular transcript SRY was shown not to be translated (Capel et al. 1993). Then, a human RNA transcript derived from the scrambled exon of MLL was reported (Caldas et al. 1998). However, the science community discredited these transcripts for a while, regarding them as background artifacts.

A genome-wide analysis of circRNAs was reported in 2012 (Salzman et al. 2012). CircRNAs with covalently linked 3' and 5' ends represent a novel class of ncRNAs, which are widespread and abundant (Salzman et al. 2012). Therefore, this study provided the foundation for a burgeoning new field. Recently, circRNA-specific RNA-seq approaches, advances in library preparation strategies, and circRNA-specific algorithms have identified thousands of circRNAs in eukaryotes (X. Zeng et al. 2017; Jiao et al. 2021). Some of these circRNAs were found to have a tissue-specific expression pattern (Yu and Kuo 2019). Protein-coding genes serve as a template for most circRNAs that consist of single or multiple exons (J. U. Guo et al. 2014). CircRNAs contain all the basic types of alternative splicing of linear RNAs. In terms of localization, circRNAs are mainly found in the cytoplasm due to the absence of poly-A tail and 5'cap (J. Zhang et al. 2019). However, exonic-intronic circRNAs (eicircRNAs) contain intron and exons that may originate from internal intron retention (A. T. He et al. 2021). Besides, failure in the debranching of intron lariats may lead to intronic circRNAs (ciRNAs) (Talhouarne and Gall 2018). ciRNAs and eicircRNAs can promote the transcription of their origin genes by regulating RNA Pol II (e.g., ci-ankrd52) or interacting with U1 snRNP (e.g., circEIF3J) (Z. Li et al. 2015).

Although back-splicing is less efficient than canonical splicing, circRNAs can accumulate in a cell-specific and temporarily regulated manner due to their high stability (Enuka et al. 2016; Bachmayr-Heyda et al. 2015). This stability results from the

covalently closed circular structure protecting circRNAs from exonuclease-mediated degradation. Due to their high abundance, stability, and unique expression pattern, circRNAs are potentially helpful for clinical diagnosis and prognosis. Majorly, linear transcripts are expressed more efficiently than circular transcripts (L. L. Chen and Yang 2015).

Bachmayr-Heyda reported that 78% of the circRNAs are higher expressed in normal compared to the tumor samples in CRC. Regardless of the abundance of the linear or circRNA alone in the tumor tissues compared to the normal tissues, qPCR analyses have revealed a reduced circRNA/mRNA ratio in all tumor tissues examined. Thus, there is reliable evidence that circRNAs are globally decreased in tumor tissues from CRC patients compared to matched normal tissues and are even more reduced in the CRC cell lines (Bachmayr-Heyda et al. 2015). The following four mechanisms could explain this trend; (1). the back splicing machinery is compromised in malignant tissues; (2). increased miRNA-mediated degradation due to deregulated miRNAs in tumor tissues; (3). circRNAs get passively diluted by cell proliferation or accumulate in non-proliferating cells (it explains neural cell accumulation and distinct roles of circRNAs), and (4). The elusive mechanisms could be the reason. *(*Bachmayr-Heyda et al. 2015*)*.

Three important assumptions must be fulfilled to understand the proliferation scenario completely. Firstly, linear and circRNAs are processed in a specific gene (and condition and cell type) ratio. It is plausible; however, only the competition between canonical splicing and back-splicing has been shown until now (L. L. Chen and Yang, 2015). Secondly, linear transcripts are accurately regulated by transcription and degradation in cells (T. I. Lee and Young 2013). Although linear transcripts also – just circular isoforms- are passively distributed into daughter cells, the required level of linear RNA is adjusted very quickly to the level before cell division, resulting in circRNA synthesis in a gene. This leads to daughter cells within the same linear/ circRNA ratio as their mother cells.

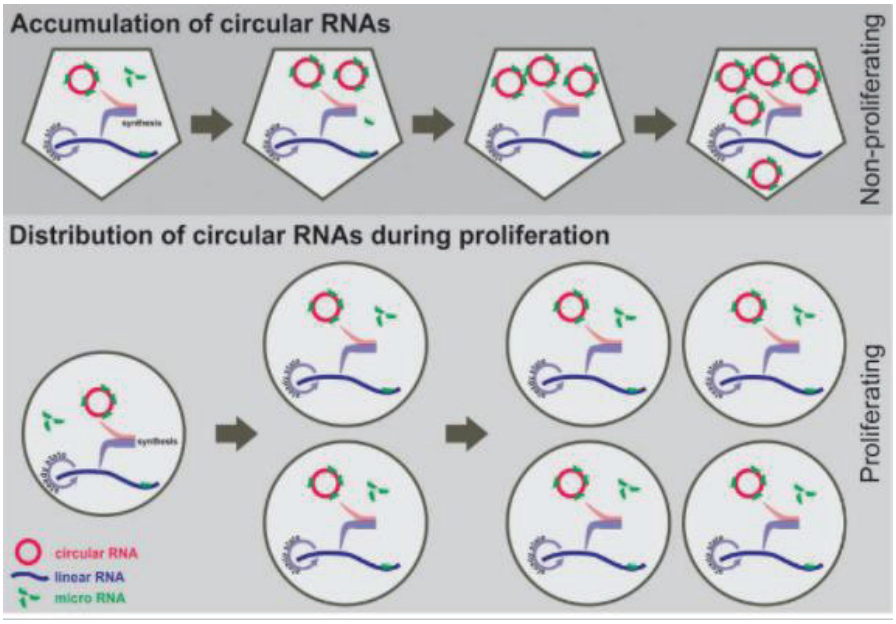

Figure 1.3. Schematic representation of circ- and linear RNAs in non-proliferating and proliferating cells (Bachmayr-Heyda et al. 2015).

Thirdly, circRNAs are more stable to exonuclease-mediated degradation than linear RNAs and are not regulated by a degradation mechanism as tight as linear RNAs. Bachmayr-Heyda et al. reported a 73.4% reduction of circRNAs in CRC samples compared to the normal colon mucosa. (12.9%) (Bachmayr-Heyda et al. 2015).

1.2.1. Biogenesis of Circular RNAs

CircRNAs are produced by back-splicing. Unlike canonical splicing, the downstream 5' splice donor site reversely attacks the upstream 3' splice acceptor site in a back-splicing reaction, leading to a covalently closed circRNA (Fig 1.4) (Jeck and Sharpless 2014; L. L. Chen and Yang 2015). The circRNAs back-splicing machinery depends on canonical splicing machinery but is accepted as an unusual type of alternative splicing (X.O. Zhang et al. 2014; Ashwal-Fluss et al. 2014). It is indicated that splicing inhibitor 'isoginkgetin' abrogates circRNA production in HeLa cells (Starke et al. 2015).

Additionally, mutagenesis analyses revealed that 99% of annotated circRNA-forming exons needed canonical 5' and 3' splice sites to carry out back-splicing using canonical spliceosomal machinery (Vo et al. 2019). No specific motifs are required for circularization rather than splice sites (L. L. Chen 2020).

Abundant circular RNAs generally originate from genes with more active promoter regions, and they tend to have long flanking introns related to back-splicing (Enuka et al. 2016). Additionally, alternative splicing is affected by DNA methylation on the gene body and epigenetic changes within histones (Shayevitch et al. 2018). Therefore, they may also have a direct impact on circRNA biogenesis. It is demonstrated that silencing DNA methyltransferase-encoded gene DNMT3B generates changes in circRNA expression independent of changes in the expression of parental linear genes (Sharma et al. 2021). However, these circRNAs may be differentially expressed, suggesting that the role of parental gene methylation in the biogenesis of circRNAs depends on the genetic composition. Moreover, the epigenetic state of the parental gene promoter can be affected by circRNAs, as shown for the oncogene FLI1 in breast cancer. The exonic circRNA FLI1 can induce the demethylation of CpG island in *cis* by recruiting TET1, which promotes DNA demethylations (N. Chen et al. 2018). Although the absence of poly(A)-tail and a 5' cap is a fundamental feature of circRNA, back-splicing is coupled with canonical pre-mRNA splicing and RNA polymerase II transcription (X.O. Zhang et al. 2014). Moreover, alternative back-splicing can generate different circRNAs from the same sequence (Gao et al. 2016). Two modes of action were proposed for back-splicing reaction coupled with transcription, the lariat-driven circularization model and the intron-pairing-driven circularization model (Kristensen et al. 2019; X.O. Zhang et al. 2014).

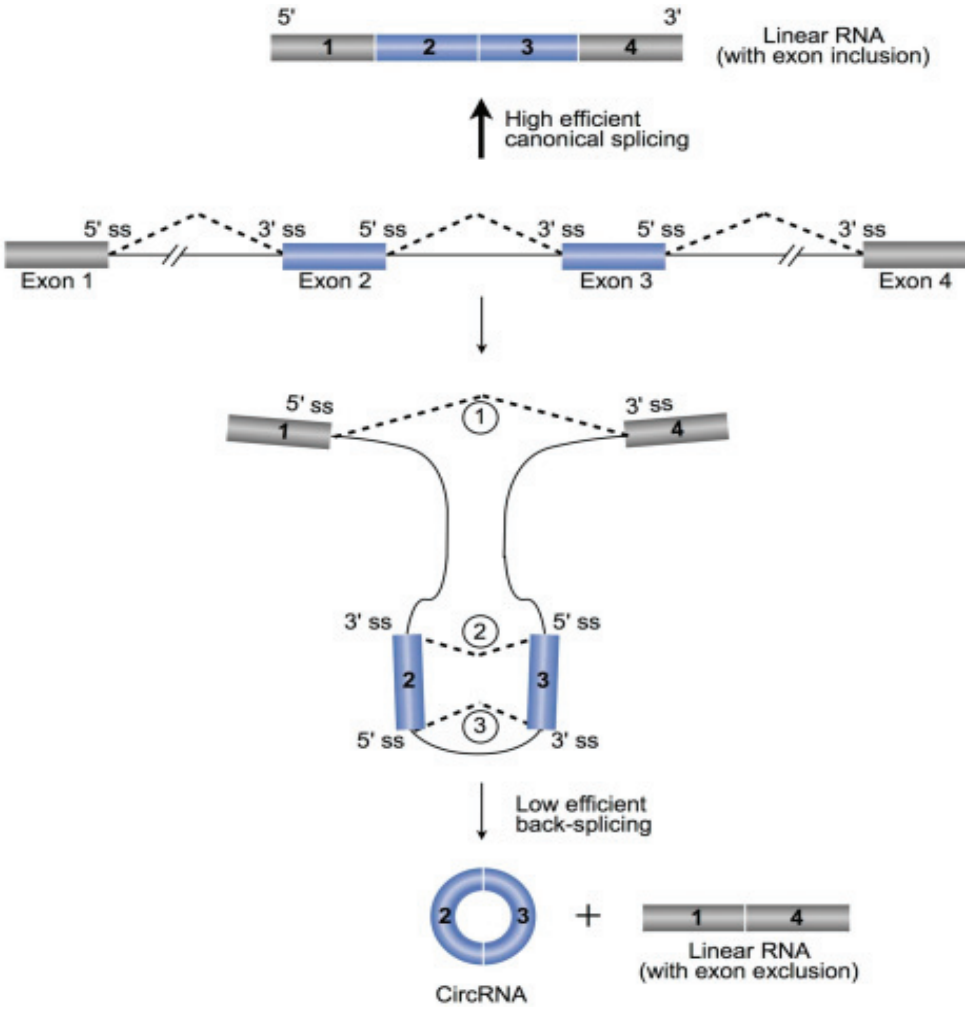

Figure 1.4. CircRNAs are derived from pre-mRNA via back-splicing (L. L. Chen and Yang 2015).

1.2.2. CircRNA Biogenesis is Coupled with the Transcription of Linear RNAs

Back-splicing is carried out both co- and post-transcriptionally. Nascent circRNAs associated with fly heads' chromatins were abundant, indicating that back-splicing may be coupling with RNA pol II transcriptions (Ashwal-Fluss et al. 2014; Y. Zhang et al. 2016). Additionally, it is demonstrated that genes producing nascent

circRNAs have a higher transcription elongation rate than non-circRNA-producing genes in humans (Y. Zhang et al. 2016). On the other hand, an appreciable portion of back-splicing reactions can occur post-transcriptionally (Wilusz 2017). This hypothesis was supported by the observation that thousands of nascent circRNAs were detected after the parental linear pre-mRNA transcription was completed (Y. Zhang et al. 2016). Two models have been proposed to show how back-splicing and canonical splicing are coupled at the same locus; (1) the lariat-driven and (2) intron-paired driven circularization modes. Broadly, the main difference between these two modes is the order of back-splicing or canonical splicing (Xiaohan Li et al. 2020).

1.2.2.1. Lariat-Driven Circularization Model (Exon-Skipping*)*

Exon skipping is the standard mode of alternative splicing reported to restore the exon content within a gene (Grau-Bové, Ruiz-Trillo, and Irimia 2018). Alternative exons are spliced out of the mature mRNA product and enclosed within the excised lariat during exon skipping (Barrett, Wang, and Salzman 2015). A long intron lariat with skipped exons is produced when the canonical splicing occurs before the back-splicing. The formation of exonic or exonic-intronic circular RNAs can originate from subsequent back-splicing of those lariats formed during exon skipping processes (Fig 1.5) (L. L. Chen and Yang 2015). However, the global correlation between exon skipping and circRNA production has not yet been supported by any biochemical evidence (Barrett, Wang, and Salzman 2015).

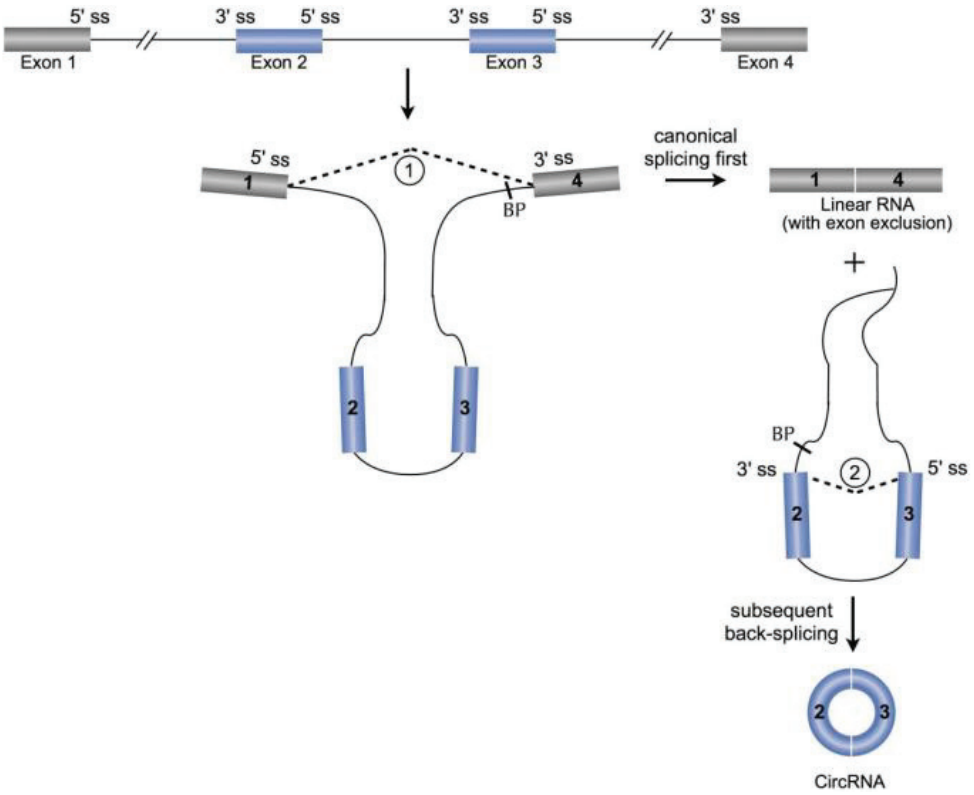

Figure 1.5. Lariat-driven circRNA biogenesis (L. L. Chen and Yang 2015).

1.2.2.2. Intron-Pairing Driven Circularization Model (Direct Back-splicing)

If the back-splicing occurs first, the circRNA and an exon-intron intermediate are generated directly. The intermediate can be potentially degraded or undergo splicing events to produce linear mRNA and skipped exons (Jeck and Sharpless 2014; Jeck et al. 2013a). The ligation between upstream 5'ss and downstream 3' ss is sterically unfavorable. To overcome this natural disadvantage, some *cis*- and *trans*-acting factors are required (X.O. Zhang et al. 2014; Jeck et al. 2013; Ivanov et al. 2015).

The inverted repeats in flanking intron sites bring donor and acceptor sites closer to facilitate back-splicing (Fig 1.6). Base pairing between inverted repeats, such as Alu elements located downstream and upstream introns, may lead to this looping (Jeck et al. 2013). In some cases, specific motifs on flanking introns are invaded by RNA-binding

proteins such as QKI (Conn et al. 2015). Surprisingly, it was proved that ADAR (ds-RNA specific adenosine deaminase) enzymes and DHX9 (ATP-dependent helicase A) repress the biogenesis of circRNAs that are associated with a base pairing of flanking inverted repeats (Aktaş et al. 2017)

It should be noted that regardless of the type of mechanism, back-splicing efficiency is low because of the sterically unfavorable ligation of an upstream 3' splice site with a downstream 5' splice site (Y. Zhang et al. 2016). Also, a global anti-correlation between circRNA formation frequency and mRNA levels supports the mutual competition between back-splicing and canonical splicing (Holdt, Kohlmaier, and Teupser 2018a). Predominantly, linear transcripts are expressed more efficiently than circular transcripts. However, circRNAs are predominant transcripts for many genes. Competition between canonical back-splicing and splicing presumably exists for the superiority of loci-producing circRNAs (Q. Zheng et al. 2016).

CircRNA splicing also has alternative modes validated by northern blotting. A given locus can produce multiple circRNAs by alternative back-splicing and the selection of splice sites within circRNAs (X.O. Zhang et al. 2016). Alternative back-splicing events can use different downstream 5' splice donors and upstream 3'splice acceptor sites. These alternative splice site selections can occur within multiple-exon circRNAs. All known types of alternative splicing, cassette exons, alternative 5' and 3' splice sites, and intron retention, were observed in multiple-exon circRNAs (Gao et al. 2016; Jeck et al. 2013a; Memczak et al. 2013; Salzman et al. 2013; X.O. Zhang et al. 2016; 2014)

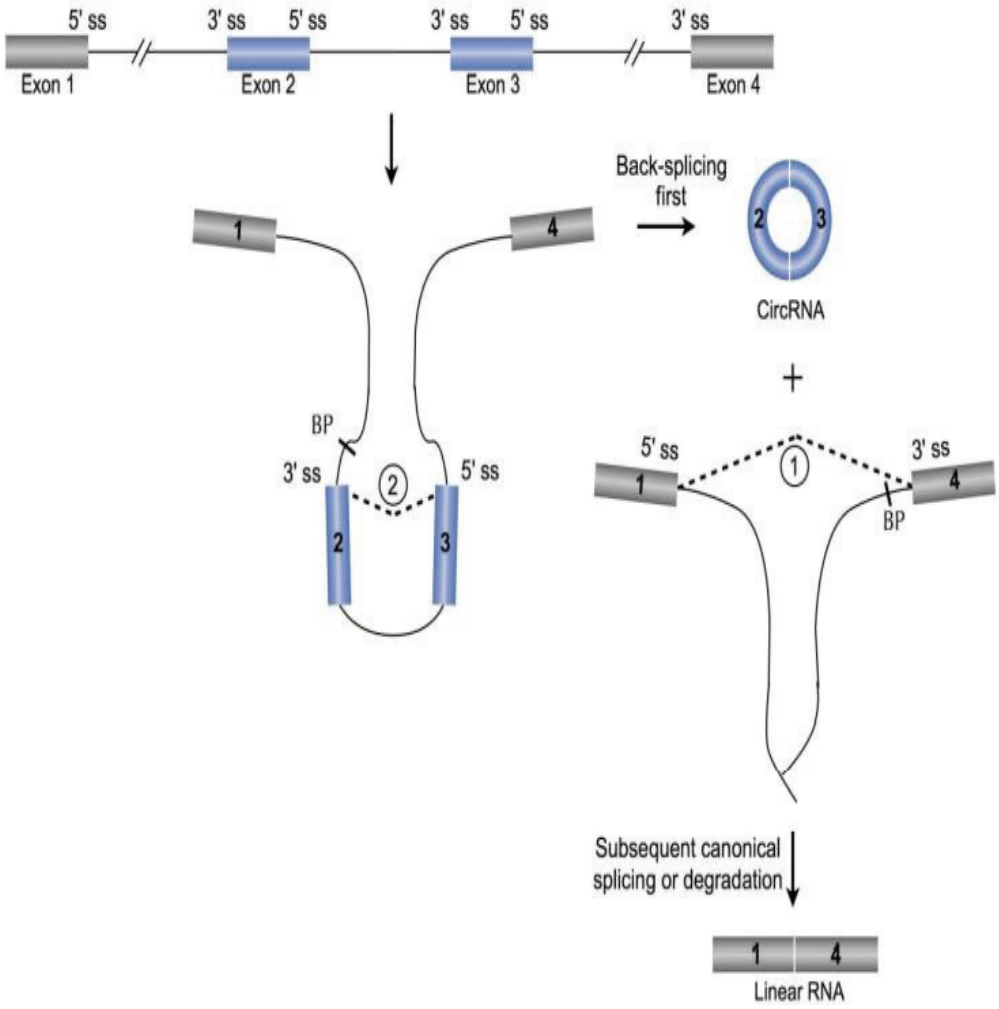

Figure 1.6. Intron-pairing driven biogenesis of circRNAs (L. L. Chen and Yang 2015).

1.2.3. CircRNA Decay

Degradation of mRNAs usually begins with poly-(A) tail shortening by a deadenylase (C.Y.A. Chen and Shyu 2011). Then, either the exoribonuclease XRN1 mediated 5'to 3' decay or exosome-mediated 3' to 5' mediated decay occurs (Jinek, Coyle, and Doudna 2011; Conti et al. 2009). Some mRNAs are cleaved by endonucleases and degraded by exonuclease-mediated decay under certain circumstances (Schoenberg 2011). Besides, mRNAs with premature stop codons are degraded by an RNA

surveillance mechanism called non-sense mediated decay (F. He and Jacobson 2015). The dynamic of biogenesis and turnover of circRNAs in eukaryotic cells is vital and has to be strictly controlled to exert particular circRNA functions. Although the mechanisms of biogenesis of circRNAs are explained roughly, how circRNAs are degraded remained unclear until very recently.

As known, circRNAs do not have 5'cap and 3' poly-A tails. Thus, it should be degraded by the endoribonucleolytic attack. Some endonucleases initiate the decay of specific circRNAs in a primary sequence-dependent manner. For example, circRNA cdr1as is cleaved with the assistance of miR-671 by AGO2. Cdr1as is one of the most characterized circRNA with sponging activity for miR-671. Recruitment of miR-671 to circCdr1as causes endonucleolytic cleavage by AGO2 and circRNA degradation (J. Xu et al. 2021) (Figure 1.7). However, another miRNA involved in AGO2-mediated circRNA decay is still elusive.

RNase P/MRP cleaves m^6A (N6-Methyladenosine) containing circRNAs in a sequence-dependent manner. In this mechanism, the m6A-containing transcript recruits the reader protein YTHDF2 and the adaptor protein HRSP12 (Park et al. 2019). A GGUUC motif is necessary to direct the binding of HRSP12. Then, HRSP12 serves as a bridge to assemble the YTHDF2 and RNase P/MRP complex to start the circRNA decay (Ren et al. 2022) (Figure 1.7). Considering the fact that the sequences of circRNAs and parental linear mRNAs are the same. Thus, it is still unknown how primary sequence-dependent decay mechanisms distinguish circular isoforms from their parental linear ones (Guo, Wei, and Peng, 2020). The distinct 3D structure of circRNAs adds a layer of complexity to their degradation mechanisms by enabling them to interact with various proteins.

In many circRNAs, 16-26 base pair imperfect RNA duplexes are formed, interacting with dsRNA-activated PKR protein. A ubiquitously expressed cytoplasmic endoribonuclease RNase L is activated and degrades circRNAs via unknown mechanisms upon viral infection and subsequently activates PKR for the innate immune response (C.-X. Liu et al. 2019) (Figure 1.7)

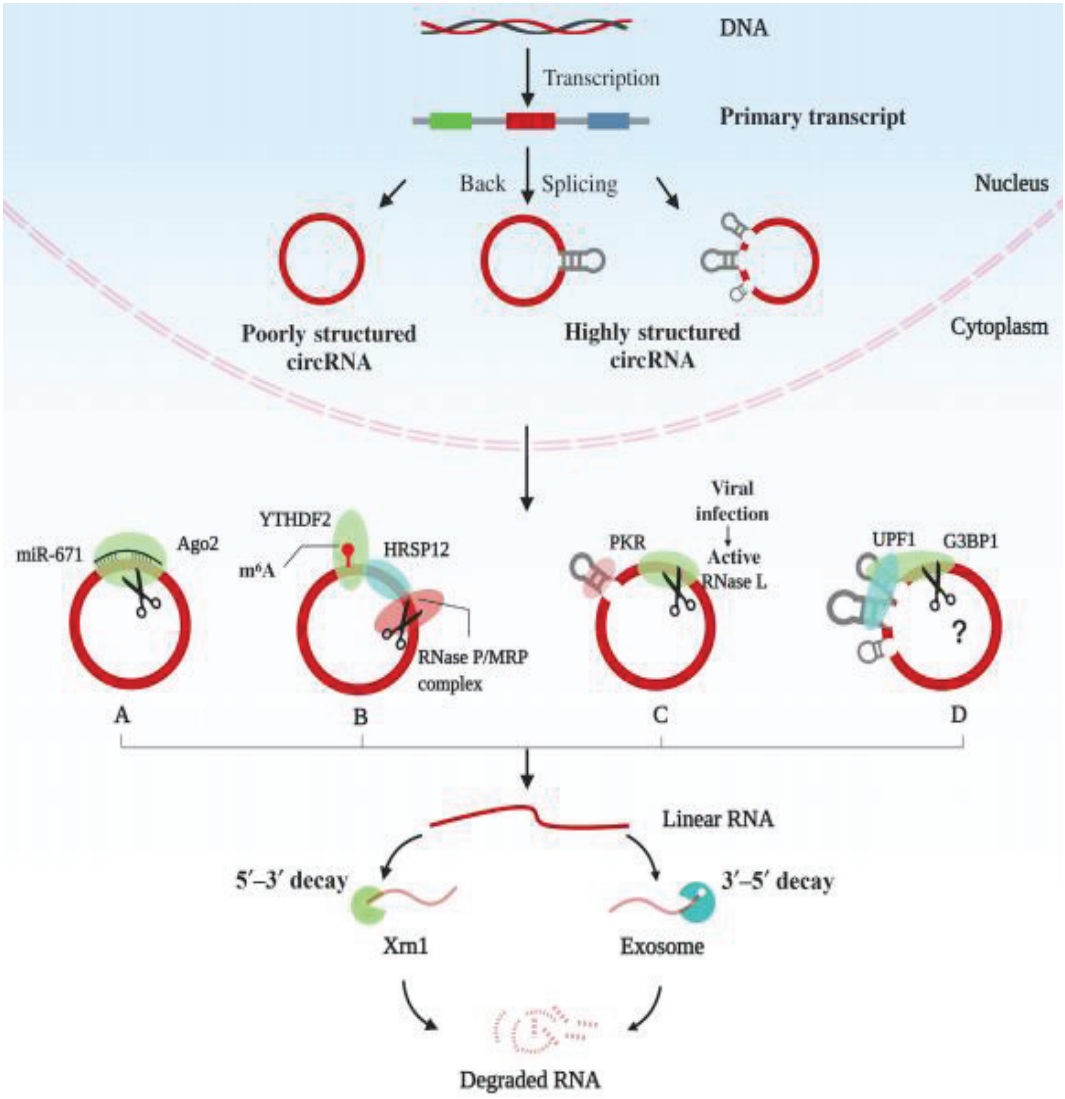

Figure 1.7. Different mechanisms in circRNA decay (Guo, Wei, and Peng, 2020).

Fisher et al. recently reported the degradation of highly structured circRNAs by UPF1 and G3BP1 under normal conditions (Fischer et al. 2020). The overall structures of circRNAs are recognized and unwinded by UPF1 and G3BP1. One-third of human circRNAs are anticipated to form a highly overall structure, and G3BP1 and UPF1 regulate their degradation. For this type of RNA degradation, RNA-binding and S149 phosphorylation activities of G3BP1 and RNA-binding and helicase activities of UPF1 are needed. It is described as structure-mediated RNA decay (SRD). Biochemical experiments suggest that G3BP1 binds highly structured circRNA, preferentially unlike UPF1. Besides, further silencing of UPF1 appears to have no additional impact on the

abundance of circRNAs in G3BP1 knockout cells. Thus, it is reported that G3BP1 is a key factor for the circRNA-SRD mechanism.

Unlike previous mechanisms, the overall structure rather than the primary sequence is the driving force of this mechanism. Nonetheless, loss of function studies has revealed that other structure-mediated decays, namely Staufen-mediated decay and nonsense-mediated decay, have minimal impact on the expression of highly structured circRNAs (Fischer et al. 2020).

1.2.4. Functions of CircRNAs

Increasing evidence suggests that circRNAs control gene expression at the transcriptional, post-transcriptional, and translational levels. Recent studies have proposed that circRNAs with various biological functions can be classified into four main concepts (Shang et al. 2019).

1.2.4.1. CircRNA Regulates the Transcription of Parental Genes

As explained in the circRNA biogenesis part, most circRNAs are produced co-transcriptionally, and canonical splice sites are necessary for circularization. Therefore, circRNA production can compete with linear splicing. It should be noted that an order of magnitude can reduce the abundance of particular circRNA because of this strong competition. It is demonstrated that flanking intron sequences are the most crucial factor that decides the biogenesis efficiency of given loci. In light of these findings, linear splicing is regulated by circRNA biogenesis (Ashwal-fluss et al. 2014).

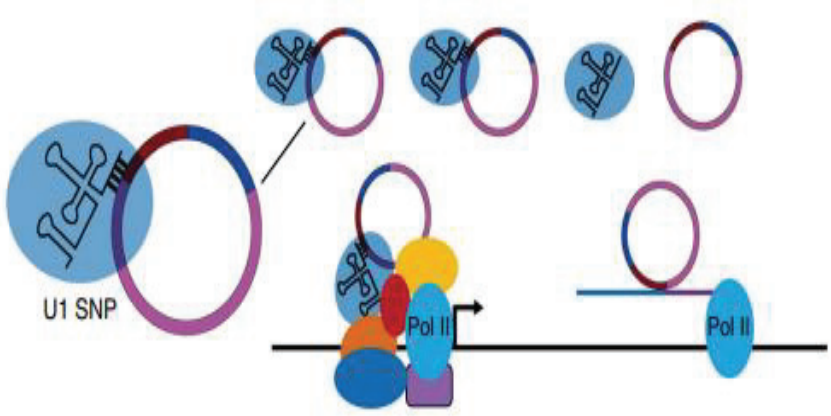

Figure 1.8. eiciRNA mediated transcription regulation of cognate mRNA (Z. Li et al. 2015).

It is reported that RNA polymerase II is associated with a distinct class of circRNA in human cells (Y. Zhang et al. 2013). circRNAs, made up of exons, and retained introns named exon-intron circRNAs (eicircRNAs), are localized predominantly in the nucleus. U1 snRNPs interact with eicircRNAs by RNA: RNA interactions, and this complex interacts with RNA Pol II and promotes expression of the linear counterpart of certain eicircRNAs (e.g., eicircRNA PAIP2 and EIF3J) (Figure 1.8). As long as the eicircRNA is produced at the transcription site, regardless of co- or –post-transcriptional production, it is said to have a *cis* function (Z. Li et al. 2015).

1.2.4.2. CircRNAs can Regulate miRNA Activity and Abundance

miRNAs are evolutionary conserved, small ncRNAs in ~22 nucleotide length, predicted to modulate mRNAs (R. C. Lee, Feinbaum, and Ambros 1993; Reinhart et al. 2000). In humans, more than 2000 miRNAs have been identified (A. Li et al. 2020). Firstly, miRNA coding genes are transcribed into pre-miRNA by RNA Pol II, followed by processing with DiGeorge Syndrome Critical Region 8 (DGCR8) and an endonuclease III enzyme, Drosha, to produce pre- miRNA (Denli et al. 2004). Pre-miRNAs are translocated into the cytoplasm and cleaved by Dicer to generate mature

miRNA (Yi et al. 2003). Usually, the translation and stability of target mRNAs are regulated by miRNAs (Bartel 2009). The level of complementarity between miRNA and target mRNA determines the action of miRNA on target mRNA (Lam et al. 2015).

miRNAs are indicated to be involved in many physiological processes, including apoptosis, proliferation, and migration (Esquela-Kerscher and Slack 2006; Bruce et al. 2015). Therefore, the regulatory mechanisms of miRNA-mediated gene regulation were a dominant area of RNA research between the early 2000s to 2015. Unsurprisingly, there is an enormous interest in understanding the regulatory mechanisms of miRNA actions. Thus, the competing endogenous RNA hypothesis has emerged. Three types of RNA, mRNA, transcribed pseudogenes, and lncRNAs, are shown on the front line of competing endogenous RNA research. Circular RNAs, following lncRNA, are a new hotspot among the competing endogenous RNA family (Panda 2018) (Figure 1.9).

Some circRNAs have multiple miRNA binding sites (Sang, Meng, Liu, et al. 2018; Sang, Meng, Sang, et al. 2018; P. Li et al. 2018). Thus, the expressions of miRNA-related target genes are upregulated upon the sponging of miRNAs by circRNAs. For example, circRNA cdr1as has more than 60 miR-7 binding sites and abrogates its function to promote miR-7 target genes (Shang et al. 2019). Other examples include circHIPK3 sponging miR-7, miR-558, miR-4288, and miR-654 and circITCH acting as a sponge for miR-17 and miR-224, resulting in p21 and PTEN upregulation in bladder cancer and glioma (Shang et al. 2019).

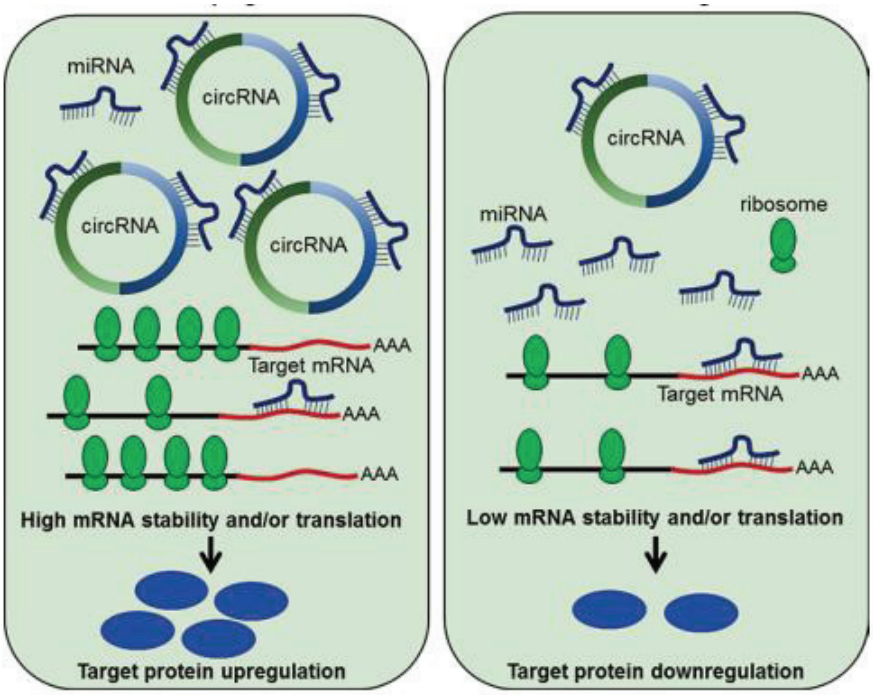

Figure 1.9. Schematic representation of circRNA mediated gene regulation by miRNA sponging (Panda 2018).

1.2.4.3. CircRNAs Interact with Proteins

CircRNAs can bind to regulatory RNA binding proteins (RBPs) by acting as protein sponges, scaffolds, decoys, or recruiters. RBPs are involved in the metabolic process of RNAs by modulating them post-transcriptionally and even forming ribonucleoprotein complexes. The RBP-circRNA interactions are sequence-dependent and affected by the tertiary structure of circRNAs (A. Huang et al. 2020). Therefore, unlike traditional mRNA-protein exchanges, a tertiary structure-dependent binding mode may be associated with specific circumstances. CircRNA-protein binding is a double-edged sword and may have bidirectional effects. It is reported that circRNAs-protein interaction influences proteins' expression and functions and the biogenesis and degradation of circRNAs (X. Huang et al. 2020). For example, circPABPN1 and parental mRNA PABPN1 compete for the HuR protein involved in translational machinery in promoting protein expression. Thus, circPABPN1 represses the PABPN1 protein

expression (Abdelmohsen et al. 2017). Furthermore, PES1 (60S ribosomal RNA assembly factor) and the pre-rRNA processing are impaired by circANRIL(Holdt et al. 2016). Thus p53 is activated in human vascular smooth muscle cells. CircRNA-protein interactions have four functions: protein sponges, protein decoys, protein scaffolds, and protein recruitment (X. Huang et al. 2020). Most circRNAs have no protein binding sites. However, many of them can act as protein sponges. For example, the QKI protein regulates circQKI biogenesis by flanking binding introns of circQKI forming exons during the EMT process (Conn et al. 2015). Besides, wound repair is mediated by circAMOT, which binds to AKT1 and PDK1 (X. Xia et al. 2019; Conn et al. 2015). The protein decoy function of circRNAs exerts as trapping target protein inappropriate cellular sites followed by abolishing its function (Du et al. 2017). For example, c-myc interacts with circAMOT and is trapped in the nucleus. Therefore, downstream target proteins of c-myc are upregulated, leading to increased cell proliferation, reduced apoptosis, and highly tumorogenic phenotype. In the circPABPN1 and HuR protein case explained above, circPABPN1 can act effectively as a protein decoy for HuR (Abdelmohsen et al. 2017). CircDHX34 and circPOLR2A bind NF90 and NF110 before viral infection in normal cells (Xiang Li et al. 2017).

In conclusion, various circRNAs serve as protein decoys across multiple cell types under different circumstances. The only regular component is that RNAs can bind proteins with high affinity and specificity, proposing that most circRNAs may assume an adversarial part regarding the typical physiological impacts of their target proteins. These RNAs may involve alternative self-regulation under stressful conditions (X. Huang et al. 2020). CircRNAs can function as a scaffold to promote interaction within protein complexes. For example, circFOXO3 and circAMOT1 serve as protein scaffolds to enhance the co-localization of enzymes and their substrates (Ou et al. 2020; Du et al. 2016; Y. Zeng et al. 2017). For example, P53 and MDM2 interactions are facilitated by circFOXO3. This interaction induces mdm2-dependent degradation of p53 (Du et al. 2016).

CircRNAs can also recruit proteins into particular cellular locations. CircFECR1 recruits TET1 protein to its host gene FLI1 promoter site to enhance the demethylation of the CpG island to promote active transcription (N. Chen et al. 2018). Moreover, circAMOT1 recruits STAT3 protein from the cytoplasm to the nucleus, leading to binding to the Dnmt3a promoter (Z.-G. Yang et al. 2017)

1.2.4.4. Translation of CircRNAs

Researchers initially thought that eukaryotic ribosomes could not be loaded onto circRNAs because circRNAs do not possess a 5' cap and 3' tail (Sinha et al. 2022). Surprisingly, it has been demonstrated that the internal ribosome entry site (IRES) specific sequence promotes translation in a cap-independent manner by binding the ribosome itself in prokaryotes (Colussi et al. 2015). IRES also allow synthetic circRNAs to be translated in vitro and cells (Pamudurti et al. 2017).

Recent reports have indicated that a subset of endogenous circRNAs might be translated into detectible peptides and short sequences (Prats et al. 2020). Interestingly, the stop codon available upstream of the start codon in the linear mRNA can be converted into in-frame termination codons upon circularization (Legnini et al. 2017) (Figure 1.10). Various direct and indirect pieces of evidence are used to interrogate the translational potential of circRNAs, such as the presence of an IRES sequence, m^6A modification sites, translation initiation sites, ORF length, sequence composition, ribosomal and polysome binding evidence, and, proteomics evidence by mass spectrometry(Yang et al. 2017; Fan, Yang, and Wang, 2018; W. Huang et al. 2020).

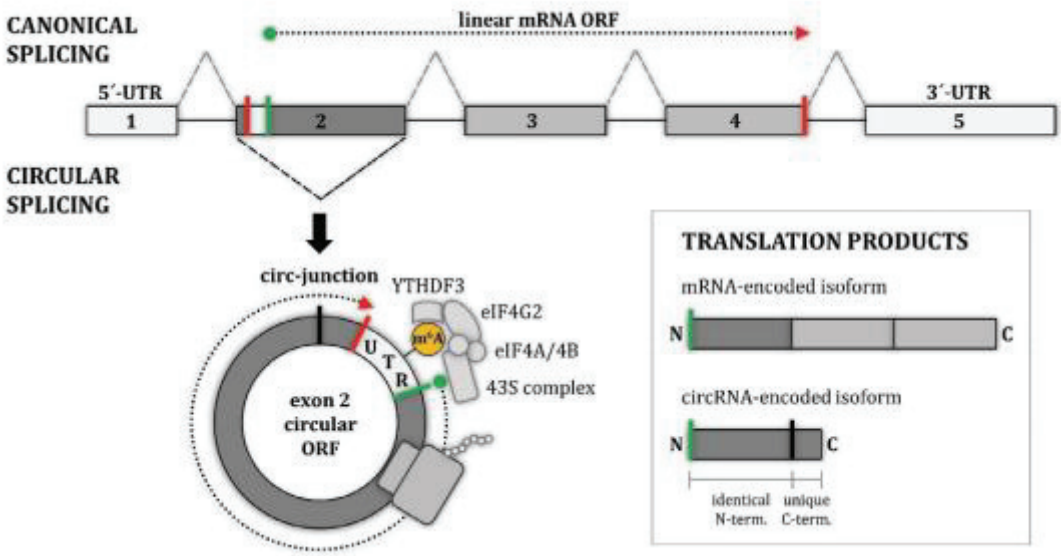

Figure 1.10. Schematic representation of circRNA translation and putative protein product (T. Schneider and Bindereif 2017).

The translation of circRNAs has to be cap-independent due to the lack of free ends (T. Schneider and Bindereif 2017). Cap-independent translation initiation must be driven by IRES RNA transcript with a unique secondary structure, which is common in viruses (Bakhshesh et al. 2008). In several cases like apoptosis, endogenous mRNAs can also use IRES to drive translation (Fitzgerald and Semler 2009). The systematic screen of IRES elements in the human genome was recently conducted. Therefore, this information can predict the translation potential of circRNAs (Fan, Yang, and Wang, 2018).

m6A is well known and the most common RNA modification available in various ncRNA and coding RNAs in the human genome (Huilin Huang, Weng, and Chen 2020). circRNAs undergo extensive m6A modifications to recruit the translation initiation complex by specifically recruiting reader protein YTHDF3 that interacts with translation initiation factor eIF4G2 (Y. Yang, Fan, Mao, Song, Wu, Zhang, Jin, et al. 2017). Therefore, the published m6A data from the REPIC database was used to map to circRNA sequences (S. Liu et al. 2020; W. Huang et al. 2020). The experimentally validated m6A sites of circRNAs are also a critical predictor for translatable circRNAs (Y. Yang, Fan, Mao, Song, Wu, Zhang, and Jin 2017). GTI-seq was used to map translation initiation site codons globally at nearly single-nucleotide resolution (S. Lee et al. 2012). Human transcriptome-wide GTI-seq indicated an obvious set of several thousand translation initiation codons as indirect evidence supporting the circRNA translation (Sinha et al. 2022).

Furthermore, long ORFs are uncommon in ncRNAs (Ruiz-Orera et al. 2014). Thus, potential ORF length should be greater than 20 aa for circRNA-encoded peptides. Notably, many small peptides were reported to be coded by ncRNAs; therefore, the length of ORF is a weak predictor (W. Huang et al. 2020). Moreover, the sequence composition of circRNA ORF is crucial to predict whether the protein outcome is functional (Hormoz 2013). It is known that the aa sequences of all-natural, stable, and functional proteins only represent a small fraction of possible sequences. Thus, the abnormal sequence proteins are mostly degraded by cells rapidly (Goldberg 2003). The sequence similarity of the natural proteins allows for predicting likely functional circRNA proteins in a random string of potential circRNA encoded amino acid pools using a machine-learning approach (W. Huang et al. 2020).

Table 1.1. CircRNAs encode novel proteins.

circRNAs	Biological functions	Types of cell/tissue	Cytoplasm/nucleus
circ-ZNF609	Regulates myoblast proliferation	Myoblast	Cytoplasm
circAβ-a	Unknown	Human Brain	-
circ-FBXW7	Tumour inhibitor	Cancer cell	Cytoplasm
circPINTexon2	Tumour inhibitor	Cancer cell	Cytoplasm
circSHPRH	Tumour inhibitor	Cancer cell	Cytoplasm
circMbl3	Translation of circRNAs	Cancer cell	Cytoplasm
circ-AKT	Tumour inhibitor	Cancer cell	Cytoplasm
circCFLAR	Unknown	Myoblast	Cytoplasm
circSLC8A1	Unknown	Myoblast	Cytoplasm
circMYBPC3	Unknown	Myoblast	Cytoplasm
circRYR2	Unknown	Myoblast	Cytoplasm

Ribosome footprinting data were published to strongly predict the potentially translatable circRNAs (Pamudurti et al. 2017). As known, the mRNAs are translated by ribosomes formed polysomes. Thus, an association of circRNA with polysomes can serve as a powerful predictor for circRNA translation. The polysome profiling approach is helpful for the comprehensive identification of peptide-coding circRNAs (Y. Ye, Wang, and Yang 2021)

Typically, mass spectrometry is used to identify and characterize proteins (Han, Aslanian, and Yates 2008). Only 50% of MS spectra can be assigned to known peptides encoded by mRNAs in the human transcriptome (W. Huang et al. 2020). This result proposes a hidden proteome, some of which may be encoded by circRNAs. MS evidence is a strong predictor for circRNA translation. However, HeLa cells' ten most abundant circRNAs are not associated with polysomes (T. Schneider et al. 2016). Arguing against the extensive translation potential of circ RNAs. Regardless, this does not exclude the possibility of natural cases of circRNA translation, such as growth conditions, or restricted to a small subset of specialized circRNAs (W. Huang et al. 2020).

Micro proteins encoded by circRNAs are generally comprised of 146-344 aa. circRNA-derived proteins are identified and characterized in metabolically active cells like myoblast and cancer using genomewide approaches. Therefore, it is suggested that

these cells promote the production of circRNA-encoded proteins to meet the additional requirements of these cells. Up to date, 11 protein-coding circRNAs have been reported (Table 1.1) (F. Ye et al. 2019; Legnini et al. 2017; Mo et al. 2020; M. Zhang, Zhao, et al. 2018; M. Zhang, Huang, et al. 2018; Pamudurti et al. 2017; van Heesch et al. 2019)

1.2.5. CircRNAs Modulate Cell Fate

Recently, the number of transcriptome-wide circRNA studies has increased owing to advances in the bioinformatics pipelines used to identify circRNAs. In 2015, has_circ_000595 was shown to regulate apoptosis in aortic-smooth muscle cells (C. Zheng et al. 2015). Chen and his group have demonstrated that the circRNA circTCF25 decreases the expression of miR-103a-3p / miR-107 by increasing CDK6 expression in bladder cancer cells in vivo and in vitro. The overexpression of circTCF25 significantly increased cell proliferation and migration. Further, it was reported that circRNA Cdr1as spontaneously pulled miR-7 and promoted heart infarction by increasing the stability of the target gene (Geng et al. 2016). It was reported that circFOXO3 increased the amount of FOXO3 protein by binding to MDM2 by preventing ubiquitination. FOXO3 causes an increase in cell apoptosis through the high expression of the target protein PUMA (Du, Yang, et al. 2017). In the same year, Deng and his group used the circRNA microarray approach to investigate the physiological roles of circRNAs in hypoxia-dependent human umbilical vein endothelial cells (HUVECs). They confirmed the high expression difference by quantitative PCR, which repressed cell proliferation and migration and suppressed apoptosis. (Dang, Liu, and Li 2017). Hsa_circ_0020397 has been shown to regulate cell viability, apoptosis, and invasion in colorectal cancer by increasing the expression of TERT and PD-L1 (H. Yang et al. 2020) circFUT10 reducing proliferation in myoblast cells and facilitated differentiation by sponging miR-133a. In this process, it was observed that circFUT10 Myo D, G and C proteins increased their expression at the mRNA and the protein level, causing cell cycle arrest in the G_O/G_1 phase (Li et al.2018). It was then reported that hsa_circ_0000799, the circular isoform of the BPTF gene, delayed the anti-oncogenic effect of miR-31-5p and increased the expression of the target gene RAB27A, and supported the development of bladder cancer (Bi et al. 2018). It was

demonstrated that hsa_circ_0036627 acts as a ceRNA (competing RNA) by targeting miR-338 to regulate MACC1 and stimulate invasive growth via the MACC / MET / ERK or AKT pathway (Li et al. 2018). Besides, silencing of has_circ_0005397 was shown to suppress pancreatic cancer cell proliferation, invasion, and migration, while hsa_circ_0102034 induced cancer progression by initiating NR2F6 expression. It was reported that the scarce circRNA hsa_circ_0001649 regulates proliferation, migration, and invasion in cholangiocarcinoma cells (Xu et al. 2018). In 2020, functional circRNAs in proliferation were screened by Li et al. using the CRISPR–Cas13 system (S. Li et al. 2020).

According to another microarray-based transcriptomic study, over-expressed circRNAs in breast cancer cells were reported. It has been shown that overexpression of hsa_circ_000911 reduces cell proliferation, migration, and invasion and supports apoptosis. The same study reported that hsa_circ_000911 sponged miR-449a with the precipitation of biotin-labeled circRNA, and the target protein of miR-449, Notch1, was significantly increased as a result of overexpression of hsa_circ_000911. It has been reported that circ_HIPK3, whose expression was decreased in death-triggered HeLa cells after CP administration, supports growth and metastasis by sponge miR-7 in colorectal cancer (Yaylak, Erdogan, and Akgul 2019; Zeng et al. 2018).

circSMAD2 differentially expressed in hepatocellular carcinoma (HCC) and neighboring non-tumor tissues and modulates proliferation, apoptosis, migration, and invasion, circSMAD2 by sponging miR-629 followed by suppression of migration, invasion, and EMT (Zhang et al. 2018). In prostate cancer cells, overexpression of hsa_circ_0102004 was shown to have a positive effect on cell proliferation has been proven (Si-Tu et al. 2019). As stated above, circRNAs are essential in cell fate due to their high stability. It has been reported that hsa_circ_0007534 can predict adverse prognosis in pancreatic ductal adenocarcinoma and regulates cell proliferation, apoptosis, and invasion by sponge miR-625 and miR-892b (Hao et al. 2019). circ_KIF4A has been shown to help the progression of ovarian cancer by sponging the miR-127 (Sheng et al. 2020). However, it has been reported that circRNA GLIS2 supports colorectal cancer cell migration by activating the NF-KB pathway (Chen et al.2020).

The transcriptome-wide analysis of circRNAs differentially expressed in apoptotic HeLa cells was reported in 2019 by our group (Yaylak, Erdogan, and Akgul 2019). Other groups reported some of these circular RNAs as regulatory molecules or

biomarkers, such as circBNC2, circLATS2, and circKDM4C, in various cancer types. However, most circRNA candidates have not been characterized yet. Undoubtedly, all uncharacterized differentially expressed circRNA candidates have a great potential to modulate apoptosis, proliferation, and cell cycle by regulating miRNAs, interacting proteins, or encoding novel proteins.

In early 2021, Li and his colleagues published a spectacular reporting that a group of circRNA candidates is essential for cell growth, mainly in a cell type-dependent manner (Li et al., 2021). gRNA libraries were constructed for 762 phenotypically important circRNAs. These gRNAs are BSJ-specific and not affected by linear mRNA. The Rfxcas13d system was chosen as the most efficient cas system to knock down circRNAs. They clearly show that only <22 nt lengths of gRNAs spanning BSJ effectively knockdown circRNA without disrupting linear mRNA level. This practical tool was used to identify circRNAs that act in a cell-type specific manner in cell proliferation by using Cas13 mediated circRNA screen (CDC Screen) pipeline that adapts MAGeCK (Li et al., 2014) and additional filtering steps (Li et al., 2021). In this design, each cell stably expresses a specific gRNA that, upon induction of Cas13, also integrated into the genome, can induce knockdown of the target transcript. Thus, each cell is barcoded by a unique gRNA sequence. The effect of the knockdown on cellular viability could then be judged by the depletion or enrichment of the specific gRNA barcodes in the cellular population (Xu et al., 2020).

Thousands of circRNAs were identified by RNA-seq approaches; however, some circRNAs may be by-products of pre-mRNA splicing without any function (C. Xu and Zhang 2021). To date, a small fraction of identified circRNAs has been described as functional circRNAs, and numerous are reportedly involved in chemotherapeutic drug resistance, proliferation, and apoptosis (J. Liu et al. 2020). Functional circRNAs have the potential to provide insight into gene regulation, disease biomarkers, and therapeutic targets, making the study of circRNAs an important and promising area of research (Y. Huang et al. 2022). The first transcriptomics analysis revealed CP-dysregulated circRNAs identified by CircExplorer (version one) were reported by our group (Yaylak, Erdogan, and Akgul 2019). Nevertheless, experimental validations to determine the cellular expression and function of circRNAs are required.

This study used CP to trigger apoptosis and repress proliferation in HeLa cells. Four novel circRNA candidates (circCLASP1, circBIRC6, circGALNT2, circBNC2)

were chosen for molecular characterization to investigate the putative function of each candidate in proliferation, apoptosis, and CP sensitivity in HeLa cells. Transcriptomics analysis was performed to identify which biological pathways are affected in response to circCLASP1 knockdown to shed light on circCLASP1-mediated regulation of proliferation and CP sensitivity.

CHAPTER 2

MATERIALS AND METHODS

2.1. Bioinformatic Analysis

A previously published study was used to identify candidate circRNAs (Yaylak, Erdogan, and Akgul 2019). Total RNAs were isolated from CP-treated Hela cells as previously described as three biological replicates. After quality control, RNAse R treatment and RNA depletion were performed to enrich for circRNAs prior to library preparation. circRNA-seq was performed by Novogene (Hong Kong), and circRNAs were identified using circExplorer (Zhang et al. 2014). According to the methodology, Total RNAs were isolated as three biological replicates. Double-stranded DNA synthesis followed by adaptor ligation and size selection was performed for PCR, library quality control, and sequencing. Due to the re-arranged exon ordering, specific algorithms are required to annotate back-splicing reads. RNA-seq reads are multiply aligned to the human reference genome using the Top-hat algorithm, and then unmapped reads were uniquely mapped with the Top-hat fusion algorithm. The Deseq2 algorithm was used to identify differentially expressed (DE) circRNAs. The DE circRNAs, which show >-1.5 and <1.5 $\log_2$ fold change (log2FC), were chosen for further steps. The read count of particular circRNA should be >5 in both CP- and DMSO-treated groups. It has a higher probability that abundant circRNAs will possibly be functional. Lastly, Co-analysis of circ-Seq data (TUBİTAK project no:215Z081) and mRNA-Seq data were performed. Circ-seq and mRNA-Seq were performed under apoptotic conditions after 16h CP treatment at different times. Log2FC >1 and log2FC <1 and p<0,05 were defined as a threshold for mRNAs, and p<0,05 was defined as selection criteria for circ-Seq (Figure 2.1).

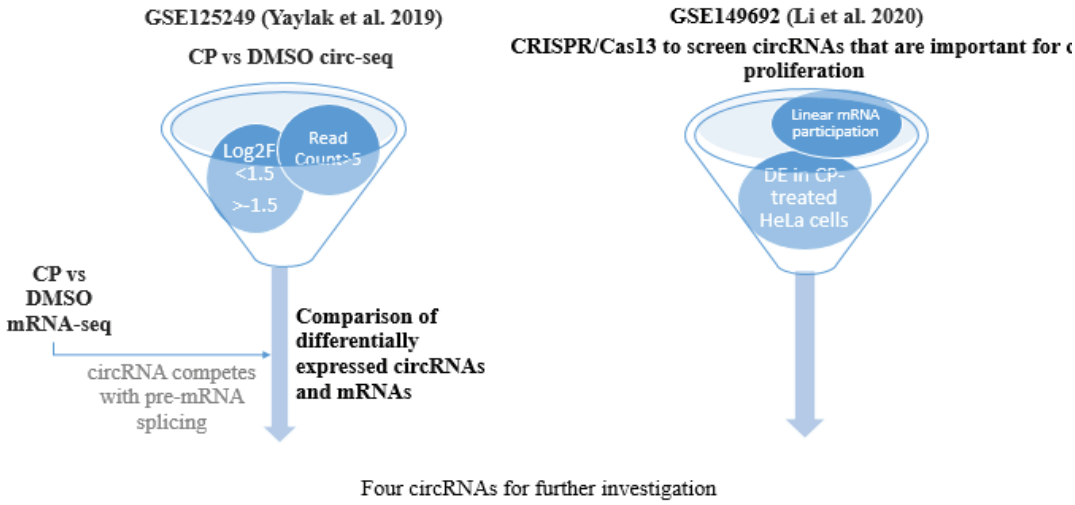

Figure 2.1. Diagram of the candidate selection process flow.

Two circular RNA candidates were selected from GSE183256 (S. Li et al. 2020) for further functional characterization on HeLa cells. Circular RNA candidates are chosen based on cognate mRNA's role in cell proliferation, apoptosis, and migration. They created CRISPR-CAS13d screening by creating a library to silence the 700 most abundant circRNAs (S. Li et al. 2020) (Figure 2.1).

2.2. Cell Culture

Since the pioneering data that form the basis of this thesis proposal were obtained from Henrietta Lacks's cells (HeLa cells) (Cell Applications), the same cells were used as a model system for examining the functions of candidate circRNAs. HeLa cells (ATCC, CCL-2) were grown in RPMI 1640 media (Gibco, USA) with 10% FBS at 37 °C and 5% CO_2. ME-180 cells (ATCC) were grown in DMEM medium with 10% FBS at 37 °C and 5% CO_2. Frozen HeLa cells were thawed within 2 minutes with gentle agitation in a 37 °C water bath, and the thawed cell suspension was transferred to a 1 ml growth medium in the 15 ml falcon tube (Sarstedt, Germany). Then the cells were collected by centrifuging at 1,000 rounds per minute (RPM) for 5 min at room

temperature (RT). The cells were grown in a cell culture flask (Sarstedt, Germany) with 5% CO_2. The HeLa cells were passaged when the culture reached 90% confluence. Passage number of cells kept between 9^{th} and 20^{th}.

2.3. CP Treatment

HeLa cells were seeded in a 0.3 X 10^6 cells/well density in six well-plates (Sarstedt, Germany). CP (Santa Cruz, USA) was used to trigger cell death. DMSO (Dimethyl sulfoxide) was used as a solvent for CP. CP was prepared freshly in every experiment because of its chemical instability. Time and dose kinetics of CP treatment was performed in the M.Sc. thesis of Ulvi Ahmadov (Ahmadov 2015). After 24 h from cell seeding, freshly prepared CP was added to the cells and incubated for 16 hours. The final concentration of CP was 80 μM. DMSO was used as mock control due to its toxicity. Annexin V/7AAD staining was performed, and apoptosis was immediately measured by flow cytometry analysis (M. Zimmermann and Meyer 2011).

Additionally, WST-8 reagent was used to measure the proliferation rate of HeLa cells. All experiments were performed three times. After transfection of HeLa cells in 6 well plates, 80 μM CP treatment was carried out 16 h before particular assays were performed. For CP-treated nuclear and cytoplasmic RNA preparation, $5x10^5$ HeLa cells were seeded in a 100 mm culture dish a day before CP treatment. Time/dose kinetics experiments were carried out to continue experiments with adequate time intervals and doses for 100 mm cell culture dishes (Sarstedt, Germany). The final concentration of CP used was 80 μM, which depends on the dose-cell# kinetics to obtain a significantly higher Annexin V+/7AAD+ population.

2.4. Primer Designing Strategy

Primers targeting circRNAs were designed manually and confirmed using circPrimer 2.0 (Zhong and Feng, 2022) to eliminate the off-target effect. The circPrimer 2.0 reveals all circular isoforms that share common BSJ. Therefore it allows for the

control of primer specificity not only for the candidate target but also for possible off-target circular isoforms deposited in available databases. A divergent primer strategy was used to design primers (Table 2.1). According to this approach, amplicon overlapped BSJ, the unique sequence of target circular RNA that is not available in linear mRNAs. Sequencing primers were designed to confirm the mature sequence of circGALNT2, circBNC2, circBIRC6, circCLASP1, and AGO2 coding sequence. Primer sequences used in this thesis are summarized (Table 2.2, Table 2.3)

Table 2.1. Quantitative Real-Time PCR primer sequences are used in this study.

Primer Name	Forward Primer	Reverse Primer	Length (bp)
circGALNT2 : hsa_circ_0000192	CTTACGCCCGCAACAAGTTCAAC	CTTTCCCTGGAGGGAGGGTCTCC	182
circCLASP1 : hsa_circ_0007052	GATTGCAGGTTGGCCAAGAAC	GAGTGAGTGGCAGAGTGATGT	201
circBNC2 : hsa_circ_0008732	ATGTCCCAACAGGCACACC	ACCCCACAACATGGGACCTT	119
circBNC2 : hsa_circ_0008732 -2nd primer pair	GCAGTTCGGAACCAGAACGAC	ATGCTGGCCAGTCTTGCTCAC	176
circBIRC6 : hsa_circ_0053535	CCAAAAAGGAGGGCACTGAG	TTTCTGGCTGTTGGAGAATG	162
GALNT2 mRNA	CTGGGCATCGCCTACTACAT	CTGGTTGAAACTTGTTGCGGG	271
CLASP1 mRNA	ATGATGCCAACAGTGATGCC	AGTAAGTTCTGCAGGCCCAG	175
BNC2 mRNA	TGTGAAACTTCACTACAGGAACG	GAGGCGTCTTCCCTGACATC	267
BIRC6 mRNA	TGTACGCTGTGATGAGGAGC	TGAATCGCACGCTATGACCA	173
circHIPK3: has_circ_0000284	TATGTTGGTGGATCCTGTTCGGCA	TGGTGGGTAGACCAAGACTTGTGA	146
GAPDH	ACTCCTCCACCTTTGACGC	GCTGTAGCCAAATTCGTTGTC	96
AGO2 mRNA	CCAGTCACCAAACATTCCCG	CAGGGGAAGGTAGGTGTGTT3	2580

Table 2.2. Cloning primer sequences are used in this study.

Cloning Primer Name	Forward Primer	Reverse Primer	Length (bp)
Cloning_circGALNT2	CCTTAATTAAGAGGACTGGAATGAAATTG	TCCCCGCGGTGGTCATGCCGGGTGTCAGG,	248
Cloning_circBNC2	CCTTAATTAAGCACACCTTGGGCCCACCC	TCCCCGCGGCTGTTGGGACATTCTGAATAAG	327
Cloning_circCLASP1	CCTTAATTAAAATGGACTGCTGAATTATGA	TCCCCGCGGCTTGTAATTGCTAGAGTTCAC	480
Cloning_circBIRC6	CCTTAATTAAGGCATACATCACAGAAGGAA	TCCCCGCGGCTTTGGTGCATGCACAGCC	1395
AGO2_Cloning_In Fusion	CCGGAATTCCATGTACTCGGGAGCCGGCC	TCCCCGCGGTCAAGCAAAGTACATGGTGC	2580

Table 2.3. Sequencing primer sequences are used in this study.

Sequencing Primer Name	Forward Primer
pMD20	CTTCCCGCTCGTAT
Laccase_MCS Exon Vector	GGCTTTGATCCTGATCAAG
circBIRC6_1	GGCATACATCACAGAAGGA
circBIRC6_2	TGGATAGTCAGGAGCAGTTG
circBIRC6_3	GCCTGAGCAGAGGAATGTTAG
AGO2_CDS_1	AAGCCAGAGAAGTGCCCGAG
AGO2_CDS_2	TCACCAAACATTCCCGCTGCA
AGO2_CDS_3	GCACCTGAAGAACACGTATGC
AGO2_CDS_4	TCGTGGTGCAGAAGAGGCAC
AGO2_CDS_5	CCACGAGTTGCTGGCCAT
AGO2_CDS_6	CATTCCAGCAGGCACGACTG
The pHTN HaloTag® CMV-neo Vector Sequencing	GTCCCGAAGCTGCTGTTCTG

2.5. RNA Isolation

Total RNAs of DMSO- and CP-treated HeLa cells and transfected HeLa cells were isolated using TRIzol reagent (Thermo Scientific). Briefly, the cell lysate was homogenized by 1 ml TRIzol reagent for drug treatments and only cell RNA isolation. Then 200 µl chloroform was added to the tube, shaken by hand aberrantly for 15 sec, and incubated at RT for 2-3 min. RNA phase separation occurred by centrifugation at 12,000 x g for 15 min. The aqueous/clear phase was transferred to a new tube, and 500 µl isopropanol was added and incubated at RT for 10 min. RNA was precipitated by centrifugation at 12,000 x g for 10 min, and the supernatant was discarded.

The pellet was washed with ethanol twice and centrifuged at 7,500 x g for 5 min. After ethanol washes, the pellet was air-dried and dissolved in 20 µl nuclease-free water. RNA isolation after transfection was performed with some exceptions; 300 µl TRIzol reagent was used for homogenization. Therefore, the chloroform, isopropanol, and ethanol volume was changed to 60 µl, 150 µl, and 300 µl. Additionally, 1 µl glycogen (20 mg/ml) was added to the mixture after adding isopropanol and incubated at -20 °C for 16 h. It should be noted that technical replicates were combined before RNA isolation for transfected HeLa cells grown 96 well-plates.

Phenol-Chloroform extraction followed by ethanol precipitation was performed to extract RNA after RNA-Immunoprecipitation and to clean up RNA after RNase R treatment. An equal volume of Phenol-Chloroform-Isoamyl alcohol (25:24:1 v/v/v) (pH:4.0) (Applichem, Germany) was added to the sample and vortexed at maximum speed for 10 sec. Then the mixture was centrifuged at 10,000 g at RT to transfer the aqueous phase into an RNase-free tube. 1/10 vol of 3 M NaOAc (Applichem, Germany) was mixed into the sample. Then the mixture was incubated at -20 °C overnight. One µl glycogen was added to the mix before incubation overnight to facilitate RNA precipitation of RNA. Moreover, RNA was precipitated by centrifuging at 15,000 x g for 10 min. The pellet was washed using 500 µl of 75% ethanol at 4°C twice by centrifuging at 7,500 x g for 5 min. Lastly, the pellet was air-dried for 10 min. The RNA pellet was dissolved in nuclease-free H_2O (Invitrogen, USA).

2.6. Validation of Differentially Expressed CircRNA Candidates by qPCR

Two total RNA groups were divided into two subgroups, and RNase R (Epicentre) treatment was performed with control RNA. cDNA was synthesized from DMSO total RNA, CP total RNA, and DMSO RNAse R groups using random primers (lack of 5'cap and 3'tail) using Revert Aid cDNA Synthesis Kit (Thermo Scientific).

The expression patterns of the candidates were determined by qPCR (Promega GoTaq qPCR Master Mix) after normalization based on the GAPDH gene by the $2^{\Delta\Delta ct}$ method using total RNA as a template. Divergent primers were specific to BSJ will be used. Nonetheless, the resistance of circRNAs compared with linear GAPDH mRNA will be determined by qPCR using the RNase R (Epicenter) treated RNAs. Additionally, the linear counterparts of circRNAs were analyzed using convergent primers by qPCR.

2.7. TA Cloning

The BSJs of candidate circRNAs were cloned into a pMD20 TA vector (Takara, Japan) to confirm non-canonical exon ordering. PCR products of circRNA were isolated from agarose gel using Gel and PCR clean-up kit (MN, Germany). The eluted PCR amplicon was poly-adenylated using a Standard Taq Polymerase kit (NEB, England). Then 1 µl dATP (2 Mm), 0.2 µL Taq Polymerase, 5 µl 10X Buffer, and eluted PCR amplicon were mixed up to 50µl volume with distilled water, incubated at 72 °C for 20 min to perform poly-adenylation. The polyadenylated amplicon was then ligated to the pMD20 TA vector using T4 DNA ligase. In detail, 0.5 µl pMD20 TA vector, 5 µl insert, 2 µl buffer (10X), and 1 µl T4 DNA ligase were mixed and then incubated at RT for 4h.

The ligation mixture was transformed to the TOP10 strain by the heat-shock method. 5 µl ligation mixture was gently added to 50 µl competent TOP10 on ice. The competent cells and the plasmid mixture were incubated on ice for 25 min. The mixture was then exposed to 42 °C for 45 sec and put immediately on ice for 2 min before adding SOC media to recover for 1 h while shaking at 180 RPM. During this period, 24 µl

IPTC/dish and 96 µl X-gal/dish were mixed and spread on ampicillin-containing LB agar media 30 min before SOC incubation was completed. At the end of the incubation, bacterial cells were harvested by centrifugation at 5,000 RPM for 5 min and plated using a Drigalski spatula on IPTC-Xgal-containing plates for blue-white screening and incubated for 16 h.

One of the white colonies was selected and confirmed by colony PCR. A small portion of bacteria from the selected colony was picked up using a toothpick, transferred into 20 µl distilled water, and incubated at 95 °C for 15 min and 10 °C for 15 min, respectively. Then 1 µl of the mixture was used as a DNA template for colony PCR using Q5 High-Fidelity DNA Polymerase. Confirmed colonies were inoculated into LB liquid and incubated for 16h. Afterward, plasmid isolations were performed using Nucleospin Plasmid Miniprep Kit (MN, Germany). BSJs of circRNAs were confirmed by Sanger Sequencing at the İYTE Integrated Research Center.

2.8. Cloning of CircRNAs into pcDNA3.1(+) Laccase2 MCS Exon Vector

The mature sequence of circRNA candidates was obtained from the Circinteractome database (Dudekula et al. 2016). Mature sequences were amplified by Q5 High Fidelity DNA polymerase (NEB). After amplification, double digestion was performed with restriction enzymes PacI and SacII and ligate double-digested pcDNA3.1(+) Laccase2 MCS Exon Vector (Kramer et al. 2015). This vector has two long laccase intron repeats flanking multiple cloning sites that facilitate back splicing and promote circRNA biogenesis in the cell. In detail, an amplified mature sequence of circRNA was cleaned up using Gel and PCR Clean-up kit (MN, Germany). Then, the insert was double-digested by PacI and SacII.

In the vector preparation step, Alkaline Phosphatase Calf Intestinal (CIP) treatment and double digestion were performed in one reaction to minimize vector loss. The pcDNA3.1(+) Laccase2 MCS Exon Vector length is 6929 bp. In detail, 4 µg pcDNA3.1(+) Laccase2 MCS Exon Vector, which has 1.868 pmol DNA ends, was digested with 4µl PacI and 4 µl SacII, 5 µl CutSmart Buffer, 0.5 µl CIP and an appropriate

amount of nuclease-free H_2O at 37 °C for 30 min. Lastly, 118 ng/µl vector with 260/280: 1,84 and 260/230:1,42 ratios was isolated for further cloning experiments using Gel and PCR clean-up kit (MN, Germany). The double-digested mature sequences of circRNA candidates were ligated with pcDNA3.1(+) Laccase2 MCS Exon Vector by T4 DNA ligase at RT for 10 min. The ligation mixture was transformed to TOP10 strain by the heat-shock method. According to the manufacturer's protocol, endotoxin-free plasmid isolation was performed by an EF-Midiprep kit (MN, Germany). Positive colonies were inoculated in 200 ml LB liquid media, grown at 37 °C overnight, and collected by centrifugation at 3200 RPM for 30 min. Bacterial pellets were resuspended with 8 ml resuspension buffer and lysed with 8 ml lysis buffer for 5 min, then adding 8 ml neutralization buffer. Lysates were loaded onto columns to bind plasmid DNAs. The endotoxin-free washes were performed with endo-EF and wash-EF buffers, respectively. Lastly, plasmid DNAs were eluted from the column using an elution buffer. Isopropanol precipitation was achieved by adding 3 ml pure isopropanol and centrifuging for 30 min at +4 °C. Pellets were air-dried and dissolved in 100 µl nuclease-free water. Sanger sequencing was performed to confirm mature sequences of candidate circRNAs. Sequencing files with .ab1 extension were confirmed using the Finch TV (FinchTV 1.4.0, USA) tool by comparing with mature circRNA sequences in the CircInteractome database. Cloning and sequencing primers were summarized in Table 2.2 and Table 2.3, respectively (Table 2.2, Table 2.3).

2.9. Small-Interfering RNA Designing for CircRNA Silencing

siRNAs targeting BSJ of candidate circRNA were designed by using CircInteractome tool siRNA designing bench. siRNA sequences used in this thesis were summarized in Table 2.4 (Table 2.4).

Table 2.4. SiRNA sequences used in this thesis.

circRNA	siRNA target sequence (sense strand)
circCLASP1	AAUUACAAGAAUGGACUGCUGdTdT
circBIRC6	CACCAAAGGGCAUACAUCACAdTdT
circBNC2	GUCCCAACAGGCACACCUUGGdTdT
circGALNT2	GCAUGACCAGAGGACUGGAAUdTdT

2.10. Transfection of Overexpression Plasmids and siRNAs

DharmaFECT-1 (Dharmacon, USA) was used in silencing assays to transfect siRNAs into HeLa cells. According to the manufacturer's protocol, $5x10^4$ HeLa cells were seeded on 96 well plates before the day of transfection for WST-8 proliferation assay. In separate tubes, 0.5 µl siRNA (5 µM) and 0.2 µl of DharmaFECT-1 transfection reaction were diluted with serum-free RPMI as 10 µl total reaction volume per tube. After 5 min incubation, tube 1 was added to tube 2 gently and incubated for 20 min. Then, the transfection mixture was mixed with an appropriate RPMI and 10%FBS volume to share 100 µl per well.

To rescue the silencing effect of siRNAs in 96 well plates, FuGENE HD (Promega, USA) transfection reagent was used to transfect overexpression plasmids to HeLa cells. After 24 h of silencing, the transfection mixture was prepared by mixing 50 ng overexpression plasmid with 0.2 µl FuGENE HD and incubated for 10 min. Then, the transfection mixture was mixed with an appropriate RPMI and 10%FBS volume to share 100 µl per well. The overexpression reaction was incubated for 1 h, and the medium was changed with RPMI 10%FBS. Non-targeting siRNA was used as mock control.

For Annexin V/7AAD and PI assays, $1.5x10^5$ HeLa cells were seeded to 6 well plates one day before transfection. The transfection mixture was prepared using the same strategy explained above by using 0.5 µl siRNA (100 µM) and 4 ul DharmaFECT-1.

After incubation, the 400 µl transfection mixture was added to wells drop-by-drop (counterclockwise). SiRNAs were incubated for 72 hours. An empty vector was used as mock control for overexpression experiments.

2.11. Cell Viability Detection Kit (CVDK-8) Assay for Proliferation Measurement

Cell viability detection kit (CVDK-8) allows a very convenient assay by utilizing its highly water-soluble tetrazolium salt, WST8 [2-(2-methoxy-4-nitrophenyl)-3-(4-nitrophenyl)-5-(2,4-disulfophenyl)-2h-tetrazolium sodium salt] produces water-soluble formazan dye upon reduction in the presence of an electron mediator (Dojindo Laboratories 2016). After transfection, 10 µl of WST-8 was added to each well of the plate. Plates were incubated for 2 h in the incubator. The absorbances were measured at 460 nm using a microplate spectrophotometer (Thermo Scientific, USA). HeLa cells were collected after spectrophotometric measurement by trypsinization for RNA isolation to confirm transfection efficiency.

2.12. Annexin V/7AAD Staining for Apoptosis Measurement

HeLa cells were collected by trypsinization 72h after transfection. One-third of the collected cells were homogenized using Trizol for RNA isolation to confirm transfection efficiency. The remaining part of the cells was washed with PBS and centrifuged at 1,200 RPM for 10 min. Then pellet was diluted with 50 µl annexin binding buffer, adding 10 µl Annexin V and 10 µl 7AAD. Then, cells were incubated at dark for 15 min and analyzed by flow cytometry.

2.13. RNA Immunoprecipitation (RIP) with AGO2-HaloTag Fusion Protein

A mature sequence of AGO2 protein was amplified by a Q5 High Fidelity DNA Polymerase kit and cloned into pHTN HaloTag® CMV-neo Vector (Promega, USA) by an In-Fusion cloning approach (Takara, Japan). Firstly, gene-specific primers with 15 bp homolog recombination site extensions were designed (Table 2.2). After amplifying the AGO2 ORF (2580 nt), the full-length cDNA was cleaned using PCR and a Gel clean-up kit (MN, Germany). Then, 2 µl In fusion cloning premix, 50 ng linearized vector, appropriate insert were mixed and filled up to 10 µl total reaction volume incubated for 15 min at 50 ºC. Clones were screened after bacterial transformation using competent TOP10 strain. Then colonies were screened by colony PCR, and one positive colony was selected. The selected colony was inoculated in 200 ml LB-liquid media and incubated for 16 h. The endotoxin-free AGO2- pHTN HaloTag® CMV-neo Vector and mock control pHTN HaloTag® CMV-neo Vector were isolated by EF Midiprep kit (MN, Germany). The coding sequence of AGO2 was confirmed by Sanger sequencing.

Transfection of AGO2- pHTN HaloTag® CMV-neo Vector and mock control pHTN HaloTag® CMV-neo Vector to HeLa cells performed by Polyethyleneimine (PEI) /Chloroquine method. 1.2 x 10^6 HeLa cells were seeded in a 150 mm dish a day before transfection. Four 150 mm dishes were transfected with AGO2- pHTN HaloTag® CMV-neo Vector, and other four 150 mm dishes were transfected with mock control pHTN HaloTag® CMV-neo Vector To reach 10 x 10^6 cells at the beginning of the RIP procedure.

On the transfection day, media was replaced with 20.319 ml RPMI 10% FBS and 20.34 µl Chloroquine at 5h before transfection. 22.6 µg plasmid added to RPMI 10% FBS up to a volume of 1,130 (1/20 of the total amount of media) RPMI 10% FBS. Due to the 1:3,5 ratio, 79,1 µg PEI (1 mg/ml) was added to RPMI 10% FBS up to a volume of 1,130 (1/20 of the total amount of media) RPMI 10% FBS. Then, the dilute PEI was added to DNA gently, and the mixture was incubated at RT for 25 min. The transfection mixture added media, pre-treated with chloroquine, dropwise. HeLa cells were harvested at 48h after transfection.

After harvesting HeLa cells, 1% of the AGO2-Overexpressed cells and pHTN HaloTag® CMV-neo-overexpressed cells were transferred to new tubes as input control. RNAs were isolated from every group using Phenol-Chloroform extraction. The rest of the cells were treated with 1% Formaldehyde for fixation.

Formaldehyde fixation began with trypsinization of transfected cells. Cells became unattached using 4 ml trypsin/EDTA for 5 min at 37 ºC. Trypsin was inhibited by adding 8 ml RPMI/10%FBS. After, cells were collected by centrifuging at 1,000 RPM, RT. Then 10 ml PBS was added to wash the cells. 100 µl/control (1% of total) was separated to confirm the overexpression of AGO2 by qPCR and expression of Halo and AGO2-Halo tag fusion protein. The cells were re-collected by centrifuging at 1,000 RPM for 5 min, and the supernatant was discarded. The pellets were mixed with RNase-free PBS containing 1% formaldehyde. The fixation was performed by incubating the mixture while shaking using an orbital shaker at RT for 10 min. 1 ml of 1.25 M Glycine was added to the cells to terminate the formaldehyde by shaking at RT for 5 min. Then the cells were collected by centrifuging at 1,000 RPM for 5min. The cells were washed with 10 ml RNase-free PBS and collected by centrifuging at 1,000 RPM for 5 min. The pellet was resuspended with 1 ml RNase-free PBS. Then the cells were collected by centrifuging at 1,000 RPM for 5 min, the supernatant was discarded carefully, and the cell pellet was stored at -80 ºC. The fixed cells were stable at -80 ºC for three months. The 1% per input materials were used for RNA extraction as an input in qPCR.

The next day, beads were washed with equilibration buffer 5 times for 5 min each. 450 µl lysis buffer was added to cell lysates of the AGO2-HaloTag overexpressed and Mock HaloTag groups and incubated for 10 min on ice, followed by sonication. The sonication was performed for 10 min (30 sec ON, 30 sec OFF, 75% amplitude).The protein: RNA hybrids were collected by centrifugation at 15,000 x g for 10 min. The 400 µl supernatant was diluted by adding an equal volume of dilution buffer.

The diluted lysates were mixed with magne halo tag beads (Promega, USA). Hybridization was performed at +4 ºC overnight. Besides, 50 µl of the unbound fraction was stored at -80 ºC for measured hybridization efficiency. Then, beads were washed using 1 ml of each high-salt PBS-T buffer, PBS-T buffer, urea wash buffer, and SDS wash buffer, respectively. The TEV protease enzyme separated the Halo Tag linker from AGO2. Then, proteinase K was used to digest AGO2 to isolate AGO2-interacted RNAs. After that, reverse-crosslink was performed by incubating samples at 65 ºC for 1 h.

Finally, RNA isolation was performed by the Phenol-Chloroform extraction method. The isolated RNAs were used as a template for cDNA synthesis, followed by qPCR. In qPCR, the expression differences of circCLASP1 in mock control and AGO2 overexpressed groups, in between input and RIP fractions, were calculated using $2^{\Delta ct}$.

2.14. Nuclear and Cytoplasmic RNA Isolation

Nuclear and cytoplasmic RNAs were isolated using a Cytoplasmic and Nuclear RNA Purification Kit (Norgen Biotech Corp., Canada). Briefly, 200 µl lysis buffer J1 was added to frozen cell pellets and lysed cells by vortexing for 15 sec. The lysate was centrifuged at maximum speed for 10 min. The cytoplasmic RNA in the supernatant was transferred to another epi (RNase-free). The pellet was saved for nuclear RNA isolation. 200 µl buffer SK was added to each nuclear and cytoplasmic RNA fraction and mixed by vortexing for 10 sec. Mixtures were applied to spin columns and centrifuged for 1 min at 4,000 x g. Then 400 µl Wash Solution A was added to columns and centrifuged for 1 min at 14,000 x g third times. Columns were spun at 14,000 x g for 2 min to dry the resin. RNAs were eluted by adding 50 µl Elution Buffer E by centrifuging at 200 x g for 2 min followed by 14,000 x g for 1 min. Eluted RNAs were stored at -70 ºC. RNAs were used as templates for cDNA synthesis, followed by qPCR.

2.15. RNA Sequencing and Analysis

Total RNAs isolated from three biological replicates of si_circCLASP1- and si_NEG-transfected HeLa cells were subjected to RNA sequencing to identify differentially expressed mRNAs upon circCLASP1 knockdown. To this end, HeLa cells were transfected with si_circCLASP1- and si_NEG for 72 h, and total RNAs were isolated, as explained earlier. The integrity of the RNAs was initially assessed by analyzing the sharpness of 18S- and 28S- rRNA bands on agarose gel electrophoresis. Additionally, the Qubit 3 photometer (Thermo Fisher, ABD, #Q33216) and 2100 Bioanalyzer (Agilent, ABD, #G2939B were used to determine the quality, quantity, and structural integrity of the samples. Illumina Stranded Total Prep kit (Illumina, USA,

#20040534) was used for library preparation (RefGEN Biotechnology, Turkey). The kit is based on the extraction of ribosomal RNAs in whole RNA, their random fragmentation, and the creation of primary and secondary cDNA strands. In the library preparation process, capture, digestion, RNA purification, cDNA synthesis, the addition of index-barcode sequences, and purification processes are performed by following the manufacturer's kit instructions, respectively. The overall process is presented in Figure 2.2 (Figure 2.2).

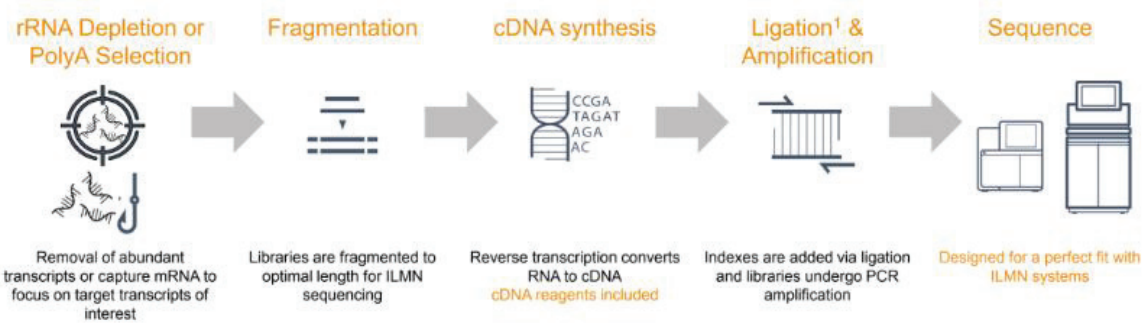

Figure 2.2. Schematic representation of the library preparation workflow (RefGEN Biotechnology, Turkey).

Illumina NovaSeq 6000, a next-generation sequencing platform, was used in the sequencing study. In this step, it is planned to obtain an average of 30 million paired-end reads with a length of 150 bp per sample (RefGEN Biotechnology, Turkey). Library measurement, dilution, and loading followed the manufacturer's instructions (Illumina, USA). After sequencing, the FASTQC tool was used to control the obtained read data quality. According to the quality control results, data amounts, read quality, GC distributions, kmer distributions, and possible adapter contaminations were examined for each sample. During the sequencing process, the reads were trimmed so that poor-quality base reads and possible adapter-index contaminations in the raw read data would not cause deviations in the subsequent analysis steps. TrimGalore (Version 0.6.10) tool was used for trimming according to quality values (Krueger et al. 2023). Then STAR alignment tool combined with GENOCODE V40 annotation and GRCh38.p13 assembly for human genome reference was used for alignment. The BAM files were counted using the Feature Counts. The Deseq2 was used for differential expression analysis.

2.16. Statistical Analysis

GraphPad Prism 6 V6.01 (La Jolla, CA, USA) was used for statistical analysis. The Student's t-test was applied to compare differences between the two groups. Each experiment was repeated in triplicate, and data were expressed as mean±SD (standard deviation). A p-value lower than 0.05 (< 0.05) is statistically significant. A padj value lower than 0.05 (<0.05) is statistically significant in differential expression analysis.

CHAPTER 3

RESULTS

3.1. Bioinformatic Analysis and Candidate Selection

3.1.1. Candidate Selection by Analysing GSE125249

Differentially expressed circRNAs in CP-treated HeLa cells were reported previously (Yaylak, Erdogan, and Akgul 2019). The heat map displays the expression differences of circular RNAs between CP-treated and DMSO-control groups (Figure 3.1.)

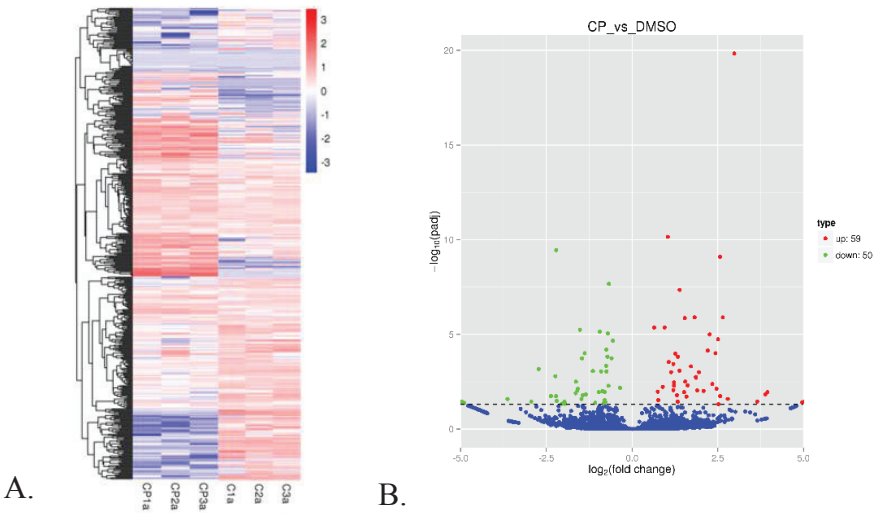

Figure 3.1. Schematic illustration of differentially expressed circRNAs in CP-treated HeLa cells. A. The heatmap of the differentially expressed circRNAs. B. The volcano plot of differentially expressed circRNAs in CP-treated HeLa cells ($p<0.05$).

Cognate mRNAs of circRNAs differentially expressed in CP-treated HeLa cells were significantly enriched in protein processing, cell cycle, and NF Kappa B signaling pathways (Figure 3.2).

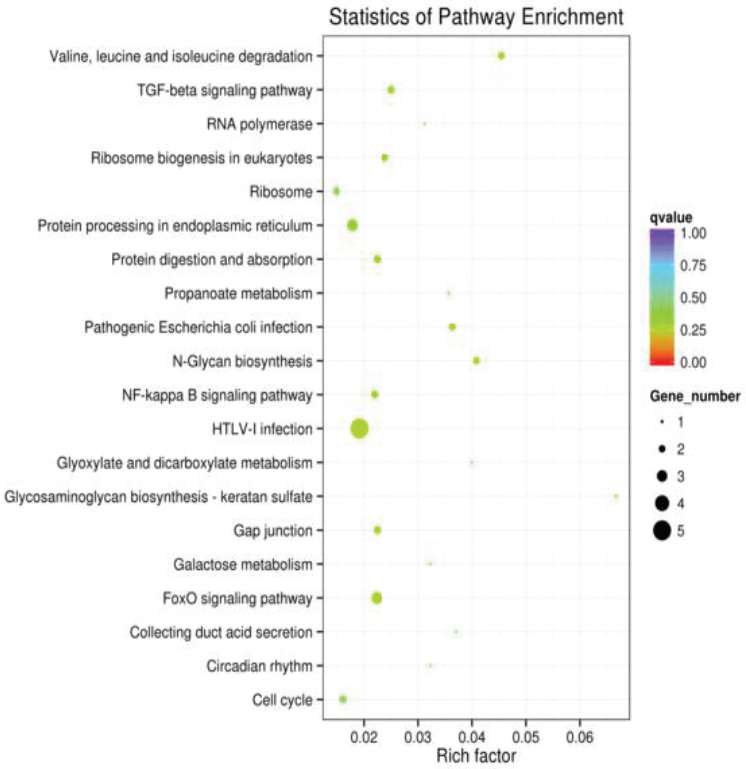

Figure 3.2. Gene ontology (GO) Pathway enrichment analysis.

GSE125249 reports 109 circRNAs differentially expressed in CP-treated HeLa cells. The candidate circRNAs for further analyses were selected based on the three following criteria; 1) their normalized read count numbers in each CP- and DMSO-treated sample should be higher than 5, 2) Log2FC of circRNAs should be greater than 1.5 or lower than -1.5 3.) Preferentially, the expression pattern of circRNA should be opposite to the cognate mRNA. circGALNT2 (has_circ_0000192) was validated as an upregulated circular RNA under apoptotic conditions. Unfortunately, the analyses did yield any circRNAs that are inversely expressed compared to their linear counterpart. circBNC2 (has_circ_0008732) was identified as a downregulated circRNA candidate under CP-treated conditions. Overall, circGALNT2 and circBNC2 were selected for further investigations. In early 2021, Li and his colleagues reported that a group of

circRNA candidates is essential for cell growth, mostly in a cell type-dependent manner (Li et al., 2021). In this strategy, the target transcript can be knocked down when Cas13, which is also integrated into the genome, is induced in each cell. Thus, a distinct gRNA sequence serves as a barcode for each cell. Depleting the particular gRNA barcodes in the cellular population would then allow one to assess the knockdown's impact on cellular viability. (Xu et al., 2020). They reported that 63 circRNAs potentially positively affect cell proliferation in HeLa cells. Most of the circRNA candidates' functions are still elusive. Two uncharacterized circRNAs, circCLASP1 (hsa_circ_0007052) and circBIRC6 (hsa_circ_0053535) were selected to investigate under CP-treated conditions. The candidate selection flowchart is summarized in Figure 3.3 (Figure 3.3).

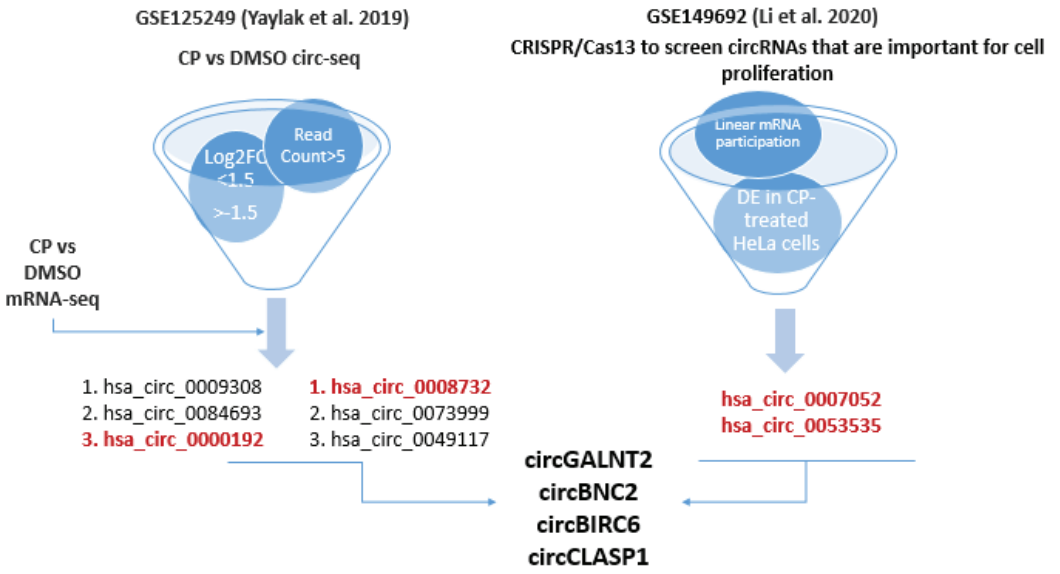

Figure 3.3. Flowchart showing the selection process of circRNA candidates.

3.2. CP Treatment Promotes Apoptosis and Represses Proliferation in HeLa Cells

HeLa cells were treated with CP to interrogate the effects of CP on HeLa cells' apoptosis and proliferation. IC50 dose was identified in time, and dose kinetics of CP treatment was reported in the M.Sc. thesis of Ulvi Ahmadov (Ahmadov 2015). The cells treated with 80 μM CP and the ~50% early and late apoptosis percentages were obtained (Figure 3.4).

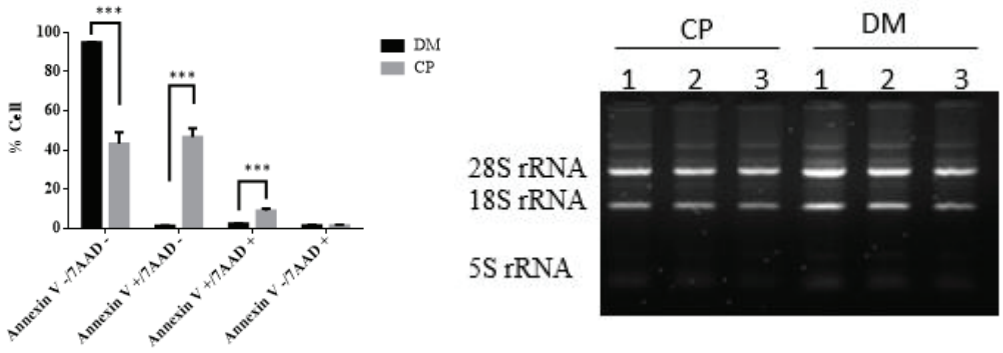

A. B.

Figure 3.4. Flow cytometric analysis of early, late apoptosis and death in treated HeLa cells with CP. A. Bar chart shows the live, early apoptosis, late apoptosis, and dead cells distribution in CP-treated HeLa cells. B. Agarose gel electrophoresis (1%, 100 V, 30 min) represents the integrity of total RNAs isolated from CP-treated and DMSO-treated control HeLa cells. C. HeLa cells treated with 80 μM CP and DMSO at ic 50 concentration and maintained 16h at. The cells were analyzed after staining with Annexin V-FITC and 7AAD by flow cytometer. The dot plot represents the DMSO-treated HeLa cells as a control group, CP-treated HeLa cells with IC50 concentration of CP. The early apoptosis events (Annexin V + /7AAD -) shown in lower right quadrant (Q4). The late stage of apoptosis/dead cells (Annexin V + /7AAD +) is shown in quadrant Q2. The dead cells (Annexin V- / 7AAD +) is indicated in upper right quadrant Q1.

Cont. on next page

Figure 3.4 (cont.)

C.

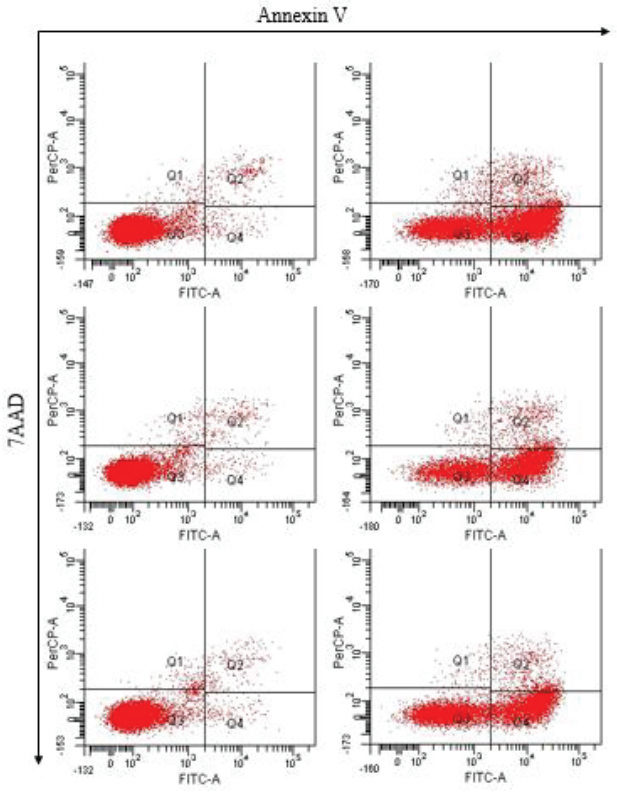

80 μM CP treatment results in approximately 50% early apoptosis, 10% late apoptosis, and 2% dead cells (Figure 3.4.B.). The total RNA from CP-treated HeLa cells and control groups were isolated and used as templates for qPCR experiments to show differential expression of circRNA candidates. RNA quality control was carried out by non-denaturing gel electrophoresis with TBE buffer. 28S rRNA and 18S rRNA bands were visualized intact and expected intensity. It is known that 28S bands should be nearly twice as intense as 18S bands in high-quality total RNA (Figure 3.4.C.). Moreover, the WST-8 assay was performed to show the effect of CP on HeLa cell proliferation. As shown below, CP represses the proliferation of HeLa in a dose-dependent manner. Therefore the circRNA candidates potentially affecting cell proliferation and apoptosis might be involved in CP-mediated regulations in HeLa cell apoptosis and proliferation

(Figure 3.5). Therefore the circRNA candidates potentially affecting cell proliferation and apoptosis might be involved in CP-mediated regulations in HeLa cell apoptosis and proliferation (Figure 3.5).

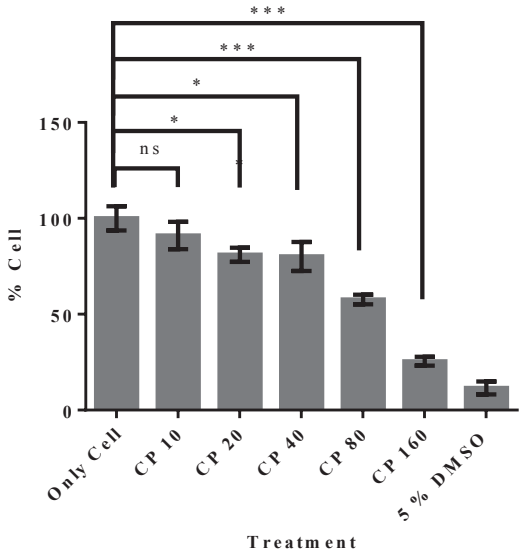

Figure 3.5. WST-8 analysis of HeLa cells treated with CP in a dose-dependent manner. Absorbance values were measured with SkanIt Spectrophotometer at 460 nm. The results are shown as mean ± sD of three independent experiments with *p,0.05. DM:DMSO.

3.3. CircCLASP1, CircBNC2, circBIRC6, and circGALNT2 Validated as CP-Modulated Circular RNAs in HeLa Cells

There are several reasons to validate circRNA before functionally characterizing them. Initially, circRNAs can be hard to detect and distinguish from other types of RNAs in cells. Their rare nature makes them difficult to detect and differentiate from other RNA species, such as mRNAs. Moreover, ribosomal RNA depletion efficiency and circular confirmation of RNAs make the library preparation and detection process challenging. Therefore, it is essential to use multiple approaches to confirm the existence of the particular circRNA before explaining them in a functional context. These complementary approaches can be summarized as the qPCR uses a divergent primer strategy, Sanger sequencing of unique back splicing junction sequence, RNase R treatment, and oligo-dt-based cDNA enrichment followed by qPCR.

3.3.1. circCLASP1 is a CP-Repressible, RNase R-resistant, Circular RNA Transcript Expressed in HeLa Cells

Firstly, circCLASP1, which is predictively located in chr2:122363276-122363756 was validated in Hela cells via a divergent primer designing strategy. The designed primers were indicated. The potential pitfalls of validating circRNAs are the availability of circRNA isoforms with common back-splicing junctions. Thus, the CircPrimers 2.0 tool (Zhong and Feng 2022) was used to eliminate possible off-target amplicons by using divergent primers specific to amplify the BSJ of circCLASP1 (Figure 3.6).

Figure 3.6. Primer designing to validate circCLASP1. A. Locations of forward and reverse primers to amplify BSJ of circCLASP1. B. Confirmation of off-target circular isoform amplicons of designed divergent primer sets. The CircPrimers 2.0 tool was used to annotate circCLASP1 and design and check divergent primers.

Designed primers were used in the subsequent experiments because the 384 bp is outside the amplicon length boundaries of qPCR are recommended to be between 150-250 bp. The results showed circCLASP1 downregulated -1 log2 FC under CP-treated conditions, while its linear mRNA CLASP1 downregulated nearly -3 log2 FC (Figures 3.7A and 3.7D).

It is hypothesized that circCLASP1 is required for HeLa cell proliferation (S. Li et al. 2020). It might be more abundantly expressed in highly proliferative cervical cancer

cell line ME-180 than HeLa. As expected, quantitative PCR showed that circCLASP1 is approximately eight-fold upregulated in the ME-180 cell line (Figure 3.7B).

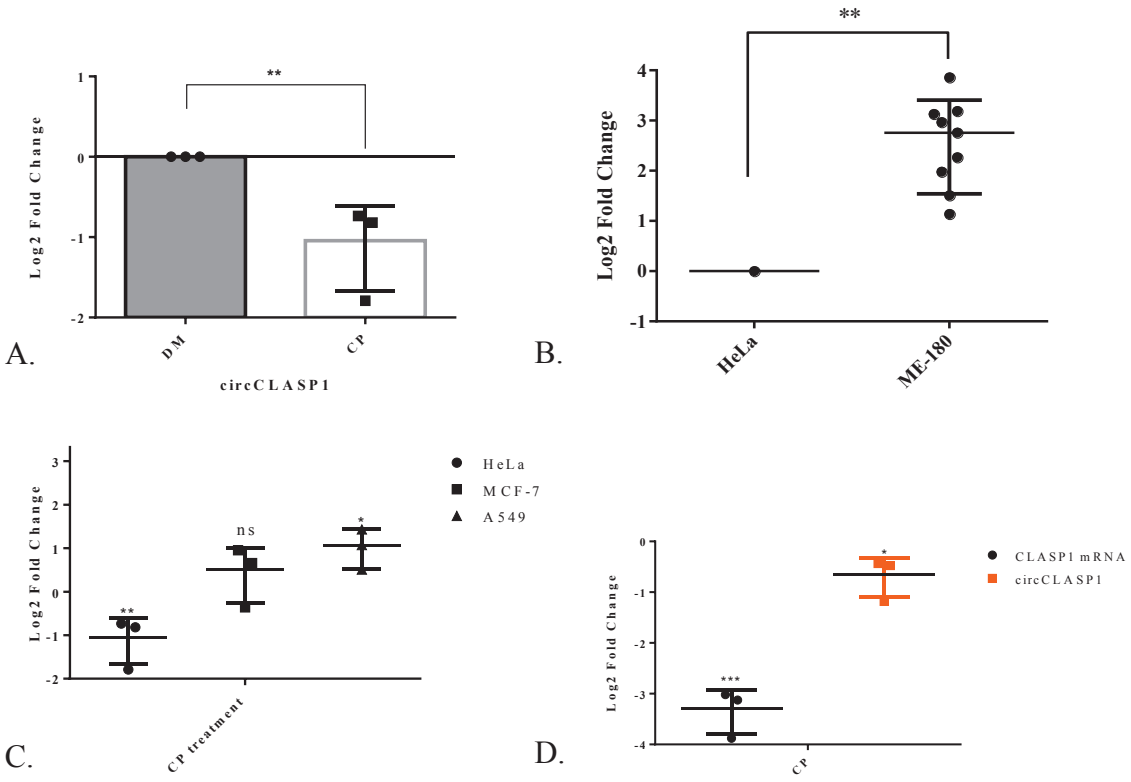

Figure 3.7. CircCLASP1 significantly downregulated in CP-treated HeLa cells while upregulated in highly proliferative cervical cancer cell line ME-180 than HeLa. A. qPCR indicates that circCLASP1 downregulated in CP-treated HeLa cells. B. circCLASP1 more abundantly expressed in ME-180 cell line compared to HeLa. C. Graphical representation of circCLASP1 expression.in HeLa, MCF-7 and A549 cell line. D. Graphical representation of linear CLASP1 and circCLASP1 indicated as orange squares) differemtial expression in CP-treated HeLa cells. Normalization were performed by $2^{\Delta\Delta Ct}$ method by using GAPDH as a reference RNA. The results are shown as mean ± sD of three independent experiments with *p,0.05. DM:DMSO

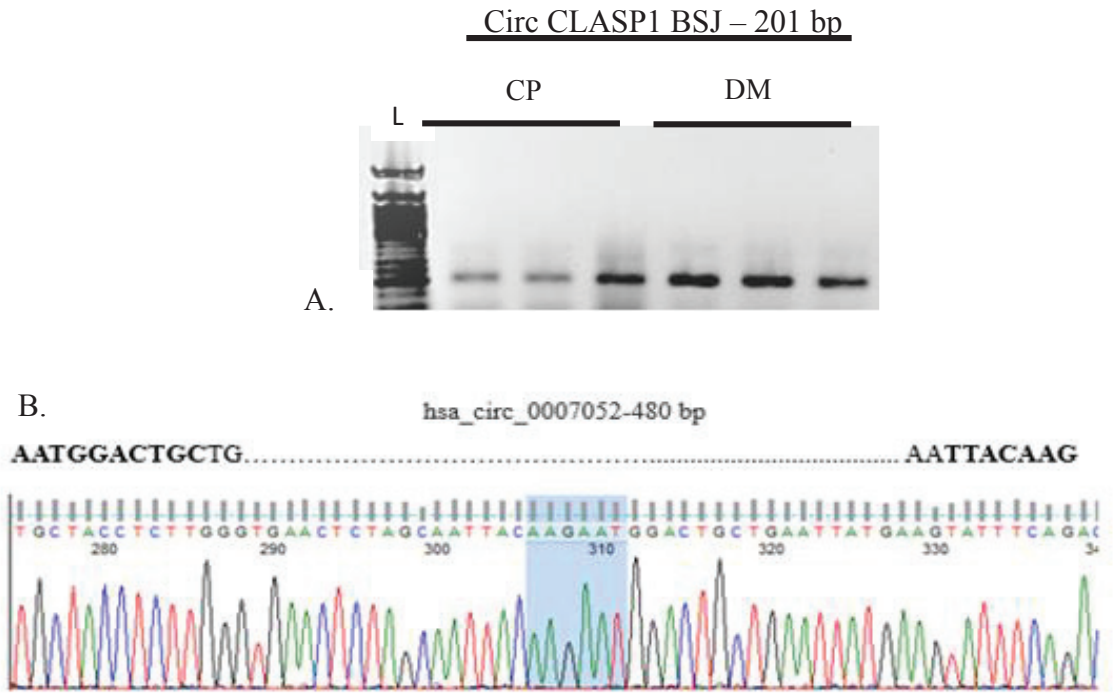

Figure 3.8. Confirmation of circCLASP1back-splicing junction by Sanger sequencing. A. Agarose gel electrophoresis (100 V, 30 min, 1%) image showed amplicon from figure 3. which was cloned into TA vector and sequenced. B. The ABI format chromatogram was observed by using Finch TV tool. L: NEB 50 bp ladder. BSJ length: 201 bp, mature sequence of circCLASP1: 480 bp.

To investigate whether the downregulation of circCLASP1 is a general trend or HeLa specific, adenocarcinoma cell lines from the breast and lung were treated with CP, and circCLASP1 expression was screened after CP treatment. Figure 3.7C indicates that circCLASP1 was upregulated in CP-treated A549 cells, whereas there is no significant change in the CP-treated MCF-7 cell line, unlike HeLa cells. It is well-known that circRNAs have cell- and tissue-specific expressions and functions (Misir, Wu, and Yang 2022) (Figure 3.7C). The 201 bp circCLASP1 BSJ amplicon was observed in agarose gel electrophoresis (Figure 3.8A), confirming the amplification of the correct product. Additionally, the back-splicing junction of circCLASP1 was confirmed by TA cloning and sanger sequencing after qPCR, a gold standard for robust circRNA research to eliminate false positives (Figure 3.8).

The ABI format chromatogram indicated that the amplicon spans the splicing junction of 5'UTR and exon2 of the CLASP1 pre-mRNA. The genomic location of circCLASP1 is chr2:122363276-122363756 (-) (Figure 3.8B).

The mature sequence of circCLASP1 begins with **AATGGACTG** and ends with *AATTACAAG*. The ABI chromatogram showed that the spanning region covers *AATTACAAG***AATGGACTG.** This observation proved that qPCR analyses addressed

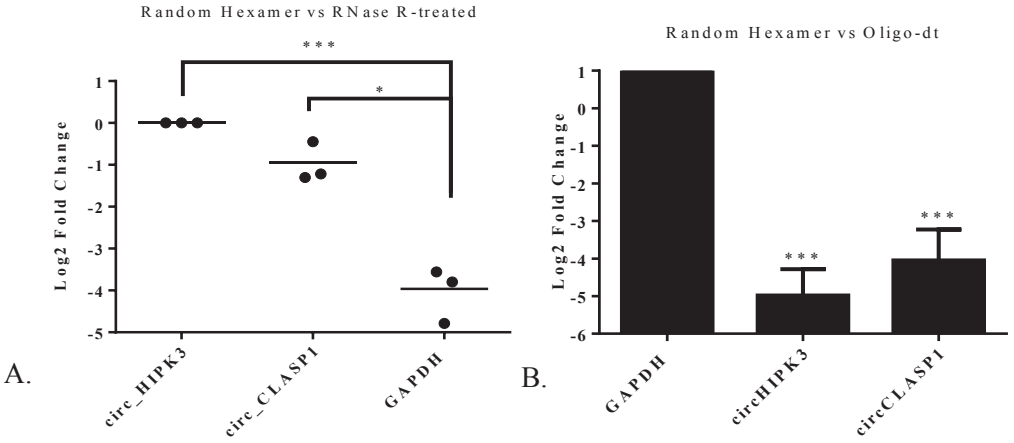

Figure 3.9. CircCLASP1 expression after RNase R treatment and oligo-dt based cDNA synthesis. A. circCLASP1 and circHIPK3 are resistant to RNAse R significantly when compared to linear GAPDH. Normalization were performed by 2 $^{\Delta\Delta Ct}$ method by using circHIPK3 as a reference RNA. B. circHIPK3 and circCLASP1 were eliminated nearly -5 log2 FC in oligo-dt-based reverse transcribed cDNA compared to random hexamer based cDNA. Normalization were performed by 2 $^{\Delta\Delta Ct}$ method by using GAPDH as a reference RNA.

specifically the has_circ_0007052 (circCLASP1) (Figure 3.7B). Identification of circRNAs relies on mapping uncommon BSJ reads to the reference genome. However, even though these approaches have been developed to uncover the discrimination problems among internal alternative splicing events, short read-based RNA-seq experiments still have caused false-positive circRNA identifications originating from trans-splicing events during library preparation or genomic rearrangements (Dodbele, Mutlu, and Wilusz 2021). Therefore, RNase R treatment was performed to ensure the circularity of circCLASP1. RNase R resistivity of circular RNAs has a spectrum (Szabo and Salzman 2016). Thus, circHIPK3, resistant to RNase R, is used as a positive control (Zhao et al. 2022). CircCLASP1 is 2-fold more sensitive to RNase R than circHIPK3;

however, 8-fold more resistant to RNase R than linear GAPDH mRNA (Figure 3.8A) (Table 3.1).

Table 3.1. Representation of linear GAPDH, circHIPK3 and circCLASP1 abundancy after RNase R treatment. After RNase R treatment, circHIPK3 ct values were shifted 3 cq whereas circCLASP1 and GAPDH were shifted 4 cq and 7 cq, respectively.

Primers	**Total RNA**			**RNaseR treated**		
GAPDH	11.02	12.1	11.9	18.54	18.51	18.54
circHIPK3	18.16	18.34	18.56	20.89	21.19	21.4
circCLASP1	22.23	22.06	21.75	25.36	26.26	25.81

3.3.2. circBNC2 is a CP-Repressible, RNase R-resistant, Circular RNA Transcript Expressed in HeLa cells

circBNC2, located in chr9:16727794-16738483 (-), was validated using the same circular RNA validation strategies explained in detail above. circBNC2, consisting of exon 2 and exon 3 of the BNC2 pre-mRNAs. Divergent primers were designed to validate circBNC2 using qPCR (Figure 3.10A). The potential off-target effect was eliminated by using circPrimer 2.0. However, the forward primer spans BSJ and overlaps with linear exon 7 bp. The primer that overlaps linear exon more than 5 bases might result in an unintended linear product. However, the primer pair is specific to desired circBNC2 isoform (Figure 3.10B). The BSJ was confirmed by Sanger sequencing and RNase R treatment. Additionally, another pair of divergent primer sets are summarized in Table 2.1. were used to amplify circBNC2 in subsequent experiments (Table 2.1).

Differential expression of circBNC2 in CP-treated HeLa cells was validated by qPCR. The -1 log2 fold change downregulation of circBNC2 was observed using qPCR, which is similar to RNAseq data which indicated a log2FC -1.5 (Figure 3.11A). Linear BNC mRNA was downregulated -6 log2 FC in CP-treated HeLa cells (Figure 3.10A, Figure 3.10C).

Interestingly, the zinc finger protein basonuclin 2 (BNC2) acts as a tumor suppressor in multiple cancers in an unidentified manner (Vanhoutteghem et al. 2011). Moreover, it was identified as a putative tumor suppressor gene in a high-grade serous ovarian carcinoma (Cesaratto et al. 2016). The CP treatment in HeLa cells dramatically decreased BNC2 expression (Figure 3.11C). It could depend on either the cell-type-specific function of BNC2 or the survival effect of HeLa cells against CP.

A.

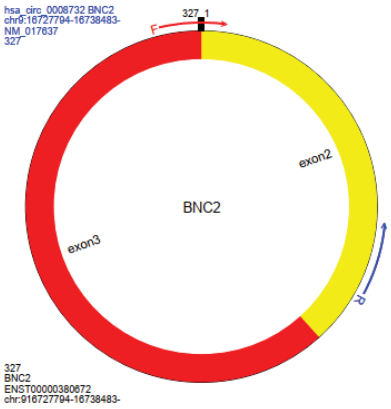

B.

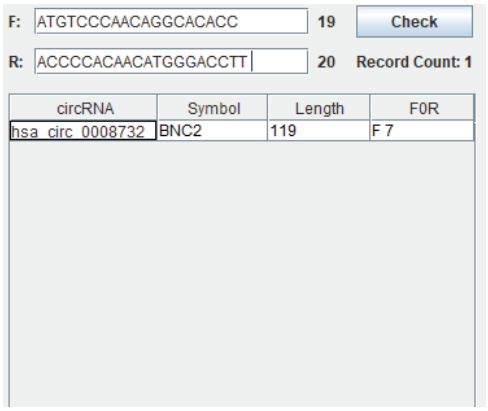

Figure 3.10. Primer designing to validate circBNC2. A. Locations of forward and reverse primers to amplify BSJ of circBNC2. B. Confirmation of off-target circular isoform amplicons of designed divergent primer sets. The CircPrimers 2.0 tool was used to annotate circBNC2.

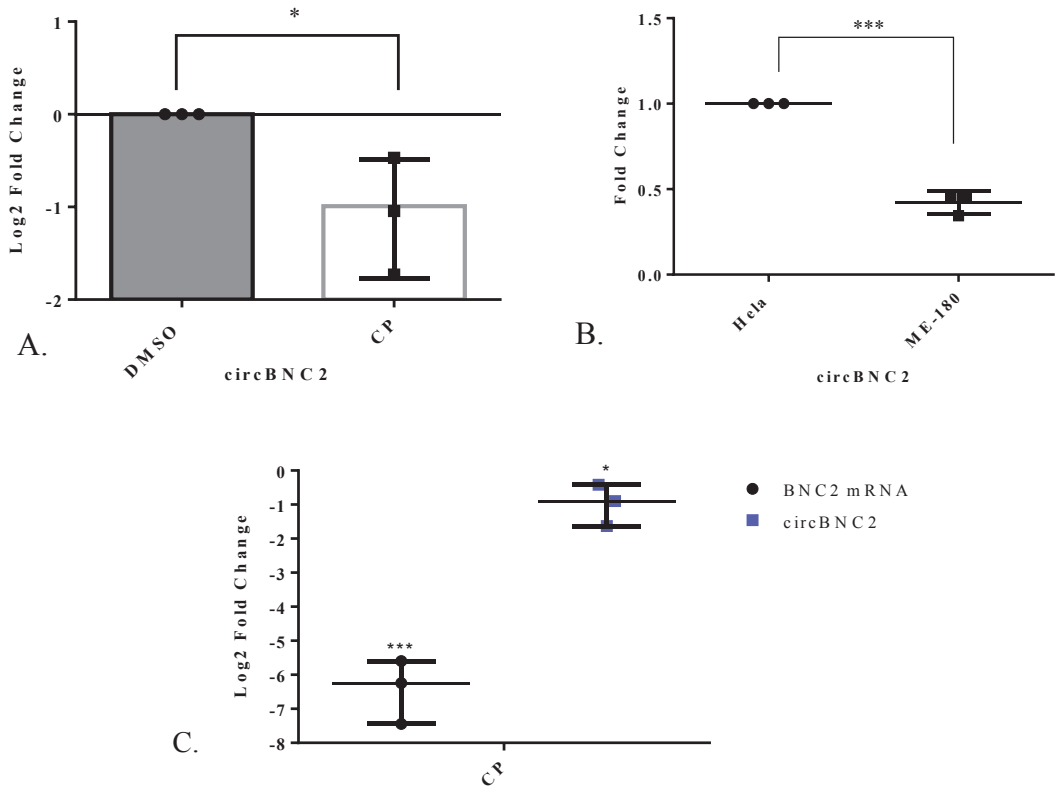

Figure 3.11. The expressions of circBNC2 and BNC2 mRNA in CP-treated HeLa cells A. qPCR indicates that circBNC2 downregulated in CP-treated HeLa cells. B. circBNC2 diminished in ME-180 cell line compared to HeLa. C. Graphical representation of linear BNC2 and circBNC2 (indicated as blue squares) differemtial expression in CP-treated HeLa cells. Normalization were performed by $2^{\Delta\Delta Ct}$ method by using GAPDH as a reference RNA. The results are shown as mean ± sD of three independent experiments with *p,0.05.

circBNC2, the CP repressible circRNA, was downregulated -1 log2 FC in highly proliferative cervical cancer cell line ME-180 (Figure 3.11B). It could be speculated that both BNC2 and circBNC2 might be tumor suppressor transcripts involved in CP resistance mechanisms in HeLa cells.

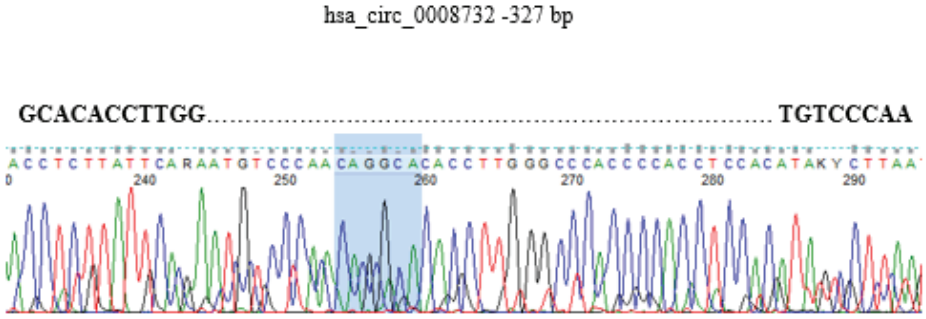

Figure 3.12. Confirmation of circBNC2 back-splicing junction by Sanger sequencing. The ABI format chromatogram was observed by using Finch TV tool. L: NEB 50 bp ladder. BSJ length: 119 bp, mature sequence of circCLASP1: 327 bp.

Confirming the circBNC2 back-splice junction (BSJ) by Sanger sequencing provides further evidence for the circular nature of particular RNA (Figure 3.12). It was shown that circBNC2 is downregulated in CP-treated cells, suggesting that it may have a specific function affected by the CP treatment. The observation that circBNC2 is RNase R resistant indicates that it has a circular structure, and the fact that it is eliminated by oligo-dT treatment supports the idea that it lacks a poly(A) tail (Figure 3.13A-B).

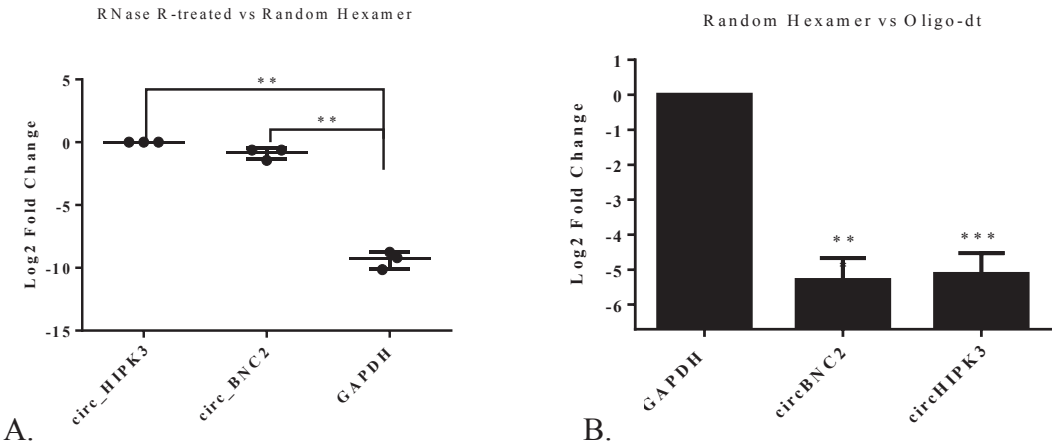

A. B.

Figure 3.13. circBNC2 expression after RNase R treatment and oligo-dt based cDNA synthesis. A. circBNC2 and circHIPK3 are resistant to RNAse R significantly when compared to linear GAPDH. Normalization were performed by 2 $^{\Delta\Delta Ct}$ method by using circHIPK3 as a reference RNA. B. circHIPK3 and circCLASP1 were eliminated nearly -5 log2 FC in oligo-dt-based reverse transcribed cDNA compared to random hexamer based cDNA. Normalization were performed by 2 $^{\Delta\Delta Ct}$ method by using GAPDH.

Overall, these findings support the existence and potential importance of circBNC2 as a functional RNA molecule in HeLa cells.

3.3.3. circGALNT2 and circBIRC6 are CP-modulated, RNase R-Resistant, Circular RNA Transcripts Expressed in HeLa Cells

circGALNT2, located in chr1:230313963-230339036(+), and circBIRC6 located in chr2:32639836-32641231 (+) were validated in HeLa cells. Results support that circGALNT2 and circBIRC6 are the covalently closed circular RNA transcript without 5'cap and 3'tail (Figure 3.14).

Based on the RnaseR-treatment followed by qPCR, circBIRC6, and circGALNT2 were enriched by approximately 2.5 and 0.5 log2FC, respectively, compared to circHIPK3 (Figure 3.14C). GAPDH mRNA degraded -3 log2FC after RNase R-treatment. The fact that they are RNase R resistant suggests that they have a circular structure, as linear RNAs are typically susceptible to degradation by this enzyme. circGALNT2 and circBIRC6 were eliminated -7 log2FC when oligo-dT-based cDNA is used, suggesting that they do not have a poly(A) tail (Figure 3.14D), a characteristic feature of most messenger RNAs (mRNAs). Instead, circular RNAs are known to be generated through back-splicing, in which a downstream splice site is joined to an upstream splice site, resulting in a circular RNA molecule that lacks a free 3' end. It was shown that circGALNT2 is upregulated 2 log2FC and circBIRC6 is downregulated -0.6 log2FC. GALNT2 mRNA and BIRC6 mRNA -2,5 and -0,8 log2FC, respectively (Figure 3.15).

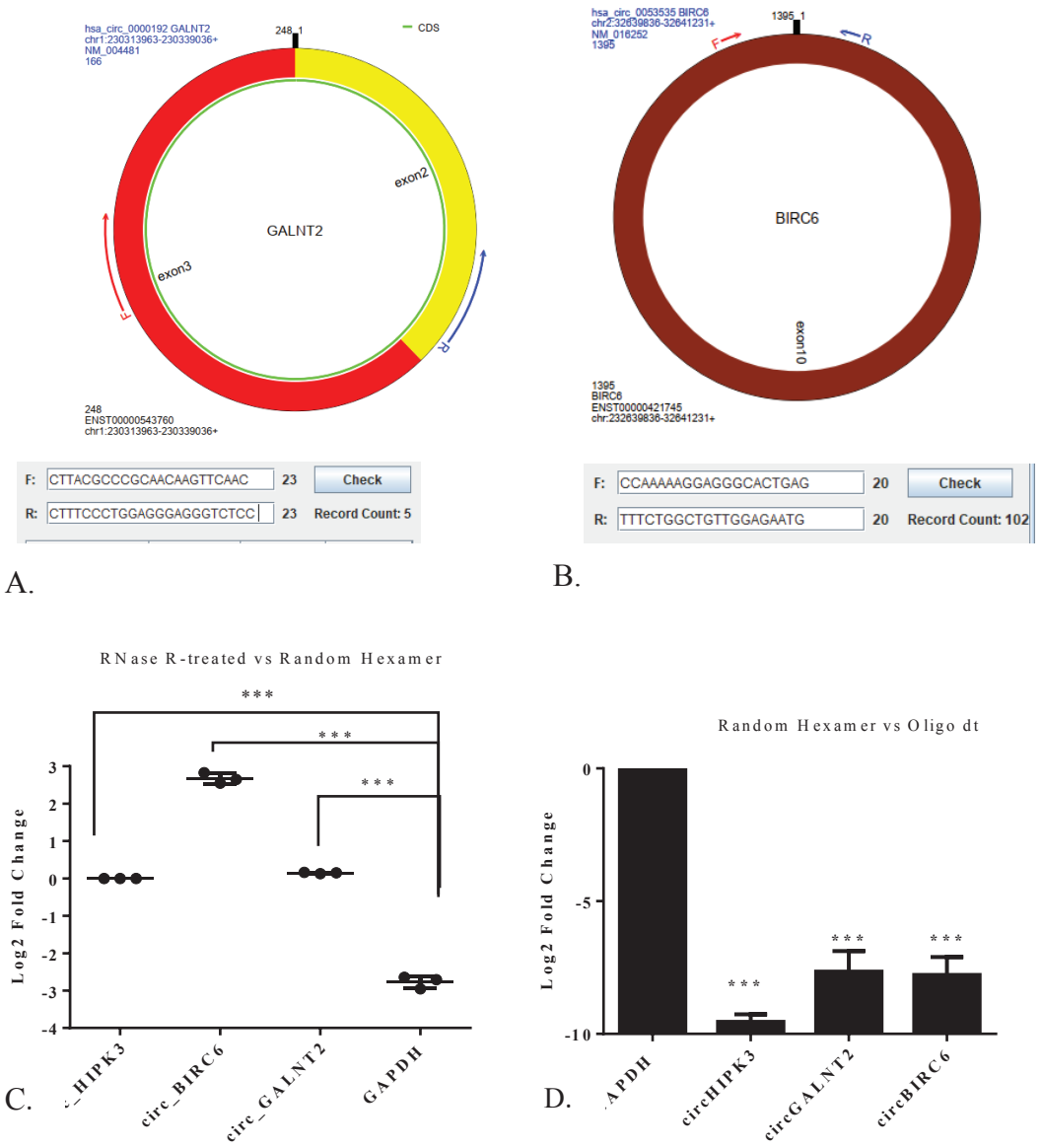

Figure 3.14. The validation of circBIRC6 and circGALNT2 in HeLa cells. A. Schematical representation of circGALNT2 and circBIRC6 indicates that divergent primers that used for Qpcr. Primer check tables shows circular isoforms amplified by using particular primer pair. C.. RNase R-resistance of circBIRC6 and circGALNT2 D. circBIRC6 and circGALNT2 were eliminated by using oligo-dt based cDNA as template for Qpcr. Normalization were performed by 2 ΔΔCt method by using GAPDH as a reference RNA. The results are shown as mean ± sD of three independent experiments with *p,0.05.

These findings suggest that circBIRC6 and circGALNT2 are circular RNAs likely to have distinct functions in HeLa cells and are structurally different from linear mRNAs. Further studies will be needed to elucidate their precise roles and mechanisms of action.

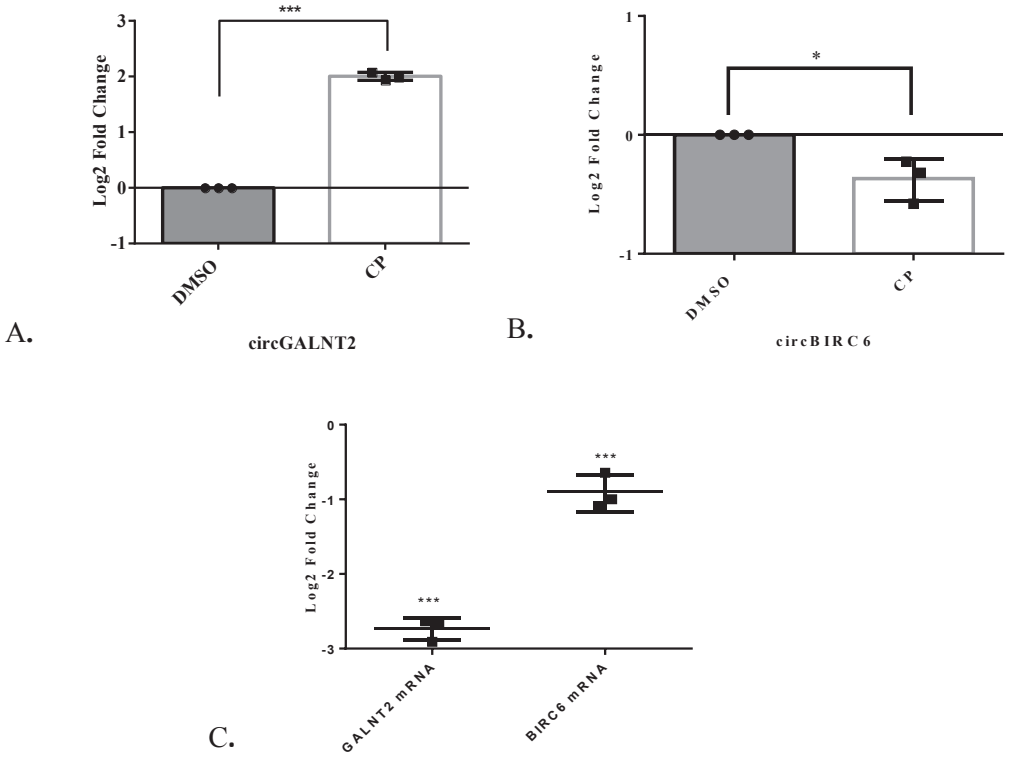

Figure 3.15. Differential expression of circGALNT2 and circBIRC6 in CP-treated HeLa cells. A. Differential expression of circGALNT2 in CP-treated HeLa cells. B. Differential expression of circBIRC6 in CP-treated HeLa cells. C. Graphical representation of linear GALNT2 and linear BIRC6 differemtial expression in CP-treated HeLa cells. Normalization were performed by $2^{\Delta\Delta Ct}$ method by using GAPDH as a reference RNA. The results are shown as mean ± sD of three independent experiments with *p,0.05. DM:DMSO (Dimethyl sulfoxide) CP:Cisplatin (Cis-diamminedichloroplatinum II). Unpaired two-tail students' t test were performed for Statistical analysis.

3.4. Functional Characterization of the Differential Expressed Circular RNAs in CP-Treated HeLa Cells

The growth curve of the HeLa cell was optimized to investigate the proliferative effect of circRNAs on HeLa cells with gain-of-function and loss-of-function studies. The best cell seeding count to observe the impact of the particular circRNA on HeLa cell proliferation is defined as 5,000 cells. Moreover, the transient transfection incubation time was 72 hours for silencing and 48 hours for overexpression experiments (Figure 3.16).

However, the experimental setup of rescue experiments was designed to be overexpressed 24 hours after silencing and incubated for 48 hours to avoid the possibility that overexpression for 24 hours after 24 hours of silencing was not sufficient to establish the phenotype.

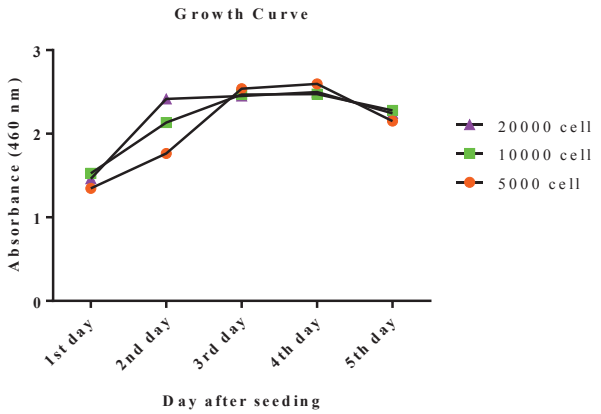

Figure 3.16. The growth curve of HeLa cells after 24-48-72-96-120 hours of incubation after 5,000, 10,000, and 20,000 cell seeding.

3.4.1. Knockdown and Overexpression of circGALNT2 have no Significant Effect on HeLa cell Apoptosis and Proliferation

To elucidate the effect of the knockdown of circGALNT2 on HeLa cell proliferation and apoptosis, WST-8 and Annexin V/7AAD assays were performed circGALNT2 knockdown. In the context of WST-8 analysis, the silenced group of HeLa cells showed no significant change (Figure 3.17D).

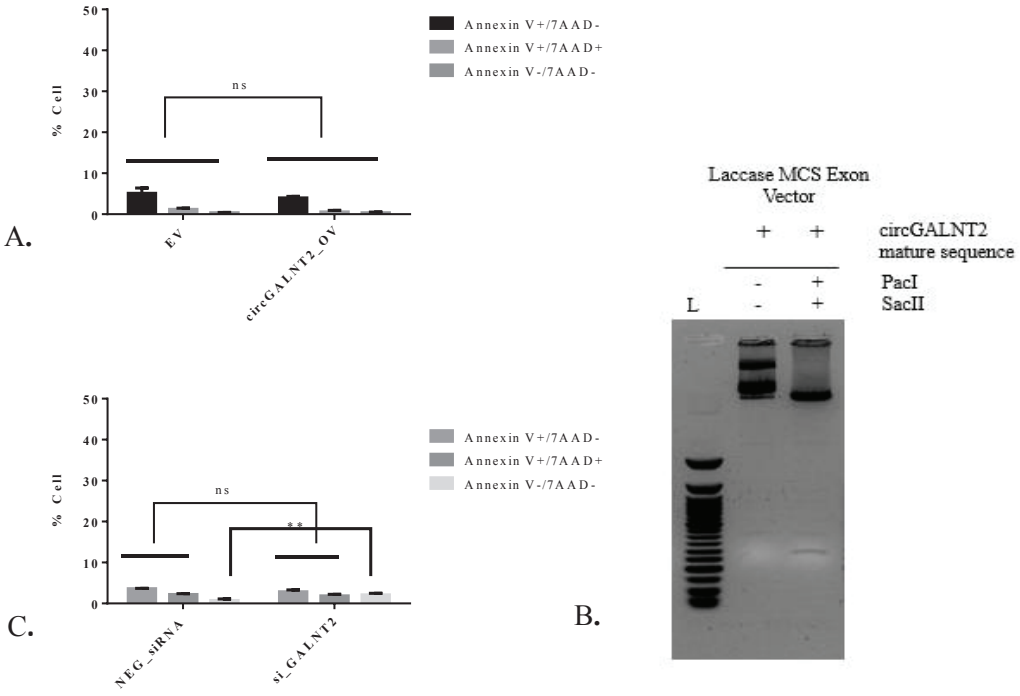

Figure 3.17. CircGALNT2 overexpression has no significant effect on HeLa cell apoptosis, whereas knockdown promotes dead cells slightly. A. Graphical representation of the circGALNT2 overexpressed HeLa cells on HeLa cell apoptosis. B. Agarose gel electrophoresis (100V, 45 min, 1%) represents circGALNT2 overexpression contruct confirmation by double digestion. C. Flow cytometry analysis of the circGALNT2 silenced HeLa cells. Cells were analyzed after staining with FITC-conjugated Annexin V and 7AAD by flow cytometer. D. WST-8 analysis of circGALNT2 knockdown HeLa cells. E.. Graphical representation of circGALNT2 knockdown followed by CP-treatment.

Cont. on next page

Figure 3.17 cont.

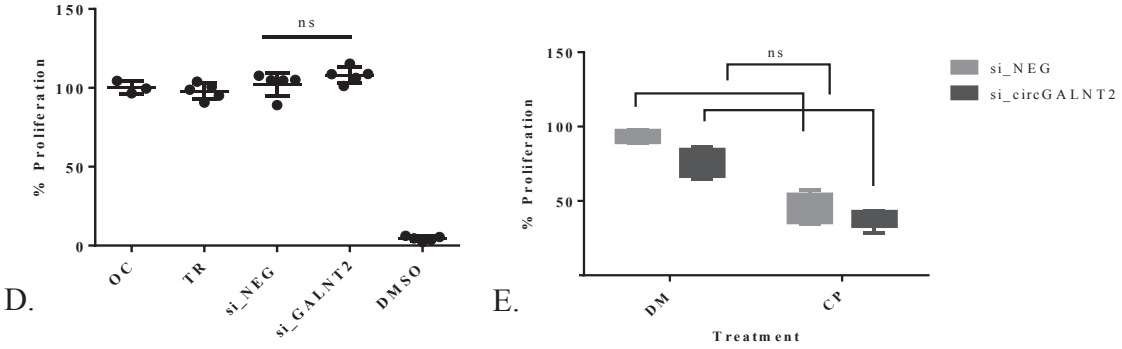

The annexin V/7AAD assay indicated that silencing of circGALNT2 knockdown promotes death cells by approximately 5% (Figure 3.17C). However, no significant changes are observed in the early or late apoptosis quadrants Q2 and Q4 (Figure 3.17C). The overexpression of circGALNT2 has no significant effects on HeLa cell apoptosis (Figure 3.17A). The WST-8 assay indicated that circGALNT2 silencing does not affect cell proliferation (Figure 3.17D).

According to the results, the circGALNT2 knockdown group and the si_NEG group showed similar patterns after 80 μM CP treatment for 16 h, repressing HeLa cell viability at 50% and 40%, respectively. It should be noted that despite a difference between the percent repression of the HeLa cell, viabilities in five replicates are statistically non-significant (Figure 3.17E).

3.4.2. Knockdown of circBNC2 does not Affect HeLa Cell Apoptosis and Proliferation

WST-8 assay was performed to elucidate the effect of the circBNC2 knockdown. As data points out, neither knockdown nor overexpression of circBNC2 significantly affects the proliferation of HeLa cells (Figure 3.18A, C).

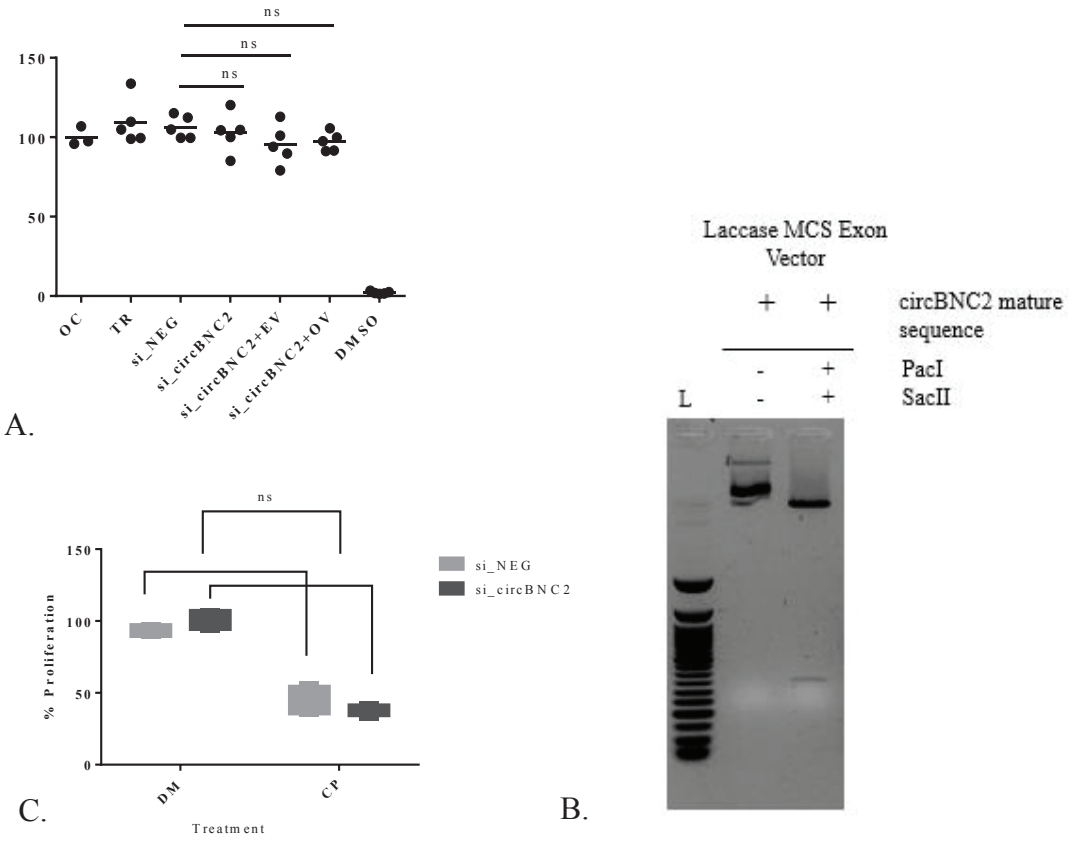

Figure 3.18. circBNC2 have no significant effect on HeLa cell proliferationa and apoptosis. A. Graphical representation of the proliferation rates of HeLa cells treated with circBNC2 silencing followed by overexpression. B. Agarose gel elctrophoresis (100V, 45 min, 1%) indicated double digestion of circBNC2 overexpression construct. C. Effect of the knockdown of circBNC2 on the HeLa cells treated with 80 μM CP. L: NEB 50 bp. CircBNC2: 327 bp. The results are shown as mean ± sD of three independent experiments with *p,0.05.

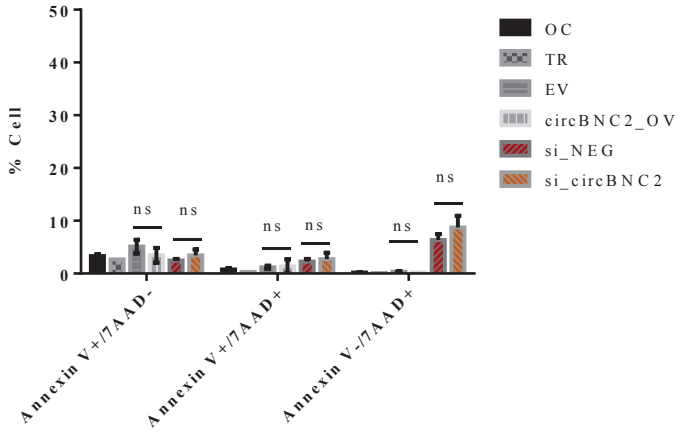

Figure 3.19. Measurement of the apoptosis rates of circBNC2 silenced and overexpressed HeLa cells by flow cytometry. CircBNC2 does not indicates significant change on HeLa cell apoptosis. Cells were analyzed after staining with FITC-conjugated Annexin V and 7AAD by flow cytometer. The results are shown as mean ± sD of three independent experiments with ns*>0.05

The graph shows the proliferation rates of HeLa cells. Proliferation % values were calculated by accepting the only-cell (OC) group as 100% after 72 hours of silencing. DMSO %5 was used as a negative control group, and consistent absorbance values of the OC group suggested that the WST-8 assay successfully detects cell proliferation. Furthermore, early- and late apoptosis and dead cell rates were not affected by the gain or loss of function of the circBNC2 (Figure 3.19). Additionally, the effect of the IC50 dose (80 μM) on HeLa cell viability did not change when circBNC2 was silenced (Figure 3.18C).

3.4.3. Knockdown of circBIRC6 Represses HeLa Cell Proliferation

WST-8 assay was used to examine the effect of circBIRC6 on HeLa cell proliferation. The graph showed the % proliferation of HeLa cells. Proliferation % values were calculated by accepting the only-cell (OC) group as 100% at 72nd hours of silencing.

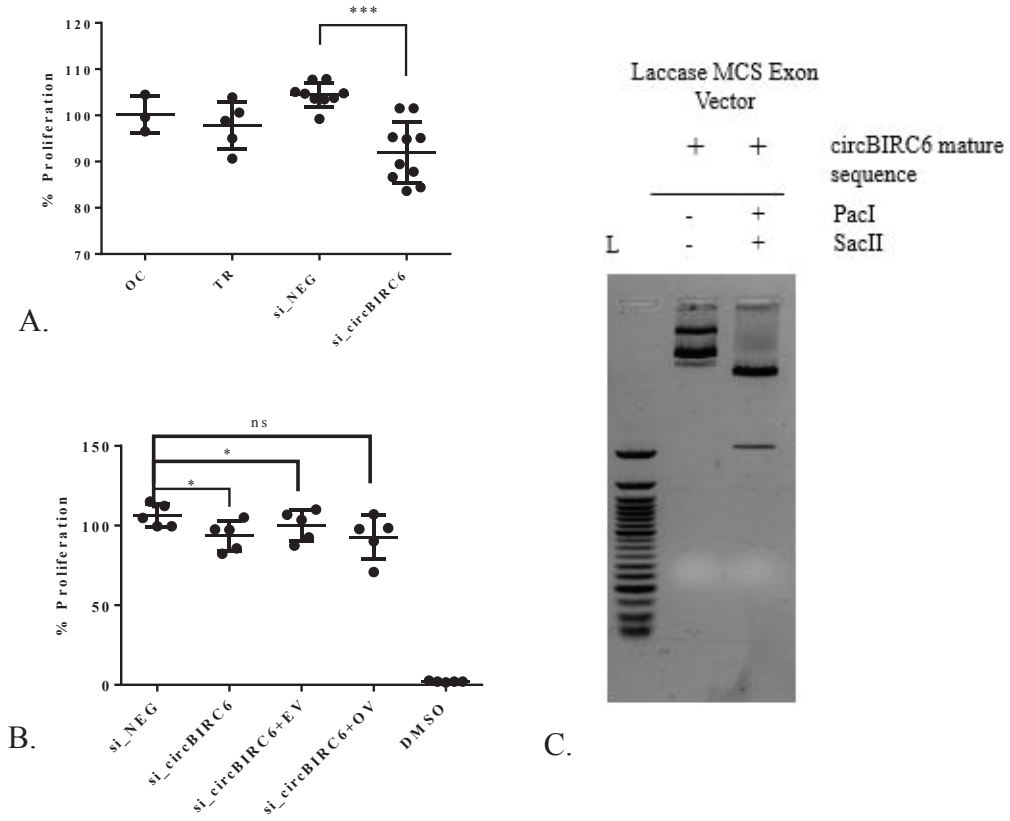

Figure 3.20. Knockdown of circBIRC6 represses HeLa cell proliferation. A. Graphical representation of the proliferation rates of circBIRC6 silenced HeLa cells. B. Graphical represeantation of rescue experiment by WST-8 assay. Absorbance readings of the WST-8 assay were measured by SkanIt Spectrophotometer at 460 nm. L: NEB 50 bp DNA ladder. CircBIRC6:1395 bp. The results are shown as mean ± sD of three independent experiments with ns>0.05 *p,0.05.

The findings indicated that circBIRC6 silencing repressed HeLa cell proliferation after 72 hours. However, subsequent overexpression experiments could not rescue this repression (Figure 3.20). The inability to rescue the phenotype by overexpression does not dismiss this circRNA as a potential candidate. Under certain circumstances, the back-splicing process often remains inefficient, producing numerous undesirable transcripts such as unspliced RNAs, concatamers, or trans-spliced RNAs (Dodbele, Mutlu, and Wilusz 2021). These mature sequence-dependent circRNAs might be toxic and thus can disrupt the protective effect of the particular circRNA.

3.4.4. circCLASP1 Promotes HeLa Cell Proliferation

3.4.4.1. CircCLASP1 Silencing Represses HeLa Cell Proliferation

CircCLASP1 overexpression plasmid was constructed by molecular cloning and confirmed by Sanger sequencing. The mature sequence of circCLASP1 was successfully cloned into laccase MCS Exon Vector (Figure 3.21A). Firstly, circCLASP1 was overexpressed in HeLa cells. The overexpression of circCLASP1 increased HeLa cell proliferation by nearly 20% in 48 hours (Figure 3.21B). Then circCLASP1 was targeted

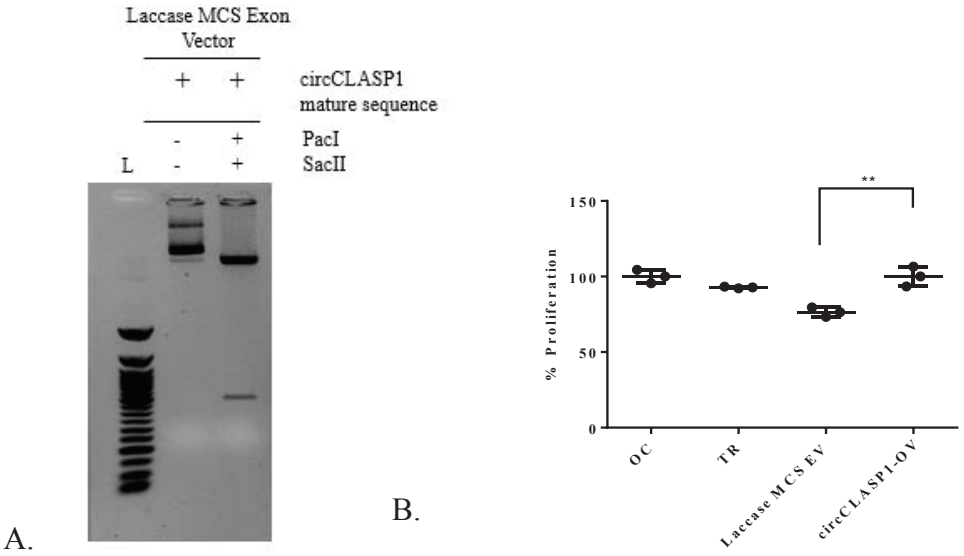

Figure 3.21. Agarose gel electrophoresis (%1, 100 V, 30 min) gel image indicates the double digestion of circCLASP1 overexpression plasmid. Mature sequence of circCLASP1 (480 bp) was confirmed by double digestigon using PazI and SacII restriction enzymes, and Sanger sequencing (Data is not shown). B. Graphical representation of proliferation rate of Hela cells after circCLASP1 overexpression L: NEB 50 bp DNA ladder. Laccase MCS EV: mock kontrol, circCLASP1_OV: overexpression vector. TR: Transfection reagent, OC: Only cell. % Proliferation is calculated by accepted OC as 100%.

by siRNA complementary to its BSJ, and the proliferation % rate of HeLa cells was measured by WST-8 reagent. The results clearly state that circCLASP1 silencing represses HeLa cell proliferation by approximately %17 and %23 in 48 and 72 hours, respectively (Figure 3.22C). The suppression of cell proliferation was measured at 24,

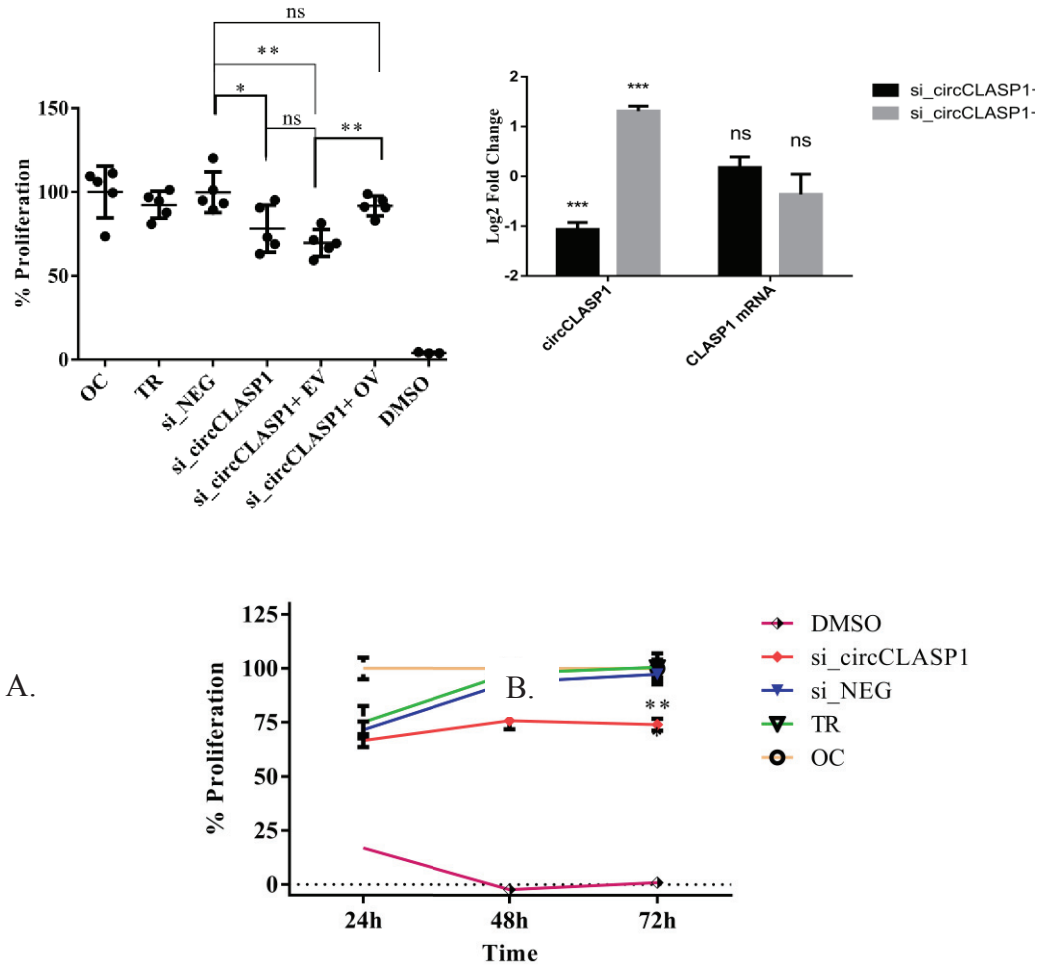

Figure 3.22. Knockdown of circCLASP1 supressed HeLa cell proliferation in a time-dependent manner. A. Knockdown of circCLASP1 inhibited proliferation. Overexpression of circCLASP1 after silencing rescued the phenotype. B. CİrcCLASP1 silenced by 55%, and overexpressed 3 simultaneously. C. Knockdown of circCLASP1 decreased HeLa cell proliferation 17% and 23% in 48, and 72 hours after transfection. si_NEG: Dharmacon On-target non-targeting siRNA, si_circCLASP1: circCLASP1 siRNA, EV: Laccase MCS Exon Vector, OV: circCLASP1 overexpression vector. The results are shown as mean ± sD of three independent experiments with *p,0.05 for A and B.

48, and 72 hours after silencing of circCLASP1. According to the results, HeLa cell proliferation had started to be repressed after 48 hours of silencing; however, the suppressive effect peaked at 72 hours after transfection (Figure 3.22C). Unfortunately, the circular RNA silencing mediated by si- and sh-RNAs have high off-target potential

because of the shared sequence with their linear mRNA counterparts (Pamudurti et al. 2020). Therefore, the only sequence that siRNA can target is the BSJ sequence which shares a common sequence with a linear mRNA counterpart of at least 8-9 nt.

The expression of linear CLASP1 mRNA was confirmed after circCLASP1 silencing to eliminate the off-target effect, and false positive phenotype originated from linear CLASP1 silencing. It was confirmed that the knockdown of circCLASP1 followed by OV (circCLASP1 overexpression) and EV(empty vector) results in any significant change in the expression of linear CLASP1 mRNA (Figure 3.22B)

3.4.4.2. CircCLASP1 Silencing Represses Proliferation by Sensitizing HeLa Cells to CP Treatment

CP treatment was performed to evaluate the effect of circCLASP1 knockdown on CP-treated HeLa cells. As seen below, the proliferation of HeLa cells was significantly suppressed when circCLASP1 was silenced. This result also confirmed the repressive effect of circCLASP1 knockdown on HeLa cell proliferation.

According to the results, the viability of only the cell group was repressed by 30% after 80 μM CP treatment for 16h. The viability (survival or growth) of the CP-treated si_NEG control group and circCLASP1 knockdown group were suppressed compared to the DMSO control groups. The suppression of viability in the si_NEG control group was 50%. Knockdown of circCLASP1 enhanced the CP effect and suppressed proliferation by up to 58% (Figure 3.23). According to flow cytometry analyses, circCLASP1 knockdown promotes early apoptosis at 2% (Figure 3.24). This change is consistent in three biological replicates. However, flow cytometry is a highly sensitive technique that can detect even small changes in cellular parameters. A 2% difference may not be biologically significant. In addition, there are no significant changes in late apoptosis and death cells (Figure 3.24).

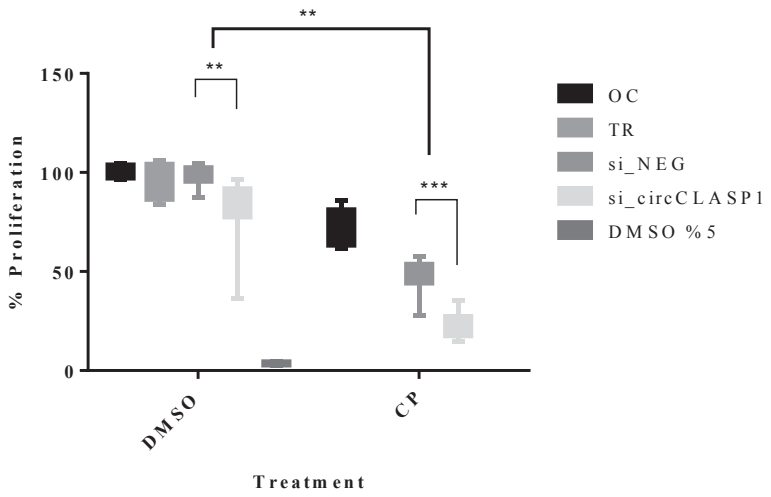

Figure 3.23. Knockdown of circCLASP1 repressed proliferation by sensitizing HeLa cells to CP. si_NEG: Dharmacon On-target non-targeting siRNA, si_circCLASP1: circCLASP1 siRNA. The results are shown as mean ± sD of three independent experiments with *p,0.05.

3.4.4.3. Knockdown of CircCLASP1 Promotes Early Apoptosis in CP-treated HeLa Cells

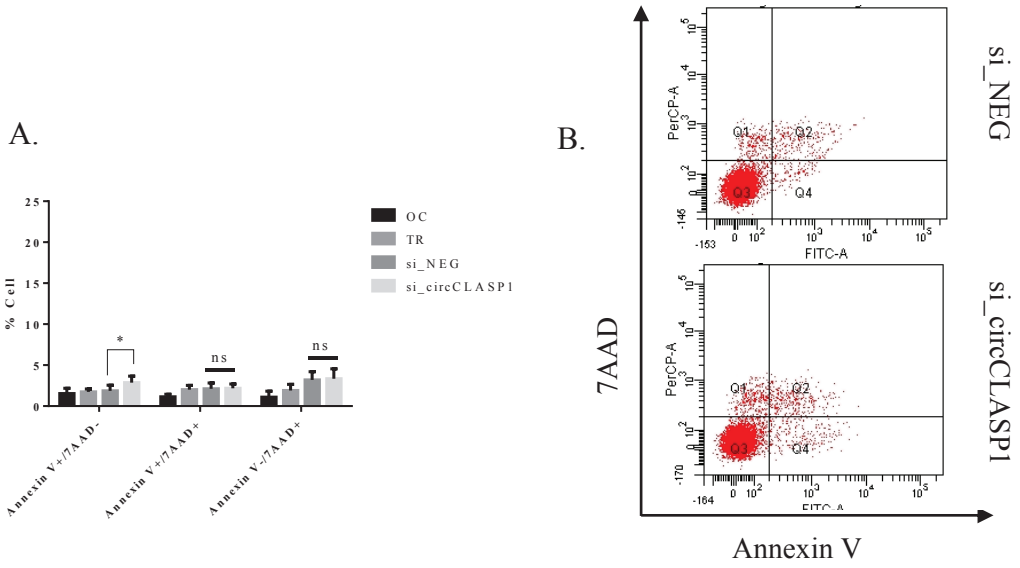

Figure 3.24. circCLASP1 knockdown promotes early apoptosis slightly. A. Knockdown of circCLASP1 promotes early apoptosis 2%, consistently. B. The cells were analyzed after staining with FITC-conjugated Annexin V and 7AAD by flow cytometer.

3.4.4.4. Knockdown of CircCLASP1 sensitizes HeLa cells against CP in a dose-dependent manner

CP treatment was performed to evaluate the effect of circCLASP1 knockdown on CP-treated HeLa cell apoptosis. The results suggest that the impact of circCLASP1 knockdown on CP-treated HeLa cells was assessed. The promotion of early apoptosis, late apoptosis, and death in response to low doses of CP (20–40 μM) and the IC50 dose (80 μM) was studied. The findings suggest that circCLASP1 silencing, followed by 20- and 40 μM of CP treatment, promotes early apoptosis. It is also interesting to note that the noticeable amount of knockdown cells dramatically shifts toward the Annexin V (-)/7AAD (+)/death quadrant, while the IC50 dose in the control group promotes nearly 45% early apoptosis as expected. The results collectively imply that circCLASP1 knockdown may increase the apoptotic response of HeLa cells to low doses of CP. However, the cell death mode might be changed when circCLASP1 was silenced and treated with 80 μM CP (Figure 3.25).

The AnnexinV-7AAD staining suggests that the knockdown of circCLASP1 enhanced the cytotoxic effect of 20 μM CP on HeLa cells for 6.4% and 2% of early apoptosis and death, respectively (Figure 3.26A). CircCLASP1 knockdown HeLa cells were sensitized to 40 μM CP for 15.3% and 4.8% as early and late apoptosis, respectively (Figure 26B). It is also interesting to note that the circCLASP1 silenced HeLa cells reached approximately IC50 (60% viability) when treated with 40 μM CP, whereas the control group viability barely decreased to 75%. Interestingly, there were noticeable differences in the circCLASP1 silenced HeLa cells treated with 80 μM CP compared to low doses. 15% of the circCLASP1 silenced HeLa cell population shifted dramatically to Annexin V-/7AAD+ dead cell Q1 quadrant compared to the control group, which is equally distributed among Annexin V-/7AAD- unstained/live and AnnexinV+/7AAD- early apoptosis quadrant as expected (Figure 3.25, Figure 3.26C).

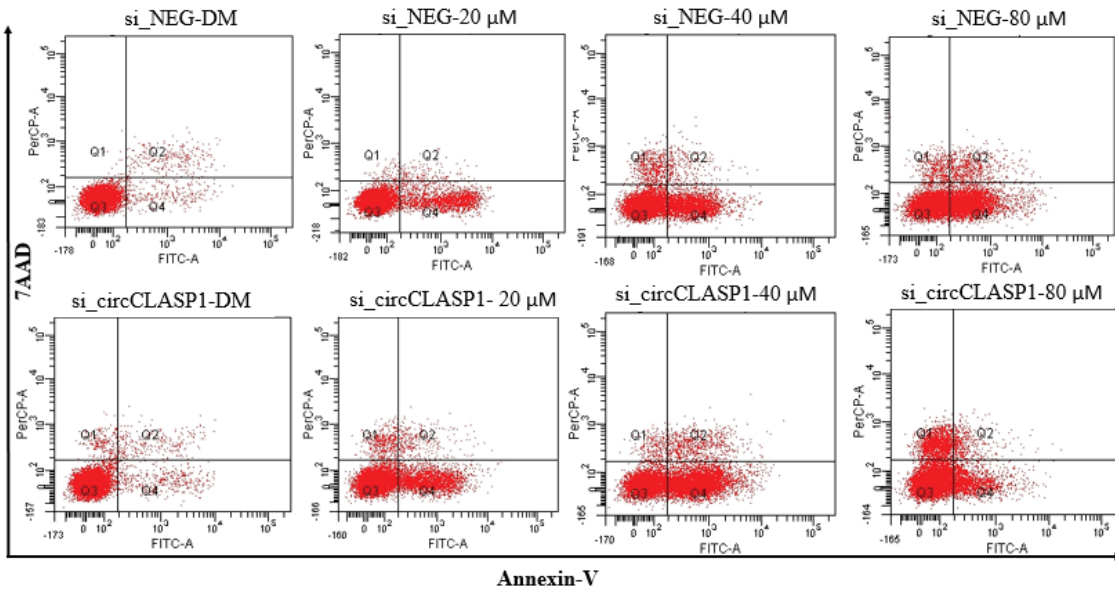

Figure 3.25. Flow cytometric analysis of early apoptosis, late apoptosis and death of circCLASP1 silenced HeLa cells followed by treatment with cisplatin (CP). CircCLASP1 knockdown and control siRNA transfected HeLa cells treated with 20-40-80 µM CP and highest amount of DMSO and maintained 16h at 37 °C CO_2 incubator. The cells were analyzed after staining with Annexin V/FITC and 7AAD by flow cytometer. The dot plot represents the DMSO-treated HeLa cells as a control group and CP-treated HeLa cells as treatment group. The early apoptosis events (Annexin V + /7AAD -) shown in lower right quadrant (Q4). The late stage of apoptosis/dead cells (Annexin V + /7AAD +) is shown in quadrant Q2. The dead cells (Annexin V- / 7AAD +) is indicated in upper right quadrant Q1. B. Bar chart shows the percentage of viable, early apoptosis, late apoptosis, and dead cells in treatment with CP on HeLa cells. The results are shown as mean ± sD of three replicates with *p,0.05.

The early apoptosis rate of si_NEG groups is 37.9% after being treated with 80 µM CP, which is barely close but not as high as the 42% early apoptosis rate of circCLASP1 silenced cells treated with 40 µM CP (Figure 3.26B, C).

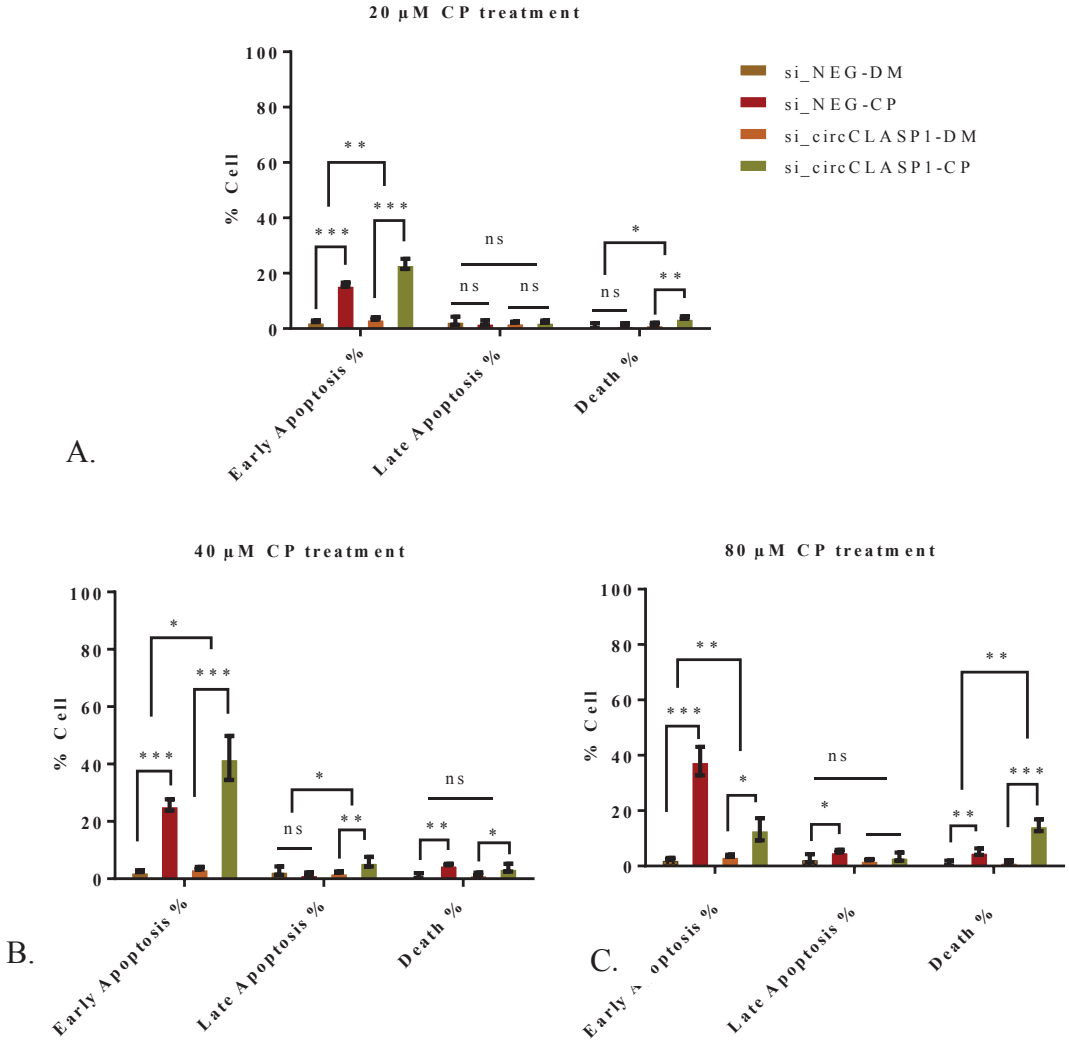

Figure 3.26. Graphical representation of Annexin V-7AAD staining of circCLASP1 silenced HeLa cells after CP treatment. A. HeLa cells were treated with 20 µM CP after circCLASP1 knockdown. B HeLa cells were treated with 40 µM CP after circCLASP1 knockdown. C. HeLa cells were treated with 80 µM CP after circCLASP1 knockdown. Early apoptosis % represents Annexin V+/ 7AAD– cells, late apoptosis % indicates Annexin V+/7AAD+ cells. Death % represents Annexin V-/7AAD+ cells. The results are shown as mean ± sD of three replicates with *p,0.05. DM:DMSO (Dimethyl sulfoxide) CP:Cisplatin (Cis-diamminedichloroplatinum II).

3.4.5. Subcellular Localization of CircCLASP1

The subcellular localization of circCLASP1 was investigated using nuclear and cytoplasmic RNA fractions. The effect of the CP treatment on the subcellular localization of circCLASP1 was also evaluated using the same approach. The GAPDH and MALAT1 were used as cytoplasmic and nuclear markers, respectively. As expected, nearly 80% of the GAPDH was in the cytoplasm, whereas 80% of the MALAT1 was in the nucleus in the DMSO-treated group (Figure 3.26A). Although circCLASP1 is an exonic circRNA, circCLASP1 is interestingly located in the nucleus in DMSO-treated control HeLa cells (Figure 3.26A).

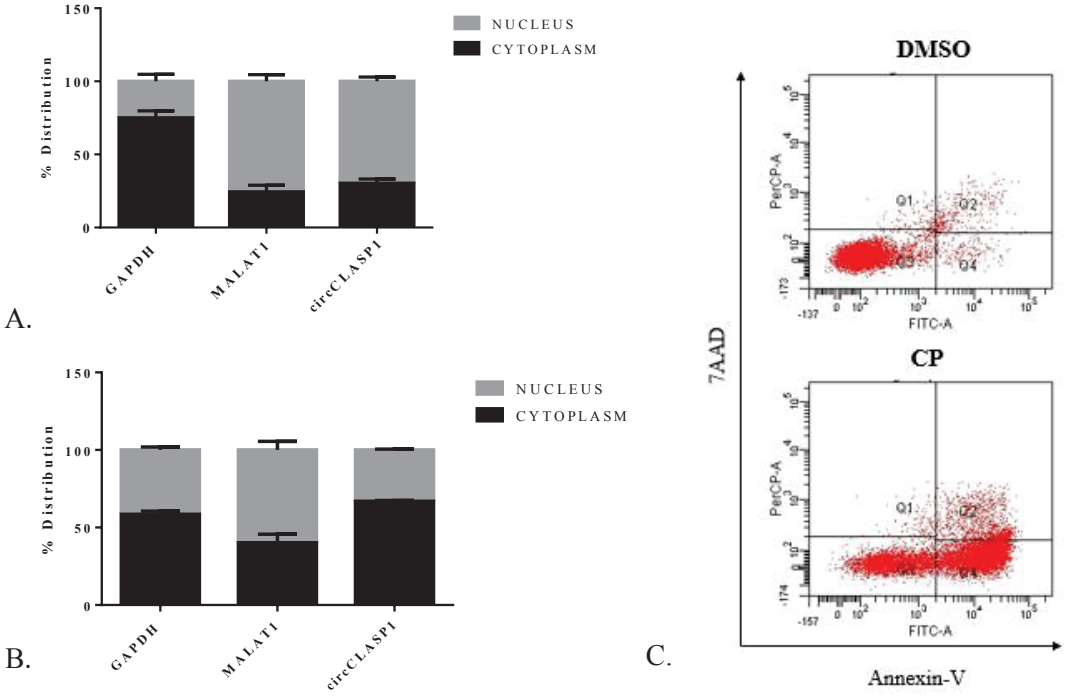

Figure 3.27. Investigation of the subcellular localization of the circCLASP1 in A. DMSO- and B. CP-treated HeLa cells. C. The dot plots represents the IC50 AnnexinV/7AAD Normalization were performed by $2^{\Delta\Delta Ct}$ method by using GAPDH as a reference RNA for cytoplasmic RNA fraction, MALAT1 RNA was used as a reference gene for nuclear RNA fraction. The results are shown as mean ± sD of three replicates with *p,0.05. DM:DMSO (Dimethyl sulfoxide) CP:Cisplatin (Cis-diamminedichloroplatinum II).

The IC50 CP dose was used to trigger apoptosis in HeLa cells to investigate whether or not circCLASP1 is localized in different subcellular compartments after CP treatment. According to the results, nearly 60% of the circCLASP1 was located in the cytoplasm. In CP-treated HeLa cells, 55% of GAPDH was found in the cytoplasm, and 60% of MALAT1 was in the nucleus. As controls, the majority of the GAPDH and the MALAT1 were located in the cytosol and nucleus, respectively. However, their distribution profiles did not disperse as dramatically as the DMSO-treated control group. As represented in dot plots, approximately 50% of the CP-treated HeLa cells are Annexin V+/7AAD- which means they lost their membrane integrities. As known, apoptotic nucleus remodeling includes increased nuclear permeability, chromatin condensation, DNA fragmentation, nuclear pore clustering, nuclear envelope blebbing, and, eventually, fragmentation. Thus, this abnormal distribution in control groups is acceptable (Figure 3.27B, C).

3.4.7. Transcriptomics Profiling of circCLASP1-Silenced HeLa Cells

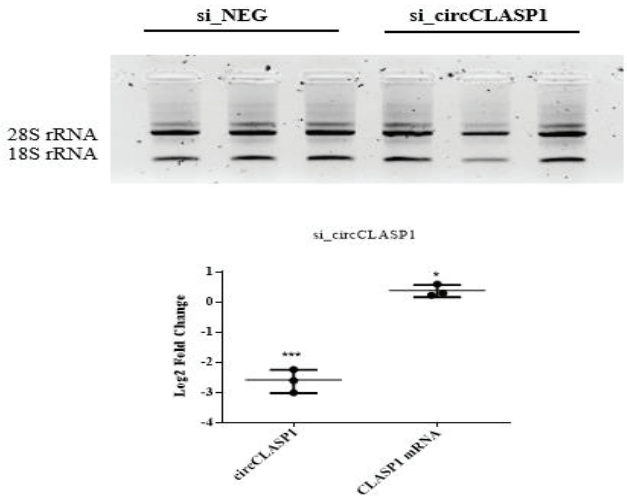

Figure 3.28. Quality control of circCLASP1 silencing for performing transcriptomics analysis to reveal transcriptomics changes followed by circCLASP1 silencing in HeLa cells. A. Agarose gel electrophoresis (100V,30 min,1%) showed the integrity of RNAs isolated from HeLa cells transfected with si_NEG and si_circCLASP1, respectively. B. Graphical representation of circCLASP1 and linear CLASP1 expression fold changes in HeLa cells after transfected with si_circCLASP1 compared to si_NEG.

Gain-of-function and loss-of-function experiments indicated that circCLASP1 silencing represses HeLa cell proliferation and significantly sensitizes HeLa cells to CP. Transcriptomics profiling of HeLa cells after circCLASP1 silencing was performed to

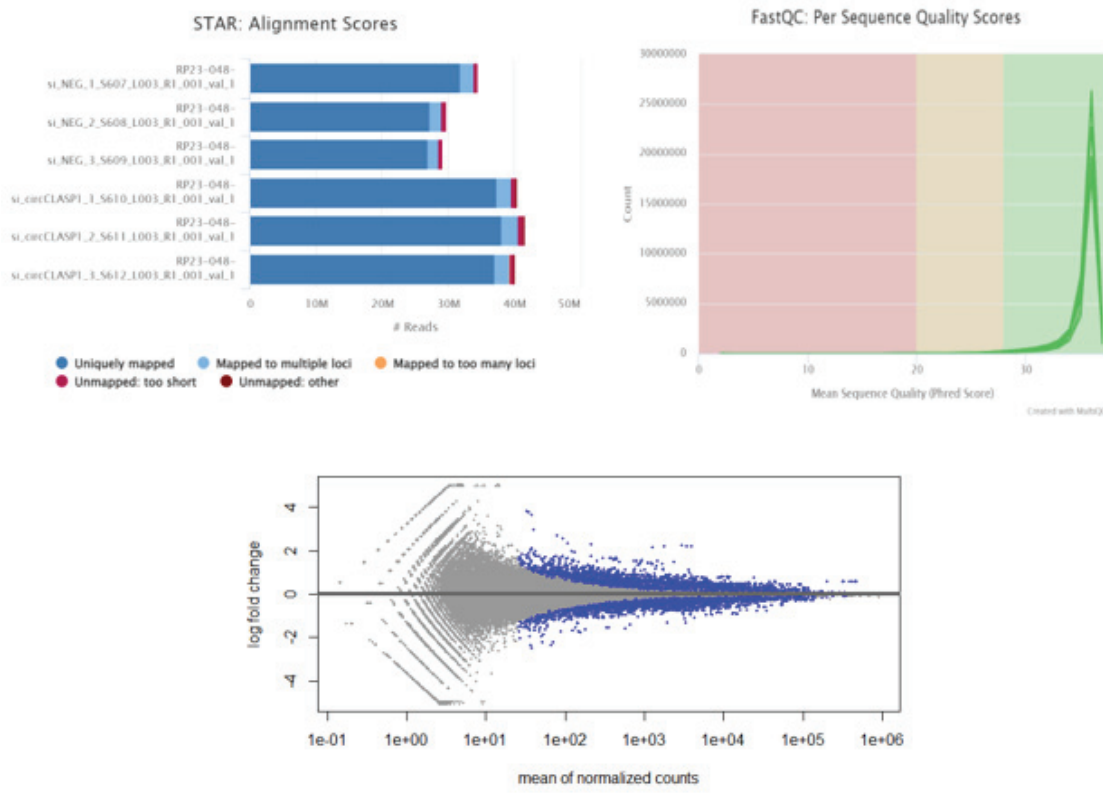

Figure 3.29. Quality control tool for high throughput sequence data with MultiQC. A. STAR alignment scores. B. Per sequence quality scores. Y axis illustrates counts while X axis shows phred score. C. The MA plot of the expression levels.

gain insight into the changes in the gene expression upon circCLASP1 knockdown (Figure 3.28). The quality control of FastQ files is performed using FASQC (Figure 3.29). The genome mapping statistics clearly showed that the ratios of the uniquely mapped reads were above 90% (Figure 3.29A).

The per sequence quality analysis showed that all samples have a phred score above 30 (Q30), and the precision of base call accuracy is above 99.9%. This is equivalent to the probability of an incorrect base call 1 in 1000 times (Figure 3.29B). The quality control of the normalization of RNA-seq data is visualized using an MA plot. MA plot is a scatter plot where the x-axis illustrates the mean of normalized counts across control and treatment samples, whereas the y-axis shows the log2FC in the given

contrast. As expected, the MA plot showed that most points are on the zero line (Figure 3.29C).

The gene expression analysis of circCLASP1 knockdown cells illustrated that 1193 transcripts were significantly upregulated and 667 transcripts were downregulated (Log2FC >0,67, Log2FC <0,67, padj<0.05). The heat map shows the top 1000 differentially expressed transcripts (Figure 3.30). The volcano plot shows the differential expression of the comparison si_circCLASP1 vs. si_NEG (Figure 3.31).

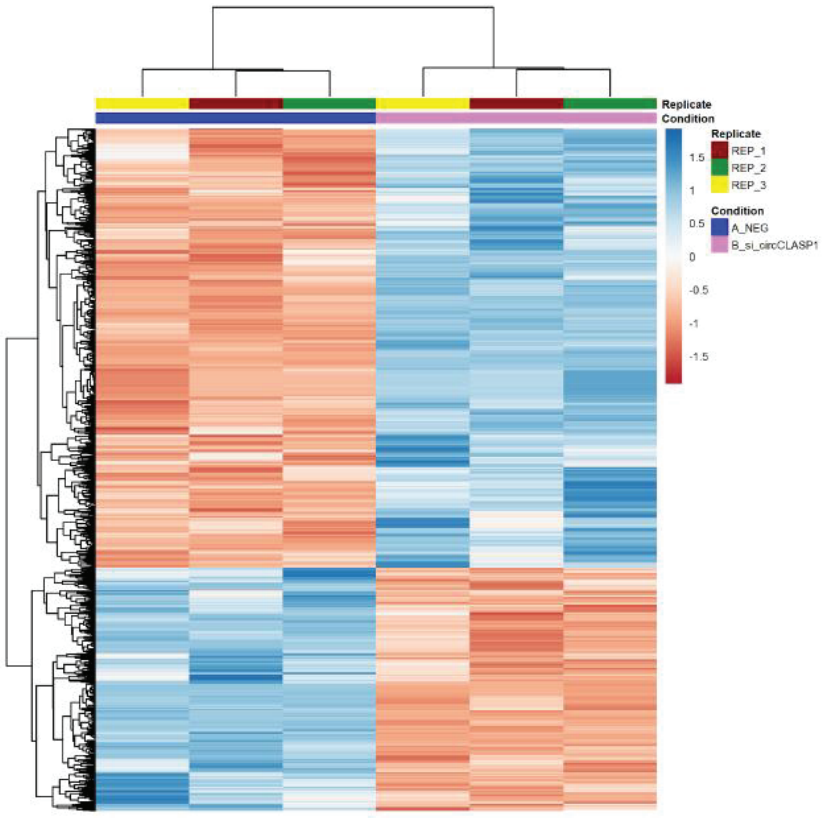

Figure 3.30. Differential gene expression pattern. The heat map shows RNA-Seq differential expression data. Pairwise comparisons are shown for each group (columns). Blue indicates higher expression in the si_circCLASP1 groups compared with the second; red shows downregulation. RNA samples are as follows: si_NEG, si_circCLASP. The graph illustrates all significant genes with log2FC>0.67 and log2FC<-0.67. Padj<0.05

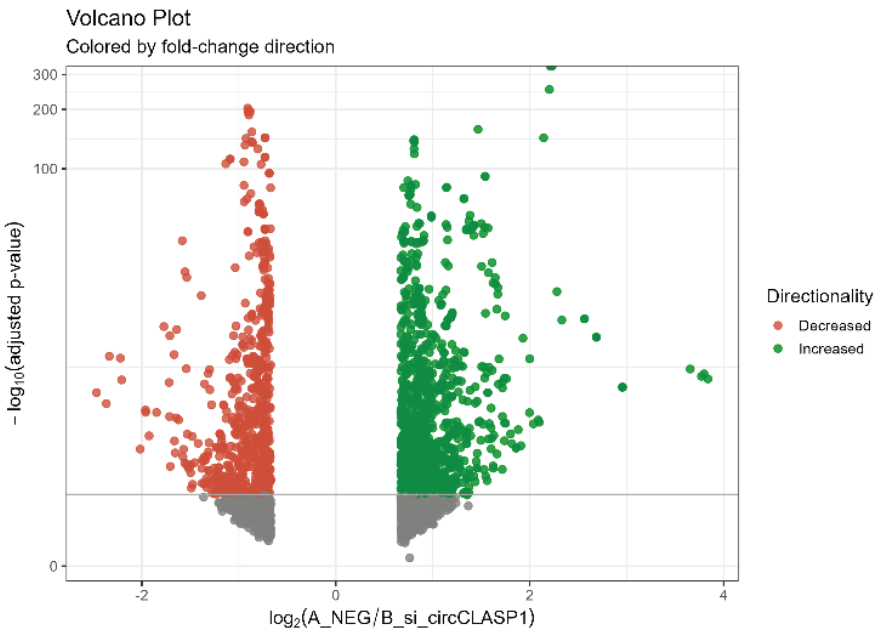

Figure 3.31. The volcano plot of differentially expressed genes was identified between the circCLASP1 knockdown and negative control groups. The green dots indicate up-regulated gene expression, the red dots indicate down-regulated gene expression, and the gray dots denote the gene expression without marked differences.Treshold is log2FC>0.67 or <-0.67.

The table showed the most differentially expressed genes according to Log2FC. The most upregulated genes are SAA2 (Serum Amyloid A2), UNC13A (Unc-13 Homolog A), HMOX1 (heme oxygenase 1), and IL1B (Interleukin-1 beta). On the other hand, MEDAG (Mesenteric Estrogen Dependent Adipogenesis), COXB2 (Cytochrome C Oxidase Subunit 6B2), ELAPOR1 (endosome-lysosome associated apoptosis and autophagy regulator 1), DOCK2 (Dedicator of cytokinesis 2), and MUSTN1 (Musculoskeletal, Embryonic Nuclear Protein 1) were the genes that most downregulated (Figure 3.32).

Gene	Log2FC		P Value	P-adj
SAA2	3.837378569	▲	4.24E-10	1.62E-08
UNC13A	2.564738904	▲	2.04E-19	2.27E-17
HMOX1	2.230910715	▲	0	0
IL1B	2.098514861	▲	2.50E-06	4.85E-05
ANKRD1	1.999814841	▲	1.43E-12	7.82E-11
MEDAG	-2.466693806	▼	1.05E-08	3.21E-07
COX6B2	-2.366032074	▼	9.68E-08	2.50E-06
ELAPOR1	-2.334852095	▼	6.41E-13	3.67E-11
DOCK2	-1.713272008	▼	7.33E-18	7.08E-16
MUSTN1	-1.706643305	▼	9.98E-07	2.11E-05

Figure 3.32. Genes showing the highest differential expression in circCLASP1 silenced HeLa cells compared to the control group. Log2FC: log2 fold change, Red arrows denote downregulated genes, green arrows denote upregulated genes.

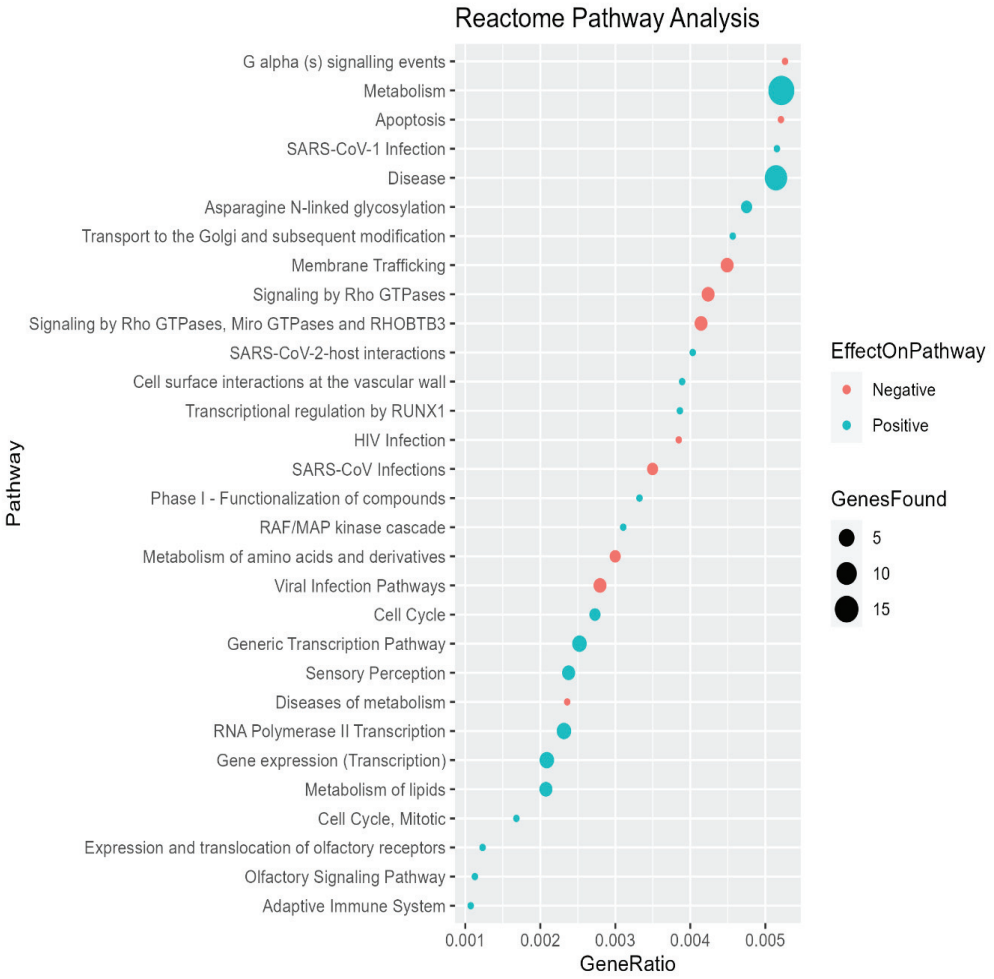

Figure 3.33. Reactome Pathway analysis

The Reactome, a comprehensive database of biological pathways, provides up-to-date knowledge of cell biological and molecular events (Griss et al. 2020). Reactome pathway analysis was performed to identify the pathways and biological processes affected by a circCLASP1 knockdown in HeLa cells. In our experimental conditions, sets of genes differentially expressed higher than log2FC 1 and lower than log2FC -1 were mapped onto the Reactome database to identify altered biological pathways. Knockdown of circCLASP1 affects the pathways metabolism, immune system, disease, apoptosis, multiple infections, RhoGTPases, RAF/MAP, surface interactions, and cell cycle (Figure 3.33).

These results suggest that silencing may be important in cellular signaling and immune response, which are important in disease development and progression. Moreover, the adaptive immune system and cytokine signaling are majorly affected, illustrating immune cell activation and cytokine signaling. The pathways of metabolism and post-translational protein modification indicate that the knockdown of the circCLASP1 may be involved in protein metabolism and modification.

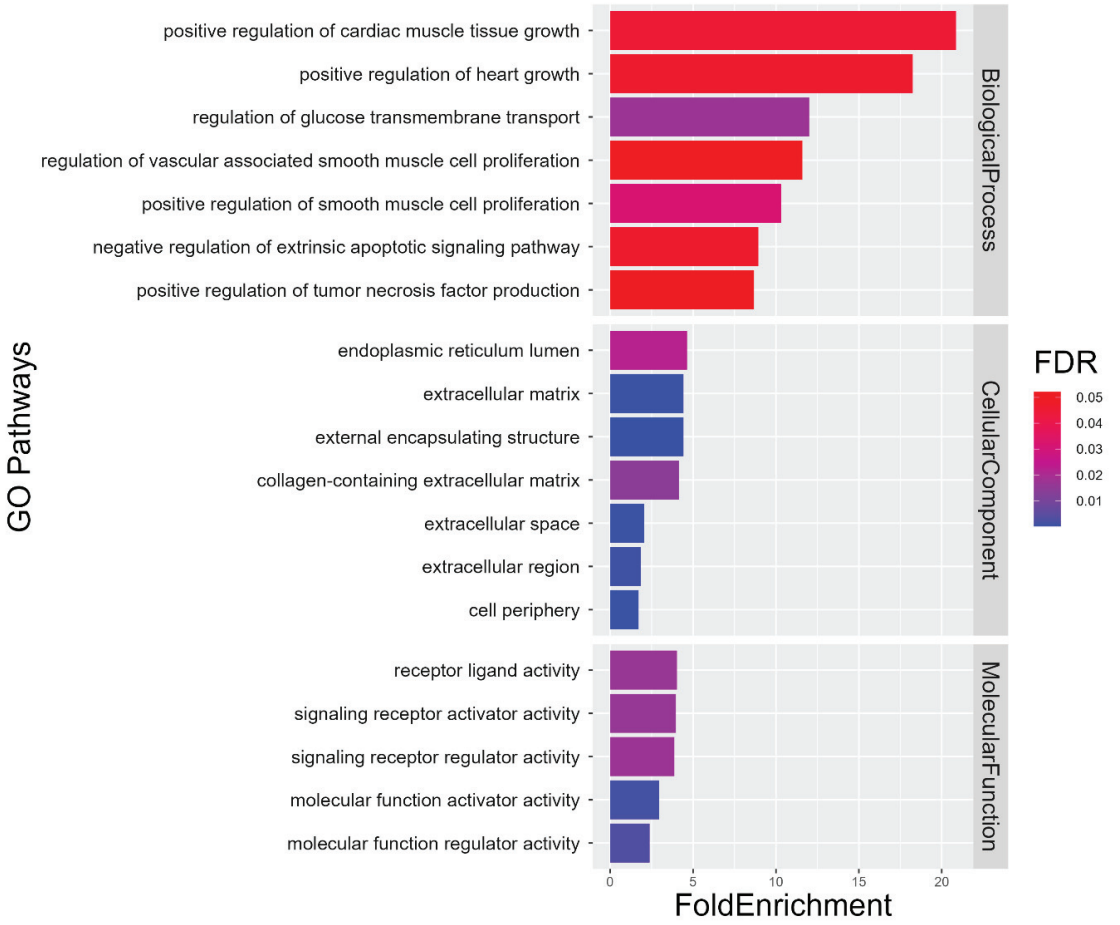

Figure 3.34. GO annotation pathway analysis. This analysis includes biological processes, cellular components, and molecular functions from top to down.

The GO analyses were performed on a differentially expressed set of genes to understand the functional roles of genes. The top pathways related to smooth muscle cell proliferation, cardiac muscle tissue growth, regulation of extrinsic apoptotic signaling,

and TNF production stimulus confirm the effect of circCLASP1 on cell proliferation (Figure 3.34).

3.4.6. AGO2-Associated Circular RNA Candidates

The mode of action of circular RNA is divided into three main groups: miRNA sponges, protein sponges/scaffolds, and regıulation of parental RNA transcription (Zhou et al. 2020). In the context of the mechanistic investigation of the role of circCLASP1 on the proliferation and CP sensitivity mechanisms, the miRNA sponging abilities of

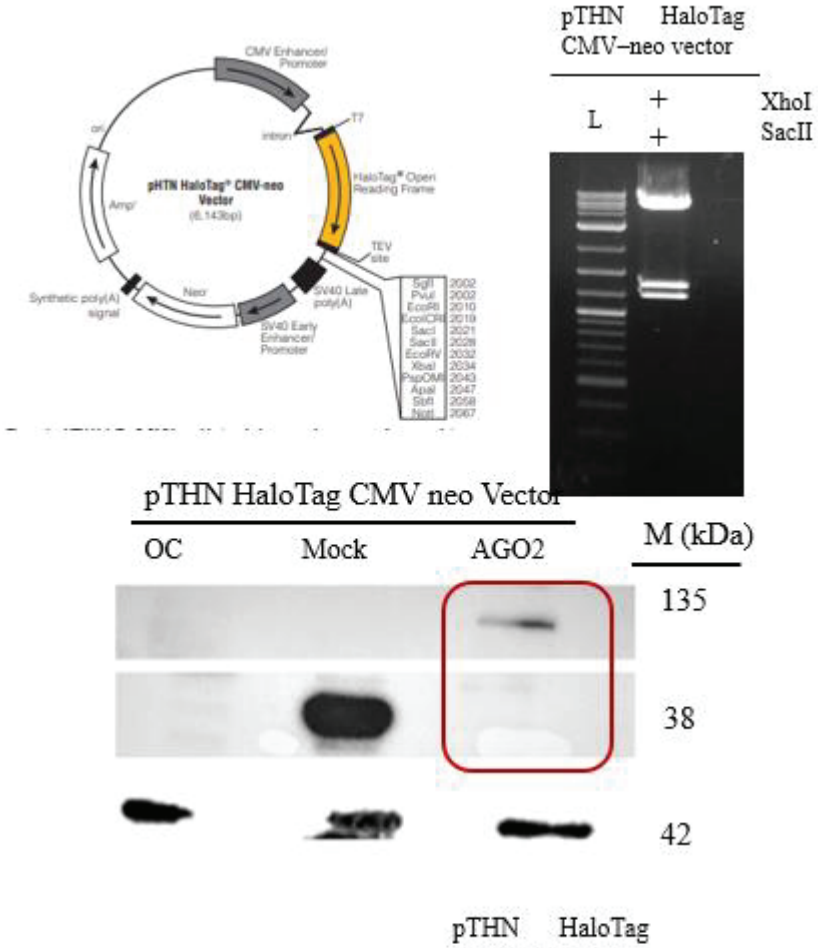

Figure 3.35. AGO2-Halo tag fusion protein production in HeLa cells.

circCLASP1 were investigated. miRNA:circRNA sponging mechanism indirectly interacts with AGO2 and circRNAs. Therefore, the miRNA sponging scenario does acceptable only if circCLASP1 is associated with AGO2. It should be noted that AGO2 is involved in the degradation of some circRNAs (J. Xu et al. 2021). However, to

investigate the miRNA sponging ability of circCLASP1, it should have interacted with AGO2. To uncover this, an AGO2-Halo Tag fusion protein plasmid was constructed (Figure 3.35). The overexpressed AGO2-HaloTag fusion protein was immunoprecipitated by the RIP method to test the enrichment of circCLASP1 in the AGO2-IP pool. In light of these findings, circCLASP1 was 15-fold enriched in the AGO2 HaloTag group compared to the HaloTag-Mock group in the AGO2-IP pool compared to Input. These results suggest that circCLASP1 is AGO2-interacted circRNA (Figure 3.36).

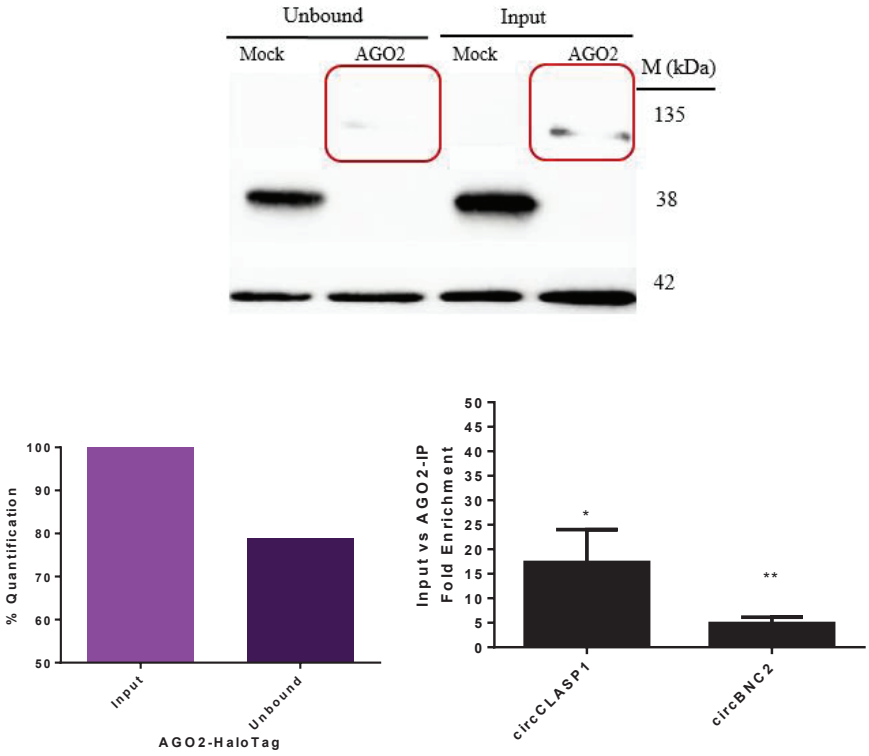

Figure 3.36. AGO2 RIP represented circCLASP1 is AGO2-interacted circRNA. A. Western blotting results illustrates the 21% of the AGO2-HaloTag fusion protein succesfully bound magnetic beads after hybridization. AGO2-HaloTag Fusion protein expression (137 kDA: 97 kDA-AGO2 + 33kDA-HaloTag + Linker). HaloTag protein+ Linker (38 kDa) and HaloTag control protein . B. Graphical representation of Image J analysis result of the calculation of the rate of AGO2-HaloTag hybridized magnetic beads, succesfully. C. The fold enrichment of circCLASP1 and circBNC2 in AGO2-HaloTag IP group when compared IP vs Input. Normalization were performed method by using the $2^{\Delta\Delta C}$t method using circCLASP1 expression in the HaloTag-control groups as the reference gene Fold enrichment was calculated using AGO2-Input and AGO2-RIP as the treatment groups.

3.4.7. Construction of circRNA-miRNA-mRNA Regulation Model for CircCLASP1-Mediated Regulation of the Proliferation, Apoptosis, and CP Response

The circRNA:miRNA:mRNA regulatory network construction was performed by a pipeline summarized below. The putative miRNA targets of the circCLASP1 were identified using CircInteractome, Cancer-Specific-CircRNA-Database, CircBank, and miRDB (Dudekula et al. 2016; S. Xia et al. 2018; M. Liu et al. 2019; Y. Chen and Wang 2020).

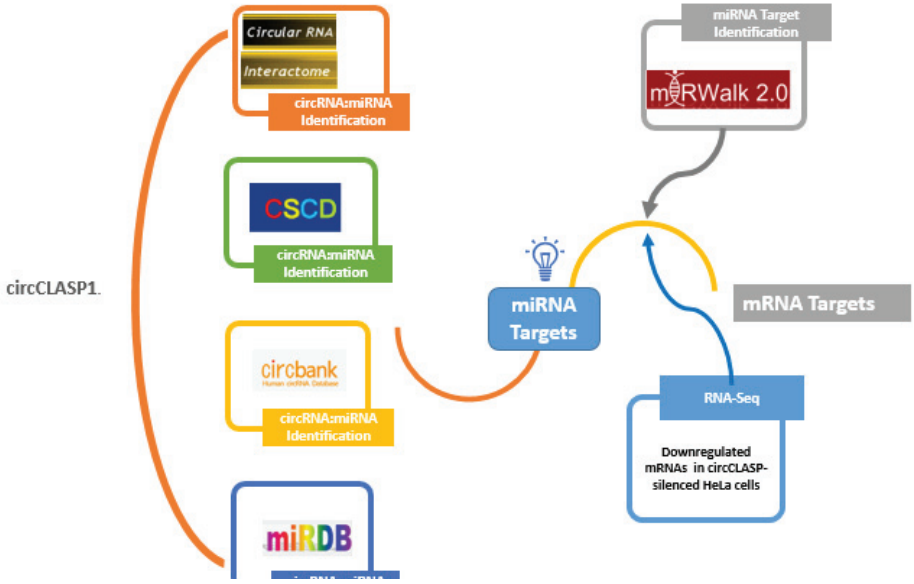

Figure 3.37. Schematic representation of circRNA-miRNA-mRNA regulatory network construction of circCLASP1.

miRNA targets identified by at least two databases were selected to identify mRNA targets using miRWalk. The downregulated genes responding to circCLASP1 knockdown were co-analyzed with miRwalk output to identify potential mRNA targets of selected miRNAs (Figure 3.37)

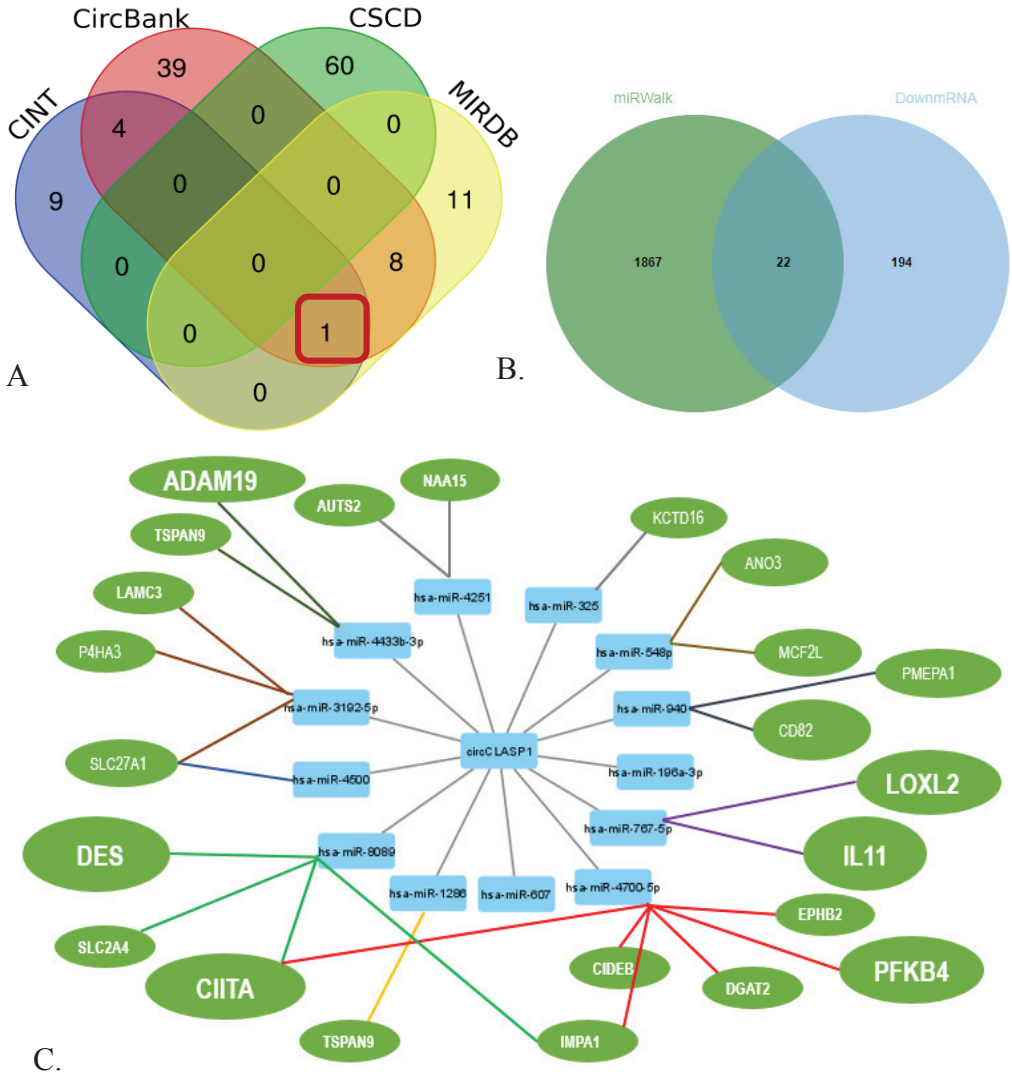

Figure 3.38. Identification of the potential circCLASP1-miRNA-mRNA regulatory networks. A. Venn diagram illustrates the miRNA targets of circCLASP1 identified by CircInteractome (CINT), circBank, Cancer-Spesific-CircRNA-Database (CSCD), and miRDB (MIRDB). B. Venn diagram shows that intersection of the mRNA targets of selected miRNAs identified by miRWalk and significantly downregulated genes in circCLASP1 silenced HeLa cells. C. Scheme illustrates the putative circCLASP1-miRNA-mRNA regulatory networks (CytoScapev3.9.1). Master regulator genes were showed in bold*, hsa-miR-767-5p indicated with red square in A

The most potent regulatory networks are circCLASP1/hsa-miR-767-5p/LOXL2, circCLASP1/hsa-miR-767-5p/IL-11, circCLASP1/hsa-miR-4700-5p/PFKB4, circCLASP1 /hsa-miR-8089/DES, circCLASP1/hsa-miR-4433b-3p/ADAM19 were identified (Figure 3.38). Among these networks, hsa-miR-767-5p is the top miRNA reported by three databases (Figure 3.38A), and IL-11 is the top downregulated mRNA among putative mRNAs. Thus, circCLASP1/ has-miR-765-5p/IL11 axis would be prioritized for investigation. IL-11 is the 6th most downregulated mRNA in circCLASP1 knockdown cells, a pro-inflammatory cytokine, and is produced by cells in an oxidative stress-dependent manner. It was reported that IL-11 pre-treatment protects various organs, including the liver. Specifically, IL-11 protects hepatocytes from IFN-gamma-induced cell death by repressing STAT1 signaling and ROS scavenging.

CHAPTER 4

DISCUSSION

Circ-seq detected 109 circRNAs (Figure 3.1), and RNA-seq detected 5426 differentially expressed mRNA in CP-treated compared with DMSO-treated HeLa cells, respectively (Figure 3.3). In CP-treated HeLa cells, Twenty-four circular RNAs expressed inversely proportional to their parental linear mRNAs. Fifty-nine circular RNAs were differentially expressed when their parental mRNAs did not indicate more than 1 log2FC. As known, back splicing is an alternative splicing mode. Unsurprisingly, circular RNAs and their linear mRNAs compete during the splicing process. This approach relies on characterizing winning circular RNA isoforms of splicing competition because cells can tend to produce RNA isoforms according to their needs. Thus, candidate circular RNAs are more likely to be a modulator of CP-triggered cellular processes. This thesis aims to validate candidate circRNAs and uncover their effects on HeLa cell phenotype (Figure 3.3).

Most circRNAs have been identified using deep-sequencing followed by identifying BSJ (Jiao et al. 2021). Reads spanning BSJ typically indicate a minor amount of the overall sequencing data, smaller than 1%. Therefore circRNA biochemical enrichment is necessary for their identification. The library preparation step of circ-seq data in Yaylak et al. consists of suitably poly-A elimination, RNase R treatment, and rRNA depletion. However, novel circRNAs were identified and annotated by CircExplorer (Version 1) (Yaylak, Erdogan, and Akgul 2019; X.O. Zhang et al. 2014). It brings several pıitfalls to investigating DE circRNA candidates functionally. Firstly, recent developments revealed that only one circRNA identification method to identify and annotate circRNAs is not recommended and should be avoided. It is shown that different circRNA prediction algorithms yielded divergent results (Hansen et al. 2016). Because different algorithms are guided by either *de novo* predictions or genome annotations. CircExplorer version 1 used genome annotation, and TopHat and TopHat fusion algorithms were used to annotate BSJ reads to the genome to identify differentially expressed circRNAs under CP treatment (Yaylak, Erdogan, and Akgul 2019). However, to identify the complex alternative splicing events and unique internal alternative splicing

regulations can be revealed by CircExplorer-2 or CIRI-AS. It is well known that apoptosis and proliferation are closely related processes. CP is one of the fundamental chemotherapeutics drugs that trigger apoptosis and represses the proliferation of cancer cells. Selected candidates from Li's study be likely a CP- dependent and might regulate CP mechanisms of action on HeLa cells. Therefore, circCLASP1 and circBIRC6 were selected to investigate under CP-treated conditions. To select circBIRC6 and circCLASP1, The criteria considered during the candidate selection processes is the participation of cognate linear mRNAs in regulating proliferation and differential expression under CP-treated conditions. In this thesis, four circRNA candidates were selected from Yaylak et al. and Li et al. to investigate their biochemical and functional properties in HeLa cells (Yaylak, Erdogan, and Akgul 2019; S. Li et al. 2020).

The main advantage of selecting circRNA candidates in addition to previously reported circRNAs by our group (Yaylak, Erdogan, and Akgul 2019) is the abundancy of target circRNAs. In 2021, Xu and Yang published a paper titled "Mammalian circular RNAs result largely from splicing errors" in Cell Press. They suggest that back splicing is much rare than linear splicing, the overall prevalence of back-splicing in a species declines with its effective population size, and circRNAs are mostly evolutionary unconserved. Therefore they suggest that only 3% of circRNAs might be functional and genome-wide trends strongly proved that circRNAs are mainly non-functional. Thus, abundance and functionality are closely related, especially in circRNAs. Li et al. used nearly 700 most abundant circRNAs in 3 different cell lines. circGALNT2 and circBNC2 are relatively abundant among our candidates.

Along with this, circBNC2 with 2 copies per cell but circGALNT2 with <1 copy per cell. However, Dodbele and Mutlu suggest that if a circular RNA is present at 1 copy or less per cell, it certainly has minimal or no effect on microRNA targeting (Dodbele and Mutlu, 2021). Thus, circCLASP1 and circBIRC6, which might impact cell proliferation, were selected for further investigation in the context of the CP mechanism on HeLa cells, in addition to circGALNT2 and circBNC2, to overcome this challenge.

CircRNAs have been shown to play essential roles in cancer progression and drug resistance, and studying their regulation and functions in response to CP treatment could provide new insights into the mechanisms underlying CP resistance and identify new therapeutic targets (X.-Y. Liu et al. 2021). Moreover, identifying specific circRNAs that are dysregulated in response to CP treatment could be biomarkers for predicting CP

resistance or prognosis in cancer patients. To provide insight into circRNAs involved in CP-mediated proliferation-repression and -apoptosis-induction, all four candidate expression patterns in CP-treated HeLa cells were measured by qPCR. The findings suggest circCLASP1 (Figure 3.7), circBIRC6 (Figure 3.15), and circBNC2 (Figure 3.11) are repressed in CP-treated HeLa cells, whereas circGALNT2 (Figure 3.15) were upregulated. Although the downregulation of circCLASP1, circBIRC6, and circBNC2 was not dramatic, the stable nature of circRNAs enables the possible phenotypic effects upon slight changes (Holdt, Kohlmaier, and Teupser 2018b).

The validation of circRNAs relies on multiple approaches. Firstly divergent primers were designed to distinguish circular isoforms from linear mRNA. Although divergent primers targets to amplify unique back-splicing junctions, different circular isoforms generated by internal alternative splicing events might be amplified with the same set of divergent primers (Zhong and Feng 2022). CircPrimers 2.0. was used to list all known annotated circRNA isoforms amplified by particular primers to eliminate the off-target effect (Zhong and Feng 2022) (Figure 3.6, Figure 3.10, Figure 3.14).

Additionally, amplified back-splicing sequences were confirmed by Sanger sequencing (Figure 3.8, Figure 3.12). However, the back-splicing junction sequence may illustrate non-linear exon order caused by reverse transcription-based false positive amplifications. A linear RNA with the apparent back-splicing junction is produced if the pre-mRNA derived from a gene is subjected to a trans-splicing event. Moreover, during cDNA synthesis, reverse transcriptase can dissociate from a template RNA and resume extension from a second template, resulting in a false-positive back-splicing junction-like sequence. Therefore, RNase R treatment was performed to ensure the circularity of candidates (Figure 3.9, Figure 3.13, Figure 3.14). The results imply that our candidates are resistant to RNase R. The circHIPK3 was used as the positive control, whereas GAPDH was used as the negative control. Each candidate has a unique level of resistance to RNase R; however, all of them are significantly resistant to RNase R when compared to GAPDH:

CircRNAs have been shown to play essential roles in various diseases and drug resistance. Studying their regulation and functions in response to CP treatment could provide new insights into the mechanisms underlying chemical stress responses, cell proliferation, and cell death. Investigating functional roles of circRNA candidates was begun with loss-of-function studies. Silencing of circRNAs relies on siRNA targeting

unique back-splicing junctions. However, designed siRNAs share a common sequence with linear mRNA exons. Therefore, off-target effect elimination is quite essential to evaluate siRNAs silencing capacity. The growth curve of different cell seeding densities of HeLa cells was constructed to observe the exponential and log phases of the cells. The 5000 cell was identified as cell seeding density for further proliferation experiments (Figure 3.16). The measurement time of transfection was identified as 48h. However, 72 hours of silencing is performed in rescue experiments.

Over-expression and knock-down of circRNA transcripts would be challenging. There are several reasons. In terms of overexpression experiments, overexpression constructs of circRNAs, including the Drosophila Laccase2 construct used in this thesis (Kramer et al. 2015). This construct produces more circular RNA transcripts than undesired flanking introns, linear concatamers, or linear exons than cDNA3.1(+) CircRNA Mini Vector. However, they still generate undesired transcripts besides the circular RNA of interest. For example, recent work has indicated that flanking introns can cause low levels of trans-spliced RNAs translated into unintended proteins (Ho-Xuan et al., 2020). The optimization of cell seeding density and transfection period were optimized to enable optimum knockdown and overexpression effects on Hela cells.

All four candidates regarding proliferation, apoptosis, and CP resistance were screened. According to the results, circGALNT2 (Figure 3.17) and circBNC2 (Figure 3.18, Figure 3.19) did not show phenotypic effects on HeLa cell proliferation and apoptosis. In terms of circGALNT2, it is clear that circGALNT2 is a circular transcript and independently regulated from its cognate linear mRNA. The circGALNT2 is nearly for 2-log2FC upregulated in HeLa cells, while GALNT2 mRNA is downregulated for -3-log2FC (Figure 3.15). The circGALNT2 was reported as one of the top 10 downregulated circRNAs in multi-drug resistant osteosarcoma cells (CP and DOX). This evidence supports the idea that circGALNT2 might be involved CP-sensitivity mechanism. However, the knockdown of circGALNT2 does not sensitize HeLa cells against CP. Although it might be an independent production of circGALNT2, it also might be an unwanted splicing product caused by decreased production of GALNT2 mRNA.

On the other hand, the effect of circBNC2, CP-repressible circRNA, and HeLa cells against CP was investigated (Figure 3.11). Lastly, circBNC2, which inhibits ovarian cancer, was reported as a diagnostic biomarker in epithelial ovarian cancer while

investigating its role in CP-treated HeLa cells. Nonetheless, WST-8 and annexin-V/7AAD assays indicated that the knockdown of circBNC2 does not affect HeLa cell apoptosis and proliferation with or without CP treatment (Figure 3.18, Figure 3.19). Additionally, the circBIRC6 knockdown repressed proliferation; however, overexpression of circBIRC6 could not restore the suppressive effect of silencing (Figure 3.20).

The knockdown of circCLASP1 showed repression of cell proliferation. Moreover, the overexpression of circCLASP1 restored the repressive effect of knockdown (Figure 3.22). Additionally, circCLASP1 knockdown promotes early apoptosis slightly (Figure 3.24). The most exciting finding about circCLASP1 is that the knockdown of circCLASP1 made HeLa cells more sensitized against low doses of CP (20 μM and 40 μM). However, 80 μM CP combined with circCLASP1 knockdown promotes Annexin V-/7AAD+ cells rather than early and late apoptosis (Figure3.25, Figure 3.26). It might point to the combined effect of circCLASP1 knockdown and chemical stress overload that forced HeLa cells to different modes of caspase-independent cell death.

After the functional characterization of circCLASP1 on cell proliferation, apoptosis, and CP-treatment, the transcriptomics approach was used to gain insight into the functional mechanism of circCLASP1. Nearly 600 mRNAs were differentially expressed in circCLASP1 knockdown HeLa cells (log2FC >1 and log2FC<-1). The Reactome pathway analysis revealed that metabolism, disease, apoptosis, g-alpha signaling pathways, metabolism of lipids, cell cycle, RAF\MAPK, and metabolic diseases are significantly modulated pathways (Figure 3.33). Besides, GO analysis indicated that proliferation-related biological processes such as cardiac muscle tissue growth, positive regulation of heart growth, vascular-associated smooth muscle cell proliferation, negative regulation of extrinsic apoptosis, and positive regulation of the tumor necrosis factor production were top biological processes which circCLASP1 knockdown likely related with (Figure 3.34). These analyses supported the proliferative effect of circCLASP1. Interestingly, top differentially expressed mRNAs are related to immune response, iron metabolism, lipid metabolism, ROS, and mitochondrial dysfunction.

It is important to note that the differential expressed gene list exhibits lots of genes involved in both the promotion and repression of survival of the cells

simultaneously. Interestingly, SAA is a well-known acute-phase protein expressed abundantly in the liver following injury or other acute traumas. IL1-B, IL6, and TNF-a are primary stimulants for the SAA gene (Getachew, Chen, and Yang, 2021). This gene generally promotes NF-kB expression to promote survival. However, it was reported that blockage of the NF-kB revealed the toxic effect of SAA1 with the appearance of caspase-3 and PARP cleavage-mediated apoptotic signature. The RNA-seq data showed significant upregulation in NF-kB inhibitors NFKB inhibitor-alpha and NFKB inhibitor-zeta.

In detail, the HOXO-1 gene metabolizes heme into bilirubin/ biliverdin, ferrous iron, and carbon monoxide. HOXO-1 is widely regarded as a survival molecule. However, numerous studies have shown the detrimental effects of HOXO-1 upregulation in which HOXO-1 is a key modulator in ferroptosis induction. The amount of cellular iron and reactive oxygen species (ROS) determines the role of HO-1, either protective or perpetrator. According to the contradictory results in the literature, the upregulation of HO-1 protects cells or governs ferroptosis events on the degree of ROS production following oxidative damage (Chiang, Chen, and Chang 2018). HO-1 induce ferroptosis is mediated by iron accumulation and lipid peroxidation (Chang et al. 2018). Interestingly, the 5th most upregulated gene, ANKRD1, regulates lipid metabolism by the peroxisome-proliferator-activated receptors (PPARs) signaling pathway. PPAR-alpha is the master regulator of fatty acid oxidation by stimulating ANKRD1. It was reported that ANKRD1 participates in forming CaOx kidney stones by activating ferroptosis by the p53/SLC7A11 pathway (J. Zhao et al. 2023). SLC7A11 is upregulated in circCLASP1 knockdown RNA-seq data.

IL1-B, one of the main stimulants of SAA1, as explained above, is the 4th most upregulated gene in circCLASP1 silenced HeLa cells. It is reported that IL-1B-induced ROS production generated mitochondrial membrane damage, which results in the accumulation of damaged mitochondria and a higher rate of apoptosis in chondrocyte cells (Ansari et al. 2017). It is known that mitochondria damage is closely related to immune response. When mitochondria are damaged, dysfunctional mitochondria continue to generate ROS and initiate immune responses (Nakahira et al. 2011).

On the other hand, the top 5 downregulated genes are MEDAG, COX6B2, ELAPOR1, DOCK2, and MUSTN1 (Figure 3.32). MEDAG is a mesenteric estrogen-dependent adipogenesis gene. It was reported as a positive regulator of PPARg (H.

Zhang, Chen, and Sairam 2012). The PPARg promotes insulin sensitization and enhances glucose metabolism (Tyagi et al. 2011). MEDAG is reported as an oncogene in breast cancer, and MEDAG silencing inhibited cell proliferation, invasion, and migration. COX6B2 gene is the cytochrome c oxidase subunit 6B2 that enhances oxidative phosphorylation proliferation and survival in various cancer types. It is reported that the depletion of COX6B2 disrupts ATP production and mitochondrial membrane potential leading to programmed cell death or senescence. In sperms, COX6B2 induces mitochondrial supercomplex formation and limits ROS production (Cheng et al. 2020). Thus it is hypothesized that COX6B2 depletion in circCLASP1 silenced cells may cause aberrant ROS production and disrupted proliferation. Additionally, ELAPOR1 endosome-lysosome-associated apoptosis and autophagy regulator 1 have been linked with survival in certain carcinomas (Schlumbrecht et al. 2011). Further, circCLASP1 is identified as AGO2-associated circRNA by RIP. To this respect, a circCLASP1 /has_miR_765-5p /IL11 regulatory network was constructed bioinformatically (Figure 3.37). Luciferase reporter assays and rescue experiments should validate it. For future perspectives, It might be speculated that circCLASP1 knockdown results in aberrant HOXO-1 activity and iron accumulation because of the high level of ROS, followed by lipid peroxidation and ferroptosis, which demands further investigations. According to transcriptomics analysis, circCLASP1 might be an essential target for smooth muscle cell growth, liver diseases, or cardiovascular diseases, requiring further investigations.

REFERENCES

Abdelmohsen, Kotb, Amaresh C Panda, Rachel Munk, Ioannis Grammatikakis, Dawood B Dudekula, Supriyo De, Jiyoung Kim, et al. 2017. "Identi Fi Cation of HuR Target Circular RNAs Uncovers Suppression of PABPN1 Translation by CircPABPN1." *RNA Biology* 14 (3): 361–69. https://doi.org/10.1080/15476286.2017.1279788.

Ahmadov, Ulvi. 2015. "Identification of Long Non-Coding Rnas That Regulate Apoptosis in Human," no. December.

Ajay, Amrendra K., Avtar S. Meena, and Manoj K. Bhat. 2012. "Human Papillomavirus 18 E6 Inhibits Phosphorylation of P53 Expressed in HeLa Cells." *Cell and Bioscience* 2 (1): 2. https://doi.org/10.1186/2045-3701-2-2.

Aktaş, Tuğçe, İbrahim Avşar Ilık, Daniel Maticzka, Vivek Bhardwaj, Cecilia Pessoa Rodrigues, Gerhard Mittler, Thomas Manke, Rolf Backofen, and Asifa Akhtar. 2017. "DHX9 Suppresses RNA Processing Defects Originating from the Alu Invasion of the Human Genome." *Nature* 544 (7648): 115–19. https://doi.org/10.1038/nature21715.

Alenzi, F. Q.B. 2004. "Links between Apoptosis, Proliferation and the Cell Cycle." *British Journal of Biomedical Science* 61 (2): 99–102. https://doi.org/10.1080/09674845.2004.11732652.

Alexander, Roger P, Gang Fang, Joel Rozowsky, Michael Snyder, and Mark B Gerstein. 2010. "Annotating Non-Coding Regions of the Genome." *Nature Reviews. Genetics* 11 (8): 559–71. https://doi.org/10.1038/nrg2814.

Alimbetov, Dauren, Sholpan Askarova, Bauyrzhan Umbayev, Terence Davis, and David Kipling. 2018. "Pharmacological Targeting of Cell Cycle, Apoptotic and Cell Adhesion Signaling Pathways Implicated in Chemoresistance of Cancer Cells." *International Journal of Molecular Sciences* 19 (6). https://doi.org/10.3390/ijms19061690.

Ashkenazi, Avi, and Vishva M Dixit. 1998. "Death Receptors: Signaling and Modulation." *Science* 281 (5381): 1305–8.

Ashwal-fluss, Reut, Markus Meyer, Nagarjuna Reddy Pamudurti, Andranik Ivanov, Osnat Bartok, Mor Hanan, Naveh Evantal, Sebastian Memczak, Nikolaus Rajewsky, and Sebastian Kadener. 2014. "Article CircRNA Biogenesis Competes with Pre-MRNA Splicing." *MOLCEL* 56 (1): 55–66. https://doi.org/10.1016/j.molcel.2014.08.019.

Ashwal-Fluss, Reut, Markus Meyer, Nagarjuna Reddy Pamudurti, Andranik Ivanov, Osnat Bartok, Mor Hanan, Naveh Evantal, Sebastian Memczak, Nikolaus Rajewsky, and Sebastian Kadener. 2014. "CircRNA Biogenesis Competes with Pre-MRNA Splicing." *Molecular Cell* 56 (1): 55–66. https://doi.org/10.1016/j.molcel.2014.08.019.

Askew, D S, R A Ashmun, B C Simmons, and J L Cleveland. 1991. "Constitutive C-Myc Expression in an IL-3-Dependent Myeloid Cell Line Suppresses Cell Cycle Arrest and Accelerates Apoptosis." *Oncogene* 6 (10): 1915–22.

Bachmayr-Heyda, Anna, Agnes T Reiner, Katharina Auer, Nyamdelger Sukhbaatar, Stefanie Aust, Thomas Bachleitner-Hofmann, Ildiko Mesteri, Thomas W Grunt, Robert Zeillinger, and Dietmar Pils. 2015. "Correlation of Circular RNA Abundance with Proliferation--Exemplified with Colorectal and Ovarian Cancer, Idiopathic Lung Fibrosis, and Normal Human Tissues." *Scientific Reports* 5 (January): 8057. https://doi.org/10.1038/srep08057.

Bakhshesh, Mehran, Elisabetta Groppelli, Margaret M Willcocks, Elizabeth Royall, Graham J Belsham, and Lisa O Roberts. 2008. "The Picornavirus Avian Encephalomyelitis Virus Possesses a Hepatitis C Virus-like Internal Ribosome Entry Site Element." *Journal of Virology* 82 (4): 1993–2003. https://doi.org/10.1128/JVI.01957-07.

Barrett, Steven P, Peter L Wang, and Julia Salzman. 2015. "Circular RNA Biogenesis Can Proceed through an Exon-Containing Lariat Precursor." *ELife* 4 (June): e07540. https://doi.org/10.7554/eLife.07540.

Bartel, David P. 2009. "MicroRNAs: Target Recognition and Regulatory Functions." *Cell* 136 (2): 215–33. https://doi.org/10.1016/j.cell.2009.01.002.

Basu, Alakananda, and Soumya Krishnamurthy. 2010. "Cellular Responses to

Cisplatin-Induced DNA Damage." *Journal of Nucleic Acids* 2010. https://doi.org/10.4061/2010/201367.

Bhattacharya, Sujoy, Ramesh M Ray, and Leonard R Johnson. 2014. "Cyclin-Dependent Kinases Regulate Apoptosis of Intestinal Epithelial Cells." *Apoptosis : An International Journal on Programmed Cell Death* 19 (3): 451–66. https://doi.org/10.1007/s10495-013-0942-3.

Bhola, Patrick D, and Anthony Letai. 2016. "Mitochondria-Judges and Executioners of Cell Death Sentences." *Molecular Cell* 61 (5): 695–704. https://doi.org/10.1016/j.molcel.2016.02.019.

Blagosklonny, Mikhail V., and Wafik S. El-Deiry. 1998. "Acute Overexpression of Wt P53 Facilitates Anticancer Drug-Induced Death of Cancer and Normal Cells." *International Journal of Cancer* 75 (6): 933–40. https://doi.org/10.1002/(SICI)1097-0215(19980316)75:6<933::AID-IJC17>3.0.CO;2-3.

Boldin, Mark P, Tanya M Goncharov, Yury V Goltseve, and David Wallach. 1996. "Involvement of MACH, a Novel MORT1/FADD-Interacting Protease, in Fas/APO-1-and TNF Receptor–Induced Cell Death." *Cell* 85 (6): 803–15.

Bretones, Gabriel, M Dolores Delgado, and Javier León. 2015. "Myc and Cell Cycle Control." *Biochimica et Biophysica Acta* 1849 (5): 506–16. https://doi.org/10.1016/j.bbagrm.2014.03.013.

Bruce, Jeff P, Angela B Y Hui, Wei Shi, Bayardo Perez-Ordonez, Ilan Weinreb, Wei Xu, Benjamin Haibe-Kains, et al. 2015. "Identification of a MicroRNA Signature Associated with Risk of Distant Metastasis in Nasopharyngeal Carcinoma." *Oncotarget* 6 (6): 4537–50. https://doi.org/10.18632/oncotarget.3005.

Caldas, Carlos, Chi W. So, Angus MacGregor, Anthony M. Ford, Bernadette McDonald, Li C. Chan, and Leanne M. Wiedemann. 1998. "Exon Scrambling of MLL Transcripts Occur Commonly and Mimic Partial Genomic Duplication of the Gene." *Gene* 208 (2): 167–76. https://doi.org/10.1016/S0378-1119(97)00640-9.

Capel, Blanche, Amanda Swain, Silvia Nicolis, Adam Hacker, Michael Walter, Peter Koopman, Peter Goodfellow, and Robin Lovell-Badge. 1993. "Circular

Transcripts of the Testis-Determining Gene Sry in Adult Mouse Testis." *Cell* 73 (5): 1019–30. https://doi.org/10.1016/0092-8674(93)90279-Y.

Cavalcante, Giovanna C, Leandro Magalhães, Ândrea Ribeiro-Dos-Santos, and Amanda F Vidal. 2020. "Mitochondrial Epigenetics: Non-Coding RNAs as a Novel Layer of Complexity." *International Journal of Molecular Sciences* 21 (5). https://doi.org/10.3390/ijms21051838.

Cesaratto, Laura, Eleonora Grisard, Michela Coan, Luigi Zandonà, Elena De Mattia, Elena Poletto, Erika Cecchin, et al. 2016. "BNC2 Is a Putative Tumor Suppressor Gene in High-Grade Serous Ovarian Carcinoma and Impacts Cell Survival after Oxidative Stress." *Cell Death and Disease* 7 (9): 1–11. https://doi.org/10.1038/cddis.2016.278.

Chen, Chyi-Ying A, and Ann-Bin Shyu. 2011. "Mechanisms of Deadenylation-Dependent Decay." *Wiley Interdisciplinary Reviews. RNA* 2 (2): 167–83. https://doi.org/10.1002/wrna.40.

Chen, Dazhi, Timothy H. Carter, and Karen J. Auborn. 2004. "Apoptosis in Cervical Cancer Cells: Implications for Adjunct Anti-Estrogen Therapy for Cervical Cancer." *Anticancer Research* 24 (5 A): 2649–56.

Chen, Jiandong. 2016. "The Cell-Cycle Arrest and Apoptotic Functions of P53 in Tumor Initiation and Progression." *Cold Spring Harbor Perspectives in Medicine* 6 (3): a026104. https://doi.org/10.1101/cshperspect.a026104.

Chen, Ling Ling. 2020. "The Expanding Regulatory Mechanisms and Cellular Functions of Circular RNAs." *Nature Reviews Molecular Cell Biology* 21 (8): 475–90. https://doi.org/10.1038/s41580-020-0243-y.

Chen, Ling Ling, and Li Yang. 2015. "Regulation of CircRNA Biogenesis." *RNA Biology* 12 (4): 381–88. https://doi.org/10.1080/15476286.2015.1020271.

Chen, Naifei, Gang Zhao, Xu Yan, Zheng Lv, Hongmei Yin, Shilin Zhang, Wei Song, et al. 2018. "A Novel FLI1 Exonic Circular RNA Promotes Metastasis in Breast Cancer by Coordinately Regulating TET1 and DNMT1." *Genome Biology* 19 (1): 218. https://doi.org/10.1186/s13059-018-1594-y.

Chen, Yuhao, and Xiaowei Wang. 2020. "MiRDB: An Online Database for Prediction

of Functional MicroRNA Targets." *Nucleic Acids Research* 48 (D1): D127–31. https://doi.org/10.1093/nar/gkz757.

Colussi, Timothy M, David A Costantino, Jianyu Zhu, John Paul Donohue, Andrei A Korostelev, Zane A Jaafar, Terra-Dawn M Plank, Harry F Noller, and Jeffrey S Kieft. 2015. "Initiation of Translation in Bacteria by a Structured Eukaryotic IRES RNA." *Nature* 519 (7541): 110–13.

Comfort, Nathaniel. 2015. "Genetics: We Are the 98%." *Nature* 520 (7549): 615–16. https://doi.org/10.1038/520615a.

Conn, Simon J., Katherine A. Pillman, John Toubia, Vanessa M. Conn, Marika Salmanidis, Caroline A. Phillips, Suraya Roslan, Andreas W. Schreiber, Philip A. Gregory, and Gregory J. Goodall. 2015. "The RNA Binding Protein Quaking Regulates Formation of CircRNAs." *Cell* 160 (6): 1125–34. https://doi.org/10.1016/j.cell.2015.02.014.

Conti, E, F Bonneau, J Ebert, J Basquin, and E Lorentzen. 2009. "Molecular Mechanisms of RNA Degradation by the Exosome." *FEBS Journal* 276 (Suppl. 1): 37–38.

CRICK, F H. 1958. "On Protein Synthesis." *Symposia of the Society for Experimental Biology* 12: 138–63.

Dang, Rui Ying, Feng Li Liu, and Yan Li. 2017. "Circular RNA Hsa_circ_0010729 Regulates Vascular Endothelial Cell Proliferation and Apoptosis by Targeting the MiR-186/HIF-1α Axis." *Biochemical and Biophysical Research Communications* 490 (2): 104–10. https://doi.org/10.1016/j.bbrc.2017.05.164.

Danial, Nika N, and Stanley J Korsmeyer. 2004. "Cell Death: Critical Control Points." *Cell* 116 (2): 205–19.

Denli, Ahmet M, Bastiaan B J Tops, Ronald H A Plasterk, René F Ketting, and Gregory J Hannon. 2004. "Processing of Primary MicroRNAs by the Microprocessor Complex." *Nature* 432 (7014): 231–35. https://doi.org/10.1038/nature03049.

Desbarats, L, A Schneider, D Müller, A Bürgin, and M Eilers. 1996. "Myc: A Single Gene Controls Both Proliferation and Apoptosis in Mammalian Cells."

Experientia 52 (12): 1123–29. https://doi.org/10.1007/BF01952111.

Dhanasekaran, Karthigeyan, Sujata Kumari, and Chandrasekhar Kanduri. 2013. "Noncoding RNAs in Chromatin Organization and Transcription Regulation: An Epigenetic View." *Sub-Cellular Biochemistry* 61: 343–72. https://doi.org/10.1007/978-94-007-4525-4_15.

Dickens, Laura S., Robert S. Boyd, Rebekah Jukes-Jones, Michelle A. Hughes, Gemma L. Robinson, Louise Fairall, John W.R. Schwabe, Kelvin Cain, and Marion MacFarlane. 2012. "A Death Effector Domain Chain DISC Model Reveals a Crucial Role for Caspase-8 Chain Assembly in Mediating Apoptotic Cell Death." *Molecular Cell* 47 (2): 291–305. https://doi.org/10.1016/j.molcel.2012.05.004.

Djebali, Sarah, Carrie A Davis, Angelika Merkel, Alex Dobin, Timo Lassmann, Ali Mortazavi, Andrea Tanzer, et al. 2012. "Landscape of Transcription in Human Cells." *Nature* 489 (7414): 101–8. https://doi.org/10.1038/nature11233.

Dodbele, Samantha, Nebibe Mutlu, and Jeremy E Wilusz. 2021. "Best Practices to Ensure Robust Investigation of Circular RNAs: Pitfalls and Tips." *EMBO Reports* 22 (3): e52072. https://doi.org/10.15252/embr.202052072.

Dojindo Laboratories, . 2016. "Technical Manual - Cell Counting Kit-8" 8: 1–2.

Du, William W., Weining Yang, Yu Chen, Zhong Kai Wu, Francis Stuart Foster, Zhenguo Yang, Xiangmin Li, and Burton B. Yang. 2017. "Foxo3 Circular RNApromotes Cardiac Senescence by Modulating Multiple Factors Associated with Stress and Senescence Responses." *European Heart Journal* 38 (18): 1402–12. https://doi.org/10.1093/eurheartj/ehw001.

Du, William W, Weining Yang, Elizabeth Liu, Zhenguo Yang, Preet Dhaliwal, and Burton B Yang. 2016. "Foxo3 Circular RNA Retards Cell Cycle Progression via Forming Ternary Complexes with P21 and CDK2." *Nucleic Acids Research* 44 (6): 2846–58. https://doi.org/10.1093/nar/gkw027.

Du, William W, Chao Zhang, Weining Yang, Tianqiao Yong, Faryal Mehwish Awan, and Burton B Yang. 2017. "Identifying and Characterizing CircRNA-Protein Interaction." *Theranostics* 7 (17): 4183–91. https://doi.org/10.7150/thno.21299.

Dudekula, Dawood B, Amaresh C Panda, Ioannis Grammatikakis, Supriyo De, Kotb

Abdelmohsen, and Myriam Gorospe. 2016. “CircInteractome: A Web Tool for Exploring Circular RNAs and Their Interacting Proteins and MicroRNAs.” *RNA Biology* 13 (1): 34–42. https://doi.org/10.1080/15476286.2015.1128065.

Dugué, Pierre-Antoine, Matejka Rebolj, Peter Garred, and Elsebeth Lynge. 2013. “Immunosuppression and Risk of Cervical Cancer.” *Expert Review of Anticancer Therapy* 13 (1): 29–42. https://doi.org/10.1586/era.12.159.

Efeyan, Alejo, and Manuel Serrano. 2007. “P53: Guardian of the Genome and Policeman of the Oncogenes.” *Cell Cycle* 6 (9): 1006–10. https://doi.org/10.4161/cc.6.9.4211.

Engeland, Kurt. 2022. “Cell Cycle Regulation: P53-P21-RB Signaling.” *Cell Death and Differentiation* 29 (5): 946–60. https://doi.org/10.1038/s41418-022-00988-z.

Enuka, Yehoshua, Mattia Lauriola, Morris E. Feldman, Aldema Sas-Chen, Igor Ulitsky, and Yosef Yarden. 2016. “Circular RNAs Are Long-Lived and Display Only Minimal Early Alterations in Response to a Growth Factor.” *Nucleic Acids Research* 44 (3): 1370–83. https://doi.org/10.1093/nar/gkv1367.

Esquela-Kerscher, Aurora, and Frank J Slack. 2006. “Oncomirs - MicroRNAs with a Role in Cancer.” *Nature Reviews. Cancer* 6 (4): 259–69. https://doi.org/10.1038/nrc1840.

Evan, Gerard I., Andrew H. Wyllie, Christopher S. Gilbert, Trevor D. Littlewood, Hartmut Land, Mary Brooks, Catherine M. Waters, Linda Z. Penn, and David C. Hancock. 1992. “Induction of Apoptosis in Fibroblasts by C-Myc Protein.” *Cell* 69 (1): 119–28. https://doi.org/10.1016/0092-8674(92)90123-T.

Fan, Xiaojuan, Yun Yang, and Zefeng Wang. n.d. “Pervasive Translation of Circular RNAs Driven by Short IRES-like Elements.”

Ferreira, Humberto J., and Manel Esteller. 2018. “Non-Coding RNAs, Epigenetics, and Cancer: Tying It All Together.” *Cancer and Metastasis Reviews* 37 (1): 55–73. https://doi.org/10.1007/s10555-017-9715-8.

Fischer, Joseph W, Veronica F Busa, Yue Shao, Anthony K L Leung, Joseph W Fischer, Veronica F Busa, Yue Shao, and Anthony K L Leung. 2020. “Article Structure-Mediated RNA Decay by UPF1 and G3BP1.” *Molecular Cell*, 1–15.

https://doi.org/10.1016/j.molcel.2020.01.021.

Fitzgerald, Kerry D, and Bert L Semler. 2009. “Bridging IRES Elements in MRNAs to the Eukaryotic Translation Apparatus.” *Biochimica et Biophysica Acta* 1789 (9–10): 518–28. https://doi.org/10.1016/j.bbagrm.2009.07.004.

Florea, Ana-Maria, and Dietrich Büsselberg. 2011. “Cisplatin as an Anti-Tumor Drug: Cellular Mechanisms of Activity, Drug Resistance and Induced Side Effects.” *Cancers* 3 (1): 1351–71. https://doi.org/10.3390/cancers3011351.

Fraser, A, and G Evan. 1996. “A License to Kill.” *Cell* 85 (6): 781–84. https://doi.org/10.1016/s0092-8674(00)81005-3.

Fraser, Michael, Brendan Leung, Arezu Jahani-Asl, Xiaojuan Yan, Winston E Thompson, and Benjamin K Tsang. 2003. “Chemoresistance in Human Ovarian Cancer: The Role of Apoptotic Regulators.” *Reproductive Biology and Endocrinology* 1 (1): 66. https://doi.org/10.1186/1477-7827-1-66.

Fulda, Simone, Adrienne M. Gorman, Osamu Hori, and Afshin Samali. 2010. “Cellular Stress Responses: Cell Survival and Cell Death.” *International Journal of Cell Biology* 2010. https://doi.org/10.1155/2010/214074.

Furuya, Y, P Lundmo, A D Short, D L Gill, and J T Isaacs. 1994. “The Role of Calcium, PH, and Cell Proliferation in the Programmed (Apoptotic) Death of Androgen-Independent Prostatic Cancer Cells Induced by Thapsigargin.” *Cancer Research* 54 (23): 6167–75.

Gao, Yuan, Jinfeng Wang, Yi Zheng, Jinyang Zhang, Shuai Chen, and Fangqing Zhao. 2016. “Comprehensive Identification of Internal Structure and Alternative Splicing Events in Circular RNAs.” *Nature Communications* 7 (May): 1–13. https://doi.org/10.1038/ncomms12060.

Gartel, Andrei L., Eugene Goufman, Charlotte Hurth, and Angela L. Tyner. 2001. “A Novel P53-Related Activity in a Colon Adenocarcinoma Cell Line With Mutant P53.” *The Scientific World JOURNAL* 1: 36–36. https://doi.org/10.1100/tsw.2001.162.

Geng, Hai Hua, Rui Li, Ya Min Su, Jie Xiao, Min Pan, Xing Xing Cai, and Xiao Ping Ji. 2016. “The Circular RNA Cdr1as Promotes Myocardial Infarction by

Mediating the Regulation of MiR-7α on Its Target Genes Expression." *PLoS ONE* 11 (3): 1–17. https://doi.org/10.1371/journal.pone.0151753.

Goldberg, Alfred L. 2003. "Protein Degradation and Protection against Misfolded or Damaged Proteins." *Nature* 426 (6968): 895–99. https://doi.org/10.1038/nature02263.

Goodwin, Edward C., and Daniel DiMaio. 2000. "Repression of Human Papillomavirus Oncogenes in HeLa Cervical Carcinoma Cells Causes the Orderly Reactivation of Dormant Tumor Suppressor Pathways." *Proceedings of the National Academy of Sciences of the United States of America* 97 (23): 12513–18. https://doi.org/10.1073/pnas.97.23.12513.

Grau-Bové, Xavier, Iñaki Ruiz-Trillo, and Manuel Irimia. 2018. "Origin of Exon Skipping-Rich Transcriptomes in Animals Driven by Evolution of Gene Architecture." *Genome Biology* 19 (1): 135. https://doi.org/10.1186/s13059-018-1499-9.

Griss, Johannes, Guilherme Viteri, Konstantinos Sidiropoulos, Vy Nguyen, Antonio Fabregat, and Henning Hermjakob. 2020. "ReactomeGSA - Efficient Multi-Omics Comparative Pathway Analysis." *Molecular & Cellular Proteomics : MCP* 19 (12): 2115–25. https://doi.org/10.1074/mcp.TIR120.002155.

Guo, Junjie U, Vikram Agarwal, Huili Guo, and David P Bartel. 2014. "Expanded Identification and Characterization of Mammalian Circular RNAs." *Genome Biology* 15 (7): 409. https://doi.org/10.1186/s13059-014-0409-z.

Guo, Yingli, Xiawei Wei, and Yong Peng. n.d. "Trends in Cell Biology Spotlight Structure-Mediated Degradation of CircRNAs Trends in Cell Biology." *Trends in Cell Biology*, 5–7. https://doi.org/10.1016/j.tcb.2020.04.001.

Han, Xuemei, Aaron Aslanian, and John R 3rd Yates. 2008. "Mass Spectrometry for Proteomics." *Current Opinion in Chemical Biology* 12 (5): 483–90. https://doi.org/10.1016/j.cbpa.2008.07.024.

Hansen, Thomas B, Morten T Venø, Christian K Damgaard, and Jørgen Kjems. 2016. "Comparison of Circular RNA Prediction Tools." *Nucleic Acids Research* 44 (6): e58–e58. https://doi.org/10.1093/nar/gkv1458.

He, Alina T, Jinglei Liu, Feiya Li, and Burton B Yang. 2021. “Targeting Circular RNAs as a Therapeutic Approach: Current Strategies and Challenges.” *Signal Transduction and Targeted Therapy* 6 (1): 185. https://doi.org/10.1038/s41392-021-00569-5.

He, Feng, and Allan Jacobson. 2015. “Nonsense-Mediated MRNA Decay: Degradation of Defective Transcripts Is Only Part of the Story.” *Annual Review of Genetics* 49: 339–66. https://doi.org/10.1146/annurev-genet-112414-054639.

Heesch, Sebastiaan van, Franziska Witte, Valentin Schneider-Lunitz, Jana F. Schulz, Eleonora Adami, Allison B. Faber, Marieluise Kirchner, et al. 2019. “The Translational Landscape of the Human Heart.” *Cell* 178 (1): 242-260.e29. https://doi.org/10.1016/j.cell.2019.05.010.

Hockenbery, D M, M Zutter, W Hickey, M Nahm, and S J Korsmeyer. 1991. “BCL2 Protein Is Topographically Restricted in Tissues Characterized by Apoptotic Cell Death.” *Proceedings of the National Academy of Sciences of the United States of America* 88 (16): 6961–65. https://doi.org/10.1073/pnas.88.16.6961.

Holdt, Lesca M., Alexander Kohlmaier, and Daniel Teupser. 2018a. “Circular RNAs as Therapeutic Agents and Targets.” *Frontiers in Physiology* 9 (OCT). https://doi.org/10.3389/fphys.2018.01262.

Holdt, Lesca M, Alexander Kohlmaier, and Daniel Teupser. 2018b. “Circular RNAs as Therapeutic Agents and Targets.” *Frontiers in Physiology* 9: 1262. https://doi.org/10.3389/fphys.2018.01262.

Hongmei, Zhao. 2012. “Extrinsic and Intrinsic Apoptosis Signal Pathway Review.” *Apoptosis and Medicine*, 3–22. https://doi.org/10.5772/50129.

Hormoz, Sahand. 2013. “Amino Acid Composition of Proteins Reduces Deleterious Impact of Mutations.” *Scientific Reports* 3 (1): 2919. https://doi.org/10.1038/srep02919.

Huang, Anqing, Haoxiao Zheng, Zhiye Wu, Minsheng Chen, and Yuli Huang. 2020. “Theranostics Circular RNA-Protein Interactions : Functions , Mechanisms , and Identification” 10 (8). https://doi.org/10.7150/thno.42174.

Huang, Haimei, Shian-Yi Huang, Ting-Ting Chen, Ja-Chi Chen, Chian-Ling Chiou,

and Ter-Mei Huang. 2004. “Cisplatin Restores P53 Function and Enhances the Radiosensitivity in HPV16 E6 Containing SiHa Cells.” *Journal of Cellular Biochemistry* 91 (4): 756–65. https://doi.org/10.1002/jcb.10769.

Huang, Huilin, Hengyou Weng, and Jianjun Chen. 2020. “M6A Modification in Coding and Non-Coding RNAs: Roles and Therapeutic Implications in Cancer.” *Cancer Cell* 37 (3): 270–88. https://doi.org/https://doi.org/10.1016/j.ccell.2020.02.004.

Huang, Wendi, Yunchao Ling, Sirui Zhang, Qiguang Xia, Ruifang Cao, Xiaojuan Fan, Zhaoyuan Fang, Zefeng Wang, and Guoqing Zhang. 2020. “TransCirc : An Interactive Database for Translatable Circular RNAs Based on Multi-Omics Evidence,” 1–7. https://doi.org/10.1093/nar/gkaa823.

Huang, Xiao-bin, Kai-jing Song, Guo-bin Chen, Rui Liu, and Zhuo-fei Jiang. 2020. “Circular RNA Hsa _ Circ _ 0003204 Promotes Cervical Cancer Cell Proliferation , Migration , and Invasion by Regulating MAPK Pathway.” *Cancer Biology & Therapy* 00 (00): 1–11. https://doi.org/10.1080/15384047.2020.1824513.

Huang, Yifan, Ying Li, Wensen Lin, Shuhao Fan, Haorong Chen, Jiaojiao Xia, Jiang Pi, and Jun-Fa Xu. 2022. “Promising Roles of Circular RNAs as Biomarkers and Targets for Potential Diagnosis and Therapy of Tuberculosis.” *Biomolecules* 12 (9). https://doi.org/10.3390/biom12091235.

Ichim, Gabriel, Jonathan Lopez, Shafiq U Ahmed, Nathiya Muthalagu, Evangelos Giampazolias, M Eugenia Delgado, Martina Haller, et al. 2015. “Limited Mitochondrial Permeabilization Causes DNA Damage and Genomic Instability in the Absence of Cell Death.” *Molecular Cell* 57 (5): 860–72. https://doi.org/10.1016/j.molcel.2015.01.018.

Ivanov, Andranik, Sebastian Memczak, Emanuel Wyler, Francesca Torti, Hagit T Porath, Marta R Orejuela, Michael Piechotta, et al. 2015. “Analysis of Intron Sequences Reveals Hallmarks of Circular RNA Biogenesis in Animals.” *Cell Reports* 10 (2): 170–77. https://doi.org/10.1016/j.celrep.2014.12.019.

Jeck, William R., Jessica A. Sorrentino, Kai Wang, Michael K. Slevin, Christin E. Burd, Jinze Liu, William F. Marzluff, and Norman E. Sharpless. 2013a. “Circular RNAs Are Abundant, Conserved, and Associated with ALU Repeats.” *Rna* 19 (2):

141–57. https://doi.org/10.1261/rna.035667.112.

Jeck, William R, and Norman E Sharpless. 2014. “Detecting and Characterizing Circular RNAs.” *Nature Biotechnology* 32 (5): 453–61. https://doi.org/10.1038/nbt.2890.

Jeck, William R, Jessica A Sorrentino, Kai Wang, Michael K Slevin, Christin E Burd, Jinze Liu, William F Marzluff, and Norman E Sharpless. 2013b. “Circular RNAs Are Abundant, Conserved, and Associated with ALU Repeats.” *RNA (New York, N.Y.)* 19 (2): 141–57. https://doi.org/10.1261/rna.035667.112.

Jekimovs, Christian, Emma Bolderson, Amila Suraweera, Mark Adams, Kenneth J O’Byrne, and Derek J Richard. 2014. “Chemotherapeutic Compounds Targeting the DNA Double-Strand Break Repair Pathways: The Good, the Bad, and the Promising.” *Frontiers in Oncology* 4: 86. https://doi.org/10.3389/fonc.2014.00086.

Jiao, Shihu, Song Wu, Shan Huang, Mingyang Liu, and Bo Gao. 2021. “Advances in the Identification of Circular RNAs and Research Into CircRNAs in Human Diseases.” *Frontiers in Genetics* 12: 665233. https://doi.org/10.3389/fgene.2021.665233.

Jinek, Martin, Scott M Coyle, and Jennifer A Doudna. 2011. “Coupled 5’ Nucleotide Recognition and Processivity in Xrn1-Mediated MRNA Decay.” *Molecular Cell* 41 (5): 600–608. https://doi.org/10.1016/j.molcel.2011.02.004.

Jost, Philipp J, and Domagoj Vucic. 2020. “Regulation of Cell Death and Immunity by XIAP.” *Cold Spring Harbor Perspectives in Biology* 12 (8). https://doi.org/10.1101/cshperspect.a036426.

Kiss, Robert C, Fen Xia, and Scarlett Acklin. 2021. “Targeting DNA Damage Response and Repair to Enhance Therapeutic Index in Cisplatin-Based Cancer Treatment.” *International Journal of Molecular Sciences*. https://doi.org/10.3390/ijms22158199.

Kramer, Marianne C, Dongming Liang, Deirdre C Tatomer, Beth Gold, Zachary M March, Sara Cherry, and Jeremy E Wilusz. 2015. “Combinatorial Control of Drosophila Circular RNA Expression by Intronic Repeats, HnRNPs, and SR

Proteins." *Genes & Development* 29 (20): 2168–82. https://doi.org/10.1101/gad.270421.115.

Kristensen, Lasse S., Maria S. Andersen, Lotte V.W. Stagsted, Karoline K. Ebbesen, Thomas B. Hansen, and Jørgen Kjems. 2019. "The Biogenesis, Biology and Characterization of Circular RNAs." *Nature Reviews Genetics* 20 (11): 675–91. https://doi.org/10.1038/s41576-019-0158-7.

Lam, Jenny K W, Michael Y T Chow, Yu Zhang, and Susan W S Leung. 2015. "SiRNA Versus MiRNA as Therapeutics for Gene Silencing." *Molecular Therapy - Nucleic Acids* 4: e252. https://doi.org/https://doi.org/10.1038/mtna.2015.23.

Lee, R C, R L Feinbaum, and V Ambros. 1993. "The C. Elegans Heterochronic Gene Lin-4 Encodes Small RNAs with Antisense Complementarity to Lin-14." *Cell* 75 (5): 843–54. https://doi.org/10.1016/0092-8674(93)90529-y.

Lee, Sooncheol, Botao Liu, Soohyun Lee, Sheng-Xiong Huang, Ben Shen, and Shu-Bing Qian. 2012. "Global Mapping of Translation Initiation Sites in Mammalian Cells at Single-Nucleotide Resolution." *Proceedings of the National Academy of Sciences of the United States of America* 109 (37): E2424-32. https://doi.org/10.1073/pnas.1207846109.

Lee, Tong Ihn, and Richard A Young. 2013. "Transcriptional Regulation and Its Misregulation in Disease." *Cell* 152 (6): 1237–51. https://doi.org/10.1016/j.cell.2013.02.014.

Legnini, Ivano, Gaia Di Timoteo, Francesca Rossi, Mariangela Morlando, Francesca Briganti, Olga Sthandier, Alessandro Fatica, et al. 2017. "Circ-ZNF609 Is a Circular RNA That Can Be Translated and Functions in Myogenesis." *Molecular Cell* 66 (1): 22-37.e9. https://doi.org/10.1016/j.molcel.2017.02.017.

Li, Aimin, Peilin Jia, Saurav Mallik, Rong Fei, Hiroki Yoshioka, Akiko Suzuki, Junichi Iwata, and Zhongming Zhao. 2020. "Critical MicroRNAs and Regulatory Motifs in Cleft Palate Identified by a Conserved MiRNA-TF-Gene Network Approach in Humans and Mice." *Briefings in Bioinformatics* 21 (4): 1465–78. https://doi.org/10.1093/bib/bbz082.

Li, Honglin, Hong Zhu, Chi-jie Xu, and Junying Yuan. 1998. "Cleavage of BID by

Caspase 8 Mediates the Mitochondrial Damage in the Fas Pathway of Apoptosis." *Cell* 94 (4): 491–501. https://doi.org/https://doi.org/10.1016/S0092-8674(00)81590-1.

Li, Min, Christian Marin-Muller, Uddalak Bharadwaj, Kwong-Hon Chow, Qizhi Yao, and Changyi Chen. 2009. "MicroRNAs: Control and Loss of Control in Human Physiology and Disease." *World Journal of Surgery* 33 (4): 667–84. https://doi.org/10.1007/s00268-008-9836-x.

Li, Peng, Xiao Yang, Wenbo Yuan, Chengdi Yang, Xiaolei Zhang, Jie Han, Jingzi Wang, et al. 2018. "CircRNA-Cdr1as Exerts Anti-Oncogenic Functions in Bladder Cancer by Sponging MicroRNA-135a." *Cellular Physiology and Biochemistry : International Journal of Experimental Cellular Physiology, Biochemistry, and Pharmacology* 46 (4): 1606–16. https://doi.org/10.1159/000489208.

Li, Siqi, Xiang Li, Wei Xue, Lin Zhang, Shi-Meng Cao, Yun-Ni Lei, Liang-Zhong Yang, et al. 2020. *Screening for Functional Circular RNAs Using the CRISPR-Cas13 System*. *Nature Methods*. Springer US. https://doi.org/10.1101/2020.03.23.002865.

Li, Xiang, Chu Xiao Liu, Wei Xue, Yang Zhang, Shan Jiang, Qing Fei Yin, Jia Wei, Run Wen Yao, Li Yang, and Ling Ling Chen. 2017. "Coordinated CircRNA Biogenesis and Function with NF90/NF110 in Viral Infection." *Molecular Cell* 67 (2): 214-227.e7. https://doi.org/10.1016/j.molcel.2017.05.023.

Li, Xiaohan, Bing Zhang, Fuyu Li, Kequan Yu, and Yunfei Bai. 2020. "The Mechanism and Detection of Alternative Splicing Events in Circular RNAs." *PeerJ* 8: e10032. https://doi.org/10.7717/peerj.10032.

Li, Zhaoyong, Chuan Huang, Chun Bao, Liang Chen, Mei Lin, Xiaolin Wang, Guolin Zhong, et al. 2015. "Exon-Intron Circular RNAs Regulate Transcription in the Nucleus." *Nature Structural & Molecular Biology*, no. November 2014: 1–11. https://doi.org/10.1038/nsmb.2959.

Lin, Min, Miaomiao Ye, Junhan Zhou, Z Peter Wang, and Xueqiong Zhu. 2019. "Recent Advances on the Molecular Mechanism of Cervical Carcinogenesis Based on Systems Biology Technologies." *Computational and Structural Biotechnology*

Journal 17 (109): 241–50. https://doi.org/10.1016/j.csbj.2019.02.001.

Liu, Chu-Xiao, Xiang Li, Fang Nan, Shan Jiang, Xiang Gao, Si-Kun Guo, Wei Xue, et al. 2019. "Structure and Degradation of Circular RNAs Regulate PKR Activation in Innate Immunity." *Cell* 177 (4): 865-880.e21. https://doi.org/https://doi.org/10.1016/j.cell.2019.03.046.

Liu, Jing, Xin Zhang, Meinan Yan, and Hui Li. 2020. "Emerging Role of Circular RNAs in Cancer." *Frontiers in Oncology* 10: 663. https://doi.org/10.3389/fonc.2020.00663.

Liu, Ming, Qian Wang, Jian Shen, Burton B Yang, and Xiangming Ding. 2019. "Circbank: A Comprehensive Database for CircRNA with Standard Nomenclature." *RNA Biology* 16 (7): 899–905. https://doi.org/10.1080/15476286.2019.1600395.

Liu, Shun, Allen Zhu, Chuan He, and Mengjie Chen. 2020. "REPIC: A Database for Exploring the N6-Methyladenosine Methylome." *Genome Biology* 21 (1): 100. https://doi.org/10.1186/s13059-020-02012-4.

Liu, Xin-Yuan, Qi Zhang, Jing Guo, Peng Zhang, Hua Liu, Zi-Bin Tian, Cui-Ping Zhang, and Xiao-Yu Li. 2021. "The Role of Circular RNAs in the Drug Resistance of Cancers." *Frontiers in Oncology* 11: 790589. https://doi.org/10.3389/fonc.2021.790589.

Marchenko, N D, and U M Moll. 2014. "Mitochondrial Death Functions of P53." *Molecular & Cellular Oncology* 1 (2): e955995. https://doi.org/10.1080/23723548.2014.955995.

Martin, Constance J, Kristen N Peters, and Samuel M Behar. 2014. "Macrophages Clean up: Efferocytosis and Microbial Control." *Current Opinion in Microbiology* 17 (February): 17–23. https://doi.org/10.1016/j.mib.2013.10.007.

McGrath, Emmet E. 2011. "The Tumor Necrosis Factor-Related Apoptosis-Inducing Ligand and Lung Cancer: Still Following the Right TRAIL?" *Journal of Thoracic Oncology* 6 (6): 983–87. https://doi.org/10.1097/JTO.0b013e318217b6c8.

McIlwain, David R, Thorsten Berger, and Tak W Mak. 2013. "Caspase Functions in Cell Death and Disease." *Cold Spring Harbor Perspectives in Biology* 5 (4):

a008656. https://doi.org/10.1101/cshperspect.a008656.

Memczak, Sebastian, Marvin Jens, Antigoni Elefsinioti, Francesca Torti, Janna Krueger, Agnieszka Rybak, Luisa Maier, et al. 2013. “Circular RNAs Are a Large Class of Animal RNAs with Regulatory Potency.” *Nature* 495 (7441): 333–38. https://doi.org/10.1038/nature11928.

Misir, Sema, Nan Wu, and Burton B Yang. 2022. “Specific Expression and Functions of Circular RNAs.” *Cell Death and Differentiation* 29 (3): 481–91. https://doi.org/10.1038/s41418-022-00948-7.

Mo, Dingding, Xinping Li, Carsten A. Raabe, Timofey S. Rozhdestvensky, Boris V. Skryabin, and Juergen Brosius. 2020. “Circular RNA Encoded Amyloid Beta Peptides-A Novel Putative Player in Alzheimer’s Disease.” *Cells* 9 (10). https://doi.org/10.3390/cells9102196.

Moyano, Miguel, and Giovanni Stefani. 2015. “PiRNA Involvement in Genome Stability and Human Cancer.” *Journal of Hematology & Oncology* 8 (April): 38. https://doi.org/10.1186/s13045-015-0133-5.

Nagata, Shigekazu. 2018. “Apoptosis and Clearance of Apoptotic Cells.” *Annual Review of Immunology* 36: 489–517. https://doi.org/10.1146/annurev-immunol-042617-053010.

Nicholson, Donald W, and Nancy A Thornberry. 1997. “Caspases: Killer Proteases.” *Trends in Biochemical Sciences* 22 (8): 299–306. https://doi.org/https://doi.org/10.1016/S0968-0004(97)01085-2.

Nigro, Janice M., Kathleen R. Cho, Eric R. Fearon, Scott E. Kern, J. Michael Ruppert, Jonathan D. Oliner, Kenneth W. Kinzler, and Bert Vogelstein. 1991. “Scrambled Exons.” *Cell* 64 (3): 607–13. https://doi.org/10.1016/0092-8674(91)90244-S.

Oltvai, Z N, C L Milliman, and S J Korsmeyer. 1993. “Bcl-2 Heterodimerizes in Vivo with a Conserved Homolog, Bax, That Accelerates Programmed Cell Death.” *Cell* 74 (4): 609–19. https://doi.org/10.1016/0092-8674(93)90509-o.

Oren, Moshe. 2019. “P53: Not Just a Tumor Suppressor.” *Journal of Molecular Cell Biology* 11 (7): 539–43. https://doi.org/10.1093/jmcb/mjz070.

Ou, Rongying, Jiangmin Lv, Qianwen Zhang, Fan Lin, Li Zhu, Fangfang Huang, Xiangyun Li, et al. 2020. "CircAMOTL1 Motivates AMOTL1 Expression to Facilitate Cervical Cancer Growth." *Molecular Therapy - Nucleic Acids* 19 (March): 50–60. https://doi.org/10.1016/j.omtn.2019.09.022.

Ovejero, Sara, Avelino Bueno, and María P Sacristán. 2020. "Working on Genomic Stability: From the S-Phase to Mitosis." *Genes* 11 (2). https://doi.org/10.3390/genes11020225.

Pabla, Navjotsingh, Shuang Huang, Qing Sheng Mi, Rene Daniel, and Zheng Dong. 2008. "ATR-Chk2 Signaling in P53 Activation and DNA Damage Response during Cisplatin-Induced Apoptosis." *Journal of Biological Chemistry* 283 (10): 6572–83. https://doi.org/10.1074/jbc.M707568200.

Pal, Asmita, and Rita Kundu. 2019. "Human Papillomavirus E6 and E7: The Cervical Cancer Hallmarks and Targets for Therapy." *Frontiers in Microbiology* 10: 3116. https://doi.org/10.3389/fmicb.2019.03116.

Pamudurti, Nagarjuna Reddy, Osnat Bartok, Marvin Jens, Reut Ashwal-Fluss, Christin Stottmeister, Larissa Ruhe, Mor Hanan, et al. 2017. "Translation of CircRNAs." *Molecular Cell* 66 (1): 9-21.e7. https://doi.org/10.1016/j.molcel.2017.02.021.

Pamudurti, Nagarjuna Reddy, Ines Lucia Patop, Aishwarya Krishnamoorthy, Reut Ashwal-Fluss, Osnat Bartok, and Sebastian Kadener. 2020. "An in Vivo Strategy for Knockdown of Circular RNAs." *Cell Discovery* 6 (1). https://doi.org/10.1038/s41421-020-0182-y.

Panda, Amaresh Chandra. 2018. "Circular RNAs Act as MiRNA Sponges." *Advances in Experimental Medicine and Biology* 1087: 67–79. https://doi.org/10.1007/978-981-13-1426-1_6.

Park, Ok Hyun, Hongseok Ha, Yujin Lee, Sung Ho Boo, Do Hoon Kwon, Hyun Kyu Song, and Yoon Ki Kim. 2019. "Endoribonucleolytic Cleavage of M6A-Containing RNAs by RNase P/MRP Complex." *Molecular Cell* 74 (3): 494-507.e8. https://doi.org/https://doi.org/10.1016/j.molcel.2019.02.034.

Pimple, Sharmila, and Gauravi Mishra. 2022. "Cancer Cervix: Epidemiology and Disease Burden." *CytoJournal* 19: 21.

https://doi.org/10.25259/CMAS_03_02_2021.

Prats, Anne-Catherine, Florian David, Leila H Diallo, Emilie Roussel, Florence Tatin, Barbara Garmy-Susini, and Eric Lacazette. 2020. “Circular RNA, the Key for Translation.” *International Journal of Molecular Sciences* 21 (22). https://doi.org/10.3390/ijms21228591.

Pucci, B, M Kasten, and A Giordano. 2000. “Cell Cycle and Apoptosis.” *Neoplasia (New York, N.Y.)* 2 (4): 291–99. https://doi.org/10.1038/sj.neo.7900101.

Qu, Shibin, Xisheng Yang, Xiaolei Li, Jianlin Wang, Yuan Gao, Runze Shang, Wei Sun, Kefeng Dou, and Haimin Li. 2015. “Circular RNA: A New Star of Noncoding RNAs.” *Cancer Letters* 365 (2): 141–48. https://doi.org/https://doi.org/10.1016/j.canlet.2015.06.003.

Reid, S., A. Ritohie, G. Hangoc, S. Cooper, L. Boring, F. Charo, and H. E. Broxmever. 1998. “Enhanced Myeloid Progenitor Cell Cycling and Apoptosis in Mice Lacking the Chemokine Receptor, CCR2.” *Experimental Hematology* 26 (8): 695. https://doi.org/10.1182/blood.v93.5.1524.405k07_1524_1533.

Reinhart, B J, F J Slack, M Basson, A E Pasquinelli, J C Bettinger, A E Rougvie, H R Horvitz, and G Ruvkun. 2000. “The 21-Nucleotide Let-7 RNA Regulates Developmental Timing in Caenorhabditis Elegans.” *Nature* 403 (6772): 901–6. https://doi.org/10.1038/35002607.

Ren, Wenjun, Yixiao Yuan, Jun Peng, Luciano Mutti, and Xiulin Jiang. 2022. “The Function and Clinical Implication of Circular RNAs in Lung Cancer.” *Frontiers in Oncology* 12: 862602. https://doi.org/10.3389/fonc.2022.862602.

Roura, Esther, Noémie Travier, Tim Waterboer, Silvia de Sanjosé, F Xavier Bosch, Michael Pawlita, Valeria Pala, et al. 2016. “The Influence of Hormonal Factors on the Risk of Developing Cervical Cancer and Pre-Cancer: Results from the EPIC Cohort.” *PloS One* 11 (1): e0147029. https://doi.org/10.1371/journal.pone.0147029.

Ruiz-Orera, Jorge, Xavier Messeguer, Juan Antonio Subirana, and M Mar Alba. 2014. “Long Non-Coding RNAs as a Source of New Peptides.” *ELife* 3 (September): e03523. https://doi.org/10.7554/eLife.03523.

Salzman, Julia, Raymond E Chen, Mari N Olsen, Peter L Wang, and Patrick O Brown. 2013. “Cell-Type Specific Features of Circular RNA Expression.” *PLoS Genetics* 9 (9): e1003777. https://doi.org/10.1371/journal.pgen.1003777.

Salzman, Julia, Charles Gawad, Peter Lincoln Wang, Norman Lacayo, and Patrick O Brown. 2012. “Circular RNAs Are the Predominant Transcript Isoform from Hundreds of Human Genes in Diverse Cell Types” 7 (2). https://doi.org/10.1371/journal.pone.0030733.

Samuel, Temesgen, H. Oliver Weber, and Jens Oliver Funk. 2002. “Linking DNA Damage to Cell Cycle Checkpoints.” *Cell Cycle (Georgetown, Tex.)* 1 (3): 161–67. https://doi.org/10.4161/cc.1.3.118.

Sang, Meixiang, Lingjiao Meng, Sihua Liu, Pingan Ding, Sheng Chang, Yingchao Ju, Fei Liu, Lina Gu, Yishui Lian, and Cuizhi Geng. 2018. “Circular RNA CiRS-7 Maintains Metastatic Phenotypes as a CeRNA of MiR-1299 to Target MMPs.” *Molecular Cancer Research : MCR* 16 (11): 1665–75. https://doi.org/10.1158/1541-7786.MCR-18-0284.

Sang, Meixiang, Lingjiao Meng, Yang Sang, Shina Liu, Pingan Ding, Yingchao Ju, Fei Liu, et al. 2018. “Circular RNA CiRS-7 Accelerates ESCC Progression through Acting as a MiR-876-5p Sponge to Enhance MAGE-A Family Expression.” *Cancer Letters* 426 (July): 37–46. https://doi.org/10.1016/j.canlet.2018.03.049.

Schleich, Kolja, Uwe Warnken, Nicolai Fricker, Selcen Oztürk, Petra Richter, Kerstin Kammerer, Martina Schnölzer, Peter H Krammer, and Inna N Lavrik. 2012. “Stoichiometry of the CD95 Death-Inducing Signaling Complex: Experimental and Modeling Evidence for a Death Effector Domain Chain Model.” *Molecular Cell* 47 (2): 306–19. https://doi.org/10.1016/j.molcel.2012.05.006.

Schneider, Eberhard, Mathias Montenarh, and Peter Wagner. 1998. “Regulation of CAK Kinase Activity by P53.” *Oncogene* 17 (21): 2733–41. https://doi.org/10.1038/sj.onc.1202504.

Schneider, Tim, and Albrecht Bindereif. 2017. “Circular RNAs: Coding or Noncoding?” *Cell Research* 27 (6): 724–25. https://doi.org/10.1038/cr.2017.70.

Schneider, Tim, Lee Hsueh Hung, Silke Schreiner, Stefan Starke, Heinrich Eckhof,

Oliver Rossbach, Stefan Reich, Jan Medenbach, and Albrecht Bindereif. 2016. "CircRNA-Protein Complexes: IMP3 Protein Component Defines Subfamily of CircRNPs." *Scientific Reports* 6 (August): 1–11. https://doi.org/10.1038/srep31313.

Schoenberg, Daniel R. 2011. "Mechanisms of Endonuclease-Mediated MRNA Decay." *Wiley Interdisciplinary Reviews. RNA* 2 (4): 582–600. https://doi.org/10.1002/wrna.78.

Sedletska, Yuliya, Marie Josèphe Giraud-Panis, and Jean Marc Malinge. 2005. "Cisplatin Is a DNA-Damaging Antitumour Compound Triggering Multifactorial Biochemical Responses in Cancer Cells: Importance of Apoptotic Pathways." *Current Medicinal Chemistry - Anti-Cancer Agents* 5 (3): 251–65. https://doi.org/10.2174/1568011053765967.

Shang, Qingfeng, Zhi Yang, Renbing Jia, and Shengfang Ge. 2019. "The Novel Roles of CircRNAs in Human Cancer," 1–10.

Sharma, Ashish Ranjan, Manojit Bhattacharya, Swarnav Bhakta, Abinit Saha, Sang-Soo Lee, and Chiranjib Chakraborty. 2021. "Recent Research Progress on Circular RNAs: Biogenesis, Properties, Functions, and Therapeutic Potential." *Molecular Therapy. Nucleic Acids* 25 (September): 355–71. https://doi.org/10.1016/j.omtn.2021.05.022.

Shayevitch, Ronna, Dan Askayo, Ifat Keydar, and Gil Ast. 2018. "The Importance of DNA Methylation of Exons on Alternative Splicing." *RNA (New York, N.Y.)* 24 (10): 1351–62. https://doi.org/10.1261/rna.064865.117.

Singh, Rumani, Anthony Letai, and Kristopher Sarosiek. 2020. "Of BCL-2 Family Proteins" 20 (3): 175–93. https://doi.org/10.1038/s41580-018-0089-8.Regulation.

Sinha, Tanvi, Chirag Panigrahi, Debojyoti Das, and Amaresh Chandra Panda. 2022. "Circular RNA Translation, a Path to Hidden Proteome." *Wiley Interdisciplinary Reviews. RNA* 13 (1): e1685. https://doi.org/10.1002/wrna.1685.

Smardová, Jana, Sárka Pavlóva, Miluska Svitákóva, Diana Grochová, and Barbora Ravcukóva. 2005. "Analysis of P53 Status in Human Cell Lines Using a Functional Assay in Yeast: Detection of New Non-Sense P53 Mutation in Codon

124." *Oncology Reports* 14 (4): 901–7. https://doi.org/10.3892/or.14.4.901.

Starke, Stefan, Isabelle Jost, Oliver Rossbach, Tim Schneider, Silke Schreiner, Lee-Hsueh Hung, and Albrecht Bindereif. 2015. "Exon Circularization Requires Canonical Splice Signals." *Cell Reports* 10 (1): 103–11. https://doi.org/10.1016/j.celrep.2014.12.002.

Statello, Luisa, Chun-Jie Guo, Ling-Ling Chen, and Maite Huarte. 2021. "Gene Regulation by Long Non-Coding RNAs and Its Biological Functions." *Nature Reviews Molecular Cell Biology* 22 (2): 96–118. https://doi.org/10.1038/s41580-020-00315-9.

Szabo, Linda, and Julia Salzman. 2016. "Detecting Circular RNAs: Bioinformatic and Experimental Challenges." *Nature Reviews. Genetics* 17 (11): 679–92. https://doi.org/10.1038/nrg.2016.114.

Taft, Ryan J, and John S Mattick. 2003. "Increasing Biological Complexity Is Positively Correlated with the Relative Genome-Wide Expansion of Non-Protein-Coding DNA Sequences." *Genome Biology* 5 (1): P1. https://doi.org/10.1186/gb-2003-5-1-p1.

Taft, Ryan J, Michael Pheasant, and John S Mattick. 2007. "The Relationship between Non-Protein-Coding DNA and Eukaryotic Complexity." *BioEssays : News and Reviews in Molecular, Cellular and Developmental Biology* 29 (3): 288–99. https://doi.org/10.1002/bies.20544.

Talhouarne, Gaëlle J S, and Joseph G Gall. 2018. "Lariat Intronic RNAs in the Cytoplasm of Vertebrate Cells." *Proceedings of the National Academy of Sciences of the United States of America* 115 (34): E7970–77. https://doi.org/10.1073/pnas.1808816115.

Thompson, E B. 1998. "The Many Roles of C-Myc in Apoptosis." *Annual Review of Physiology* 60: 575–600. https://doi.org/10.1146/annurev.physiol.60.1.575.

Tomari, Yukihide, and Phillip D Zamore. 2005. "Perspective: Machines for RNAi." *Genes & Development* 19 (5): 517–29. https://doi.org/10.1101/gad.1284105.

Trinidad, Antonio Garcia, Patricia A.J. Muller, Jorge Cuellar, Marta Klejnot, Max Nobis, José María Valpuesta, and Karen H. Vousden. 2013. "Interaction of P53

with the CCT Complex Promotes Protein Folding and Wild-Type P53 Activity." *Molecular Cell* 50 (6): 805–17. https://doi.org/https://doi.org/10.1016/j.molcel.2013.05.002.

Vanhoutteghem, Amandine, Cyril Bouche, Anna Maciejewski-Duval, Françoise Hervé, and Philippe Djian. 2011. "Basonuclins and Disco: Orthologous Zinc Finger Proteins Essential for Development in Vertebrates and Arthropods." *Biochimie* 93 (2): 127–33. https://doi.org/https://doi.org/10.1016/j.biochi.2010.09.010.

Verma, Sonia, Rajnikant Dixit, and Kailash C Pandey. 2016. "Cysteine Proteases: Modes of Activation and Future Prospects as Pharmacological Targets." *Frontiers in Pharmacology* 7: 107. https://doi.org/10.3389/fphar.2016.00107.

Vermeulen, Katrien, Zwi N. Berneman, and Dirk R. Van Bockstaele. 2003. "Cell Cycle and Apoptosis." *Cell Proliferation* 36 (3): 165–75. https://doi.org/10.1046/j.1365-2184.2003.00267.x.

Vo, Josh N, Marcin Cieslik, Yajia Zhang, Sudhanshu Shukla, Lanbo Xiao, Yuping Zhang, Yi-Mi Wu, et al. 2019. "The Landscape of Circular RNA in Cancer." *Cell* 176 (4): 869-881.e13. https://doi.org/10.1016/j.cell.2018.12.021.

Vogt, Carl. 1842. *Untersuchungen Über Die Entwicklungsgeschichte Der Geburtshelferkröte (Alytes Obstetricans)*. Jent & Gassmann.

Vousden, Karen H. 2006. "Outcomes of P53 Activation - Spoilt for Choice." *Journal of Cell Science* 119 (24): 5015–20. https://doi.org/10.1242/jcs.03293.

Vries, Elisabeth G.E. De, Jourik A. Gietema, and Steven De Jong. 2006. "Tumor Necrosis Factor-Related Apoptosis-Inducing Ligand Pathway and Its Therapeutic Implications." *Clinical Cancer Research* 12 (8): 2390–93. https://doi.org/10.1158/1078-0432.CCR-06-0352.

Wang, Chen, Jiawei Zhang, Jie Yin, Yichao Gan, Senlin Xu, Ying Gu, and Wendong Huang. 2021. "Alternative Approaches to Target Myc for Cancer Treatment." *Signal Transduction and Targeted Therapy* 6 (1): 117. https://doi.org/10.1038/s41392-021-00500-y.

Wang, Qifang, Xin Li, Liqin Wang, Ying-Hong Feng, Robin Zeng, and George Gorodeski. 2004. "Antiapoptotic Effects of Estrogen in Normal and Cancer

Human Cervical Epithelial Cells." *Endocrinology* 145 (12): 5568–79. https://doi.org/10.1210/en.2004-0807.

Wang, Zhixiang. 2021. "Regulation of Cell Cycle Progression by Growth Factor-Induced Cell Signaling." *Cells* 10 (12). https://doi.org/10.3390/cells10123327.

Wawryk-Gawda, Ewelina, Patrycja Chylińska-Wrzos, Marta Lis-Sochocka, Katarzyna Chłapek, Kamila Bulak, Marian Jędrych, and Barbara Jodłowska-Jędrych. 2014. "P53 Protein in Proliferation, Repair and Apoptosis of Cells." *Protoplasma* 251 (3): 525–33. https://doi.org/10.1007/s00709-013-0548-1.

Wei, Jian Wei, Kai Huang, Chao Yang, and Chun Sheng Kang. 2017. "Non-Coding RNAs as Regulators in Epigenetics (Review)." *Oncology Reports* 37 (1): 3–9. https://doi.org/10.3892/or.2016.5236.

Westphal, D, R M Kluck, and G Dewson. 2014. "Building Blocks of the Apoptotic Pore: How Bax and Bak Are Activated and Oligomerize during Apoptosis." *Cell Death & Differentiation* 21 (2): 196–205. https://doi.org/10.1038/cdd.2013.139.

Wilusz, Jeremy E. 2017. "Circular RNAs: Unexpected Outputs of Many Protein-Coding Genes." *RNA Biology* 14 (8): 1007–17. https://doi.org/10.1080/15476286.2016.1227905.

Wiman, K G, and B Zhivotovsky. 2017. "Understanding Cell Cycle and Cell Death Regulation Provides Novel Weapons against Human Diseases." *Journal of Internal Medicine* 281 (5): 483–95. https://doi.org/10.1111/joim.12609.

Woods, Derek, and John J Turchi. 2013. "Chemotherapy Induced DNA Damage Response: Convergence of Drugs and Pathways." *Cancer Biology & Therapy* 14 (5): 379–89. https://doi.org/10.4161/cbt.23761.

Wsierska-Gdek, Józefa, Daniela Schloffer, Vladimir Kotala, and Marcel Horky. 2002. "Escape of P53 Protein from E6-Mediated Degradation in HeLa Cells after Cisplatin Therapy." *International Journal of Cancer* 101 (2): 128–36. https://doi.org/10.1002/ijc.10580.

Wu, Fengqin, and Jingjing Zhou. 2019. "CircAGFG1 Promotes Cervical Cancer Progression via MiR-370-3p/RAF1 Signaling." *BMC Cancer* 19 (1): 1–10. https://doi.org/10.1186/s12885-019-6269-x.

Xia, Siyu, Jing Feng, Ke Chen, Yanbing Ma, Jing Gong, Fangfang Cai, Yuxuan Jin, et al. 2018. “CSCD: A Database for Cancer-Specific Circular RNAs.” *Nucleic Acids Research* 46 (D1): D925–29. https://doi.org/10.1093/nar/gkx863.

Xia, Xin, Xixi Li, Fanying Li, Xujia Wu, Maolei Zhang, Huangkai Zhou, Nunu Huang, et al. 2019. “A Novel Tumor Suppressor Protein Encoded by Circular AKT3 RNA Inhibits Glioblastoma Tumorigenicity by Competing with Active Phosphoinositide-Dependent Kinase-1.” *Molecular Cancer* 18 (1): 1–16. https://doi.org/10.1186/s12943-019-1056-5.

Xu, Chuan, and Jianzhi Zhang. 2021. “Mammalian Circular RNAs Result Largely from Splicing Errors.” *Cell Reports* 36 (4): 109439. https://doi.org/10.1016/j.celrep.2021.109439.

Xu, Juan, Xiyi Chen, Yu Sun, Yaqian Shi, Fang Teng, Mingming Lv, Chen Liu, and Xuemei Jia. 2021. “The Regulation Network and Clinical Significance of Circular RNAs in Breast Cancer.” *Frontiers in Oncology*. Switzerland. https://doi.org/10.3389/fonc.2021.691317.

Yang, Hongbao, Xiaobo Li, Qingtao Meng, Hao Sun, Shenshen Wu, Weiwei Hu, Guilai Liu, and Xianjing Li. 2020. “CircPTK2 (Hsa _ Circ _ 0005273) as a Novel Therapeutic Target for Metastatic Colorectal Cancer,” 1–15.

Yang, Yun, Xiaojuan Fan, Miaowei Mao, Xiaowei Song, Ping Wu, Yang Zhang, and Yongfeng Jin. 2017. “Extensive Translation of Circular RNAs Driven By.” *Nature Publishing Group*, 1–16. https://doi.org/10.1038/cr.2017.31.

———. 2017. “Extensive Translation of Circular RNAs Driven by N 6 - Methyladenosine.” *Cell Research* 27 (5): 626–41. https://doi.org/10.1038/cr.2017.31.

Yang, Zhen-Guo, Faryal Mehwish Awan, William W Du, Yan Zeng, Juanjuan Lyu, De Wu, Shaan Gupta, Weining Yang, and Burton B Yang. 2017. “The Circular RNA Interacts with STAT3, Increasing Its Nuclear Translocation and Wound Repair by Modulating Dnmt3a and MiR-17 Function.” *Molecular Therapy : The Journal of the American Society of Gene Therapy* 25 (9): 2062–74. https://doi.org/10.1016/j.ymthe.2017.05.022.

Yaylak, B., I. Erdogan, and B. Akgul. 2019. “Transcriptomics Analysis of Circular RNAs Differentially Expressed in Apoptotic HeLa Cells.” *Frontiers in Genetics* 10 (MAR). https://doi.org/10.3389/fgene.2019.00176.

Ye, Feng, Guanfeng Gao, Yutian Zou, Shaoquan Zheng, Lijuan Zhang, Xueqi Ou, Xiaoming Xie, and Hailin Tang. 2019. “CircFBXW7 Inhibits Malignant Progression by Sponging MiR-197-3p and Encoding a 185-Aa Protein in Triple-Negative Breast Cancer.” *Molecular Therapy. Nucleic Acids* 18 (December): 88–98. https://doi.org/10.1016/j.omtn.2019.07.023.

Ye, Yanwen, Zefeng Wang, and Yun Yang. 2021. “Comprehensive Identification of Translatable Circular RNAs Using Polysome Profiling.” *Bio-Protocol* 11 (18): e4167. https://doi.org/10.21769/BioProtoc.4167.

Yi, Rui, Yi Qin, Ian G Macara, and Bryan R Cullen. 2003. “Exportin-5 Mediates the Nuclear Export of Pre-MicroRNAs and Short Hairpin RNAs.” *Genes & Development* 17 (24): 3011–16. https://doi.org/10.1101/gad.1158803.

Ying, Shao-Yao, Donald C Chang, and Shi-Lung Lin. 2008. “The MicroRNA (MiRNA): Overview of the RNA Genes That Modulate Gene Function.” *Molecular Biotechnology* 38 (3): 257–68. https://doi.org/10.1007/s12033-007-9013-8.

Yu, Chun-Ying, and Hung-Chih Kuo. 2019. “The Emerging Roles and Functions of Circular RNAs and Their Generation.” *Journal of Biomedical Science* 26 (1): 29. https://doi.org/10.1186/s12929-019-0523-z.

Zeng, Xiangxiang, Wei Lin, Maozu Guo, and Quan Zou. 2017. “A Comprehensive Overview and Evaluation of Circular RNA Detection Tools.” *PLOS Computational Biology* 13 (6): e1005420. https://doi.org/10.1371/journal.pcbi.1005420.

Zeng, Yan, William W Du, Yingya Wu, Zhenguo Yang, Faryal Mehwish Awan, Xiangmin Li, Weining Yang, et al. 2017. “A Circular RNA Binds To and Activates AKT Phosphorylation and Nuclear Localization Reducing Apoptosis and Enhancing Cardiac Repair.” *Theranostics* 7 (16): 3842–55. https://doi.org/10.7150/thno.19764.

Zhang, Ju, Xiuli Zhang, Cuidan Li, Liya Yue, Nan Ding, Tim Riordan, Li Yang, et al. 2019. “Circular RNA Profiling Provides Insights into Their Subcellular Distribution and Molecular Characteristics in HepG2 Cells.” *RNA Biology* 16 (2): 220–32. https://doi.org/10.1080/15476286.2019.1565284.

Zhang, Lirui, Xiaofeng Yang, Xu Li, Chen Li, Le Zhao, Yuanyuan Zhou, and Huilian Hou. 2015. “Butein Sensitizes HeLa Cells to Cisplatin through the AKT and ERK/P38 MAPK Pathways by Targeting FoxO3a.” *International Journal of Molecular Medicine* 36 (4): 957–66. https://doi.org/10.3892/ijmm.2015.2324.

Zhang, Maolei, Nunu Huang, Xuesong Yang, Jingyan Luo, Sheng Yan, Feizhe Xiao, Wenping Chen, et al. 2018. “A Novel Protein Encoded by the Circular Form of the SHPRH Gene Suppresses Glioma Tumorigenesis.” *Oncogene* 37 (13): 1805–14. https://doi.org/10.1038/s41388-017-0019-9.

Zhang, Maolei, Kun Zhao, Xiaoping Xu, Yibing Yang, Sheng Yan, Ping Wei, Hui Liu, et al. 2018. “A Peptide Encoded by Circular Form of LINC-PINT Suppresses Oncogenic Transcriptional Elongation in Glioblastoma.” *Nature Communications* 9 (1). https://doi.org/10.1038/s41467-018-06862-2.

Zhang, Xiao-Ou, Rui Dong, Yang Zhang, Jia-Lin Zhang, Zheng Luo, Jun Zhang, Ling-Ling Chen, and Li Yang. 2016. “Diverse Alternative Back-Splicing and Alternative Splicing Landscape of Circular RNAs.” *Genome Research* 26 (9): 1277–87. https://doi.org/10.1101/gr.202895.115.

Zhang, Xiao-Ou, Hai-Bin Wang, Yang Zhang, Xuhua Lu, Ling-Ling Chen, and Li Yang. 2014. “Complementary Sequence-Mediated Exon Circularization.” *Cell* 159 (1): 134–47. https://doi.org/https://doi.org/10.1016/j.cell.2014.09.001.

Zhang, Yang, Wei Xue, Xiang Li, Jun Zhang, Siye Chen, Jia-Lin Zhang, Li Yang, and Ling-Ling Chen. 2016. “The Biogenesis of Nascent Circular RNAs.” *Cell Reports* 15 (3): 611–24. https://doi.org/10.1016/j.celrep.2016.03.058.

Zhang, Yang, Xiao-Ou Zhang, Tian Chen, Jian-Feng Xiang, Qing-Fei Yin, Yu-Hang Xing, Shanshan Zhu, Li Yang, and Ling-Ling Chen. 2013. “Circular Intronic Long Noncoding RNAs.” *Molecular Cell* 51 (6): 792–806. https://doi.org/https://doi.org/10.1016/j.molcel.2013.08.017.

Zhao, Yi, Caiming Zhang, Haibo Tang, Xiaomin Wu, and Qiugan Qi. 2022. "Mechanism of RNA CircHIPK3 Involved in Resistance of Lung Cancer Cells to Gefitinib." *BioMed Research International* 2022: 4541918. https://doi.org/10.1155/2022/4541918.

Zheng, Chengfei, Hui Niu, Ming Li, Hongkun Zhang, Zhenggang Yang, Lu Tian, Ziheng Wu, Donglin Li, and Xudong Chen. 2015. "Cyclic RNA Hsa-Circ-000595 Regulates Apoptosis of Aortic Smooth Muscle Cells." *Molecular Medicine Reports* 12 (5): 6656–62. https://doi.org/10.3892/mmr.2015.4264.

Zheng, Qiupeng, Chunyang Bao, Weijie Guo, Shuyi Li, Jie Chen, Bing Chen, Yanting Luo, et al. 2016. "Circular RNA Profiling Reveals an Abundant CircHIPK3 That Regulates Cell Growth by Sponging Multiple MiRNAs." *Nature Communications* 7. https://doi.org/10.1038/ncomms11215.

Zhong, Shanliang, and Jifeng Feng. 2022. "CircPrimer 2.0: A Software for Annotating CircRNAs and Predicting Translation Potential of CircRNAs." *BMC Bioinformatics* 23 (1): 215. https://doi.org/10.1186/s12859-022-04705-y.

Zhou, Wei-Yi, Ze-Rong Cai, Jia Liu, De-Shen Wang, Huai-Qiang Ju, and Rui-Hua Xu. 2020. "Circular RNA: Metabolism, Functions and Interactions with Proteins." *Molecular Cancer* 19 (1): 172. https://doi.org/10.1186/s12943-020-01286-3.

Zimmermann, H, R Degenkolbe, H U Bernard, and M J O'Connor. 1999. "The Human Papillomavirus Type 16 E6 Oncoprotein Can Down-Regulate P53 Activity by Targeting the Transcriptional Coactivator CBP/P300." *Journal of Virology* 73 (8): 6209–19. https://doi.org/10.1128/JVI.73.8.6209-6219.1999.

Zimmermann, Maya, and Norbert Meyer. 2011. "Annexin V/7-AAD Staining in Keratinocytes." *Methods in Molecular Biology (Clifton, N.J.)* 740: 57–63. https://doi.org/10.1007/978-1-61779-108-6_8.

VITA

Bilge Yaylak

2011-16	B.Sc. in Molecular Biology and Genetics, Izmır Institute of Technology, Turkey
2016-18	M.Sc. in Molecular Biology and Genetics, Izmır Institute of Technology, Turkey
2016-23	Research Scholar, Izmır Institute of Technology, Turkey
2018-23	Ph.D. in Molecular Biology and Genetics, Izmır Institute of Technology, Turkey

FIELD OF STUDY

Characterization of Circular RNAs

PUBLICATIONS

Yaylak, B., Erdogan, I. and Akgul, B. 2019. “Transcriptomics Analysis of Circular RNAs Differentially Expressed in Apoptotic HeLa Cells.” Frontiers in Genetics. 10.3389/fgene.2019.00176.

Tüncel, Ö. Kara, M., Yaylak, B., Erdogan, I., Akgül, B. 2022. "Noncoding RNAs in Apoptosis: Identification and Function," Turkish Journal of Biology. 10.3906/biy-2109-35.

Yaylak, B, Akgül, B. 2022. “Experimental MicroRNA Detection Methods” Methods Mol Biol. 10.1007/978-1-0716-1170-8_2.